Novel Immunogens Of Cellular Immunity Revealed Using In Vitro Human Cell-based Approach

2012

Brian Schanen
University of Central Florida

NOVEL IMMUNOGENS OF CELLULAR IMMUNITY REVEALED USING AN *IN VITRO* HUMAN CELL-BASED APPROACH

by

BRIAN CHRISTOPHER SCHANEN
M.S. University of Central Florida, 2010

A dissertation submitted in partial fulfillment of the requirements
for the degree of Doctor of Philosophy
in the Burnett School of Biomedical Sciences
in the College of Medicine
at the University of Central Florida
Orlando, Florida

Summer Term
2012

Major Professors:
William Self
William Warren

ABSTRACT

In the last 150 years, tremendous headway has been made in our understanding of the human immune system. Pioneers in the field such as Paul Ehrlich, Elie Metchnikoff, Louis Pasteur, Robert Koch and Walter Reed carried out seminal studies that established the groundwork for our understanding of humoral and cellular immunity in humans. However, this direct line of evidence into human immunology was diverted in the mid-20th century with the adoption of a model which allowed for investigators to use a reductionist-approach with the promise to resolve immunity at a molecular level. This revolutionary model was the scientific commercialization of various inbred strains of mice. It seems inconceivable how a four-legged nocturnal rodent managed to become the focus of billions of dollars of research to improve our understanding of human immunity. Nevertheless, this strange surrogate for human immunity did provide us with major conceptual advances in areas, such as identification of dendritic cell population heterogeneity, T cell help for B cell antibody production, MHC-restricted recognition of virus-infected cells, and even the discovery of cell types like NKT cells. However, these prior advances have now been prefaced with decades-worth of disappointing, non-translational findings. The best examples of such disappointments are in murine models of autoimmunity, cancer immunotherapy, and vaccinology where numerous studies have revealed promising outcomes in mice but were met with failure or limited success upon translation into humans. We do not look at this as a failure of the murine model; rather we consider it a *call to arms* to innovate *in vitro* surrogates to examine human immunity when otherwise bound by ethical limitation from working directly in humans.

To overcome these challenges, we developed a system to interrogate novel immunogens that begins by generating human dendritic cells (DCs), a cell type necessary to mounting a protective immune response. DCs for research and clinical applications are typically derived from purified blood monocytes that are cultured in a cocktail of cytokines for a week or more. Because it has been

suggested that these cytokine-derived DCs may be deficient in some important immunological functions and might not accurately represent antigen presenting cell (APC) populations found under normal conditions *in vivo*, there is an interest in developing methods that permit the derivation of DCs in a more physiologically relevant manner *in vitro*. Here, we describe a simple and reliable technique for generating large numbers of highly purified DCs that is based on a one-way migration of blood monocytes through a layer of human umbilical vein endothelial cells (HUVECs) that are cultured to confluency in the upper chamber of a Transwell device. The resultant APCs, harvested from the lower Transwell chamber, resemble other cultured DC populations in their expression of major histocompatibility (MHC) and costimulatory molecules, ability to phagocytose protein antigens and capacity to trigger primary antigen-specific T cell responses. This technique offers several advantages over the standard method of *in vitro* cytokine-driven DC development, including: (1) the rapidity of this approach, as DC differentiation occurs in only 2 days, (2) the differentiation process itself, which is more akin to the development of DCs under physiologic conditions and (3) the cost effectiveness of the system, since no monocyte pre-selection is required and DC development occurs in the absence of expensive recombinant cytokines. Taken together, this approach allows for the exploration of novel immunogens utilizing a physiologically representative population of APCs enriched from circulating blood.

The outbreak of the swine-origin H1N1 influenza in the spring of 2009 took epidemiologists, immunologists, and vaccinologists by surprise and galvanized a massive worldwide effort to produce millions of vaccine doses to protect against this single virus strain. Of particular concern was the apparent lack of pre-existing antibody capable of eliciting cross-protective immunity against this novel virus, which fueled fears this strain would trigger a particularly far-reaching and lethal pandemic. Given that disease caused by the swine-origin virus was far less severe than expected, we hypothesized

cellular immunity to cross-conserved T cell epitopes might have played a significant role in protecting against the pandemic H1N1 in the absence of cross-reactive humoral immunity. We collaborated with bioinformaticians to develop an immunoinformatics approach to predict CD4+ T cell epitopes conserved between the 2008-2009 seasonal H1N1 vaccine strain and pandemic H1N1 (A/California/04/2009) hemagglutinin proteins that could act as novel immunogens and function as potential vaccine candidates or compliments to current vaccine formulations. We examined these peptides using T cells from human donors not exposed to the pandemic virus demonstrating that pre-existing CD4+ T cells can elicit cross-reactive effector responses against the pandemic H1N1 virus. As well, we showed the computational tools created by our collaborators were 80-90% accurate in predicting CD4+ T cell epitopes and their HLA-DRB1-dependent response profiles in donors that were chosen at random for HLA haplotype. Combined, these results confirm the power of coupling immunoinformatics to define broadly reactive CD4+ T cell epitopes with a highly sensitive *in vitro* model to verify these *in silico* predictions as a means to understand human cellular immunity, including cross-protective responses, and to define CD4+ T cell epitopes for potential vaccination efforts against future influenza viruses and other pathogens.

It is thought that utilizing highly conserved peptides as novel immunogens of cellular immunity for future vaccination strategies may require an adjuvant for efficacy. However, the FDA has approved the use of only two adjuvant compounds (Alum or MPL®) which may not be compatible or offer effective immune enhancement in novel vaccine preparations, thereby soliciting the need for novel adjuvants. Nanoparticles have since been a topic of adjuvant potential. Nanoparticles harbor great potential because they possess unique physicochemical properties compared to their larger counter parts as a result of quantum-size effects and their inherent large surface area to volume ratio. These physicochemical properties govern how a nanoparticle will behave in its environment. However,

researchers have only just begun to catalogue the biological effect these properties illicit. Moreover, little is known about the interaction between the immune system and NPs. However, in light of the recent development in new adjuvants that involves composites and coatings of polymers, lipids, ligands, TLR agonist, the ability of a simple metal oxide nanopowder to effectively induce or couple immunomodulation would provide researchers a basic alternative to costly and complex adjuvant development. Considering the evidence suggesting NPs can act as immunopotentiators, we questioned whether these materials can act not only as innate adjuvants, but as novel immunogens to cellular immunity.

To accomplish this, we under took a set of studies to investigate any nanoparticle size-induced effects using TiO_2, one of the most widely manufactured nanoparticles, as a model. We explored titanium dioxide synthesized into its three most commonly nanoarchitectures: anatase (7-10 nm), rutile (15-20 nm), and nanotube (10-15 nm diameters, 70-150 nm length) in comparison to a micron-sized formulation. We used the fully human autologous MIMIC® immunological construct has been utilized as a predictive, nonanimal alternative to diagnose nanoparticle immunogenicity. Cumulatively, treatment with titanium dioxide nanoparticles in the MIMIC® system led to elevated levels of proinflammatory cytokines and increased maturation and expression of costimulatory molecules on dendritic cells. Additionally, these treatments effectively primed activation and proliferation of naïve $CD4^+$ T cells in comparison to dendritic cells treated with titanium dioxide microspheres, characteristic of an *in vivo* inflammatory response, providing evidence of a size induced difference between the nano-sized and micron-sized material, revealing novel immune cell recognition and activation by a crystalline nanomaterial in a size-dependent manner.

Having identified nanomaterial size as a contributing feature of nanoparticle induced immunopotentiation, we became interested if additional physicochemical properties such as surface

reactivity or catalytic behavior could also be immunostimulatory. Moreover, because we witnessed a stimulatory effect to dendritic cells following nanoparticle treatment, we were curious how these nanoparticle-touched dendritic cells would impact adaptive immunity. Since TiO_2 acts as an oxidant we chose an antioxidant nanoparticle, CeO_2, as a counterpart to explore how divergent nanoparticle surface reactivity impacts innate and adaptive immunity. We focused on the effect these nanoparticles had on human dendritic cells and T_H cells as a strategy towards defining their impact to cellular immunity. Combined, we report that TiO_2 nanoparticles potentiate DC maturation inducing the secretion of IL-12p70 and IL-1B, while treatment with CeO_2 nanoparticles induced IL-10, a hallmark of suppression. When delivered to T cells alone TiO_2 nanoparticles induced stronger proliferation in comparison to CeO_2 which also stimulated T_{Reg} differentiation. When co-cultured in allogeneic T cell assays, the materials directed alternate T_H polarization whereby TiO_2 drives largely a T_H1 dominate response, whereas CeO_2 drove a T_H2 bias. Combined, we report a novel immunomodulatory capacity of nanomaterials with catalytic activity. While unintentional exposure to these nanomaterials could pose a serious health risk, development and targeted use of such immunomodulatory nanoparticles could provide researchers with new tools for novel adjuvant strategies or therapeutics.

I dedicate this dissertation to the love of my life, my beloved wife Amanda. I eagerly (and anxiously) await to see what the future will hold for us as we both embark upon our career-life leaving behind our academic-life (finally). Also, I extend my gratitude to my family (Deborah and David Schanen- without you none of this would be possible) as well as my extended family (Jim Baker and Lisa Sanchez- your support has been invaluable) and all my friends for their support provided to me throughout my education.

I also want to extend a special *degree* of appreciation to my friends for their seemingly constant query of when I would be finished with my PhD.

Additionally, I would like to dedicate this to Broker Brown, the greyhound who kept me company the myriad of late nights spent editing what always seemed like the final draft of the next manuscript in preparation.

Finally, I would like to thank the creative cinematic sci-fi thinkers like Gene Roddenberry, whose stories about man's futuristic trek through the stars inspired me to take stock in the betterment of humanity and pursue a career in science.

ACKNOWLEDGMENTS

I would like to express my debt of gratitude to my PhD advisors, Dr. William Self and Dr. William Warren for your guidance, support, and inspiration. Working between the Self lab and Dr. Warren's company, Vaxdesign, has been a challenging journey, yet straddling these positions has provided me a unique and valuable life experience which no doubt will propel my career in science. Thank you. You both have helped me find a balance between the worlds of academia and industry.

I could not go without acknowledging my mentor of immunology, Dr. Donald Drake III. You have been so much more to me than a supervisor at Vaxdesign. You have mentored me through my development as an immunologist and have always pushed me to be a better scientist whether I'm at the bench, in the conference room, or through my written word.

I would also like to acknowledge my committee members Dr. Sudipta Seal, Dr. Annette Khaled, and Dr. Antonis Zervos for their assistance, insights, and suggestions which have added to the success of my dissertation research.

TABLE OF CONTENTS

LIST OF FIGURES

LIST OF TABLES

LIST OF ACRONYMS/ABBREVIATIONS

APC	Antigen Presenting Cell
CFSE	Carboxyfluorescein Succinimidyl Ester
DC	Dendritic Cell
DCF-DA	2-,7-Dichlorodihydrofluorescein Diacetate
DLS	Dynamic Light Scattering
EU	Endotoxin Unit
FACS	Fluorescence Activated Cell Sorting
HA	Hemagglutinin
HRTEM	High Resolution Transmission Electron Microscopy
HUVEC	Human Umbilical Vein Endothelial Cell
ICP-MS	Inductively Coupled Plasma-Mass Spectroscopy
IL	Interleukin
iTEM	Individualized T cell Epitope Measure
LPS	Lipopolysaccharide
LTE	Lymphoid Tissue Equivalent
MFI	Mean Fluorescence Intensity
MIMIC®	Modular Immune *In vitro* Construct
MHC	Major Histocompatibility Complex
MTT	3-[4,5-dimethylthiazol-2-yl]-2,5-diphenyl tetrazolium bromide
NP(s)	Nanoparticle(s)
PBMC	Peripheral Blood Mononuclear Cells

PBS	Phosphate Buffered Saline
PC	Polycarbonate
PHA	Phytohemagglutinin
PTE	Peripheral Tissue Equivalent
PWM	Pokeweed mitogen
ROS	Reactive Oxygen Species
SI	Stimulation Index
S-OIV	Swine-Origin Influenza A virus
TEER	Trans-Endothelial Electrical Resistance
T_H	T helper cell
TIV	Seasonal Trivalent Vaccine

CHAPTER ONE: A NOVEL APPROACH FOR THE GENERATION OF HUMAN DENDRITIC CELLS FROM BLOOD MONOCYTES IN THE ABSENCE OF EXOGENOUS FACTORS

Abridgment

This body of evidence presented here in this thesis is built upon the development of a human model of immunity to gain more-accurate insights into the effects of agents upon human immunity. Development of such a model of interrogation begins at the ground floor with cells of the innate immune system. Henceforth, we chose to investigate human dendritic cells (DCs) because of their important role as antigen presenting cells (APCs) and their unique ability to bridge innate and adaptive immunity. DCs for research and clinical applications are typically derived from purified blood monocytes that are cultured in a cocktail of cytokines for a week or more. Because it has been suggested that these cytokine-derived DCs may be deficient in some important immunological functions and might not accurately represent APC populations found under normal conditions in vivo, there is an interest in developing methods that permit the derivation of DCs in a more physiologically relevant manner in vitro. Here, we describe a simple and reliable technique for generating large numbers of highly purified DCs that is based on a one-way migration of blood monocytes through a layer of human umbilical vein endothelial cells (HUVECs) that are cultured to confluency in the upper chamber of a Transwell device. The resultant APCs, harvested from the lower Transwell chamber, resemble other cultured DC populations in their expression of major histocompatibility (MHC) and costimulatory molecules, ability to phagocytose protein antigens and capacity to trigger primary antigen-specific T cell responses. This technique offers several advantages over the standard method of in vitro cytokine-driven DC development, including: (1) the rapidity of this approach, as DC differentiation occurs in only 2 days, (2)

the differentiation process itself, which is more akin to the development of DCs under physiologic conditions and (3) the cost effectiveness of the system, since no monocyte pre-selection is required and DC development occurs in the absence of expensive recombinant cytokines.

Introduction

The generation of protective immunity against infection and tumors requires specialized cells that can present foreign or altered-self antigens to T cells. While several cell types can act as APCs, DCs are the most potent of these populations and the only ones capable of inducing $CD4^+$ and $CD8^+$ T cell responses against naïve antigens. Under normal conditions, immature DCs actively acquire antigen via various pathways of endocytosis, but express low levels of surface major histocompatibility complex (MHC) and T cell costimulatory molecules. An encounter with inflammatory signals or common pathogen motifs (Toll-like receptor ligands) triggers a maturation program in DCs that lessens their ability to take up exogenous proteins, increases their surface expression of MHC/peptide complexes and ligands important for T cell activation and enhances their migration towards secondary lymphoid tissues [1, 2]. It is these matured, antigen-loaded DCs that are particularly well-suited for inducing primary T cell responses within secondary lymphoid tissues. Tissue-resident DCs comprise a heterogeneous population of cells found in most organs of the body. Short-lived circulating monocytes, which give rise to DCs, traverse the vascular endothelium into peripheral tissues in a constitutive manner, though infection or injury triggers an increased accumulation of these cells at the inflamed site [3-6]. Within tissues, a fraction of the extravasated monocytes differentiate into DCs, with the milieu of the local microenvironment often influencing the phenotype and functional activity of APCs residing in a particular site [7-9]. For example, gut-associated DCs populate Peyer's patches, where they receive

antigens from M cells and act as the resident APCs of mucosal tissue [10]. Langerhans cells, on the other hand, are found primarily in the skin and play a key role in the induction of adaptive responses following infection [11]. DCs for research and clinical applications are usually obtained by culturing PBMC-derived monocytes in a cocktail of cytokines for about 1 week. However, several laboratories have worked to develop in vitro systems which more closely recapitulate the cell interactions and signaling pathways that trigger monocyte to DC differentiation in vivo. For instance, the groups of Muller and Randolph pioneered the development of a tissue construct consisting of primary HUVEC grown atop a collagen support matrix that promotes the differentiation of blood monocytes into APCs which resembled DCs by phenotype and function [5, 6, 12-14]. While this tissue model generates a diverse APC population that may accurately represent DC populations found in vivo, its complexity makes it impractical for widespread use. In another approach, adherent monocytes cocultured directly with human or porcine endothelial cells gave rise to potent APCs that produced proinflammatory cytokines, expressed high levels of costimulatory ligands and efficiently stimulated allogeneic T cells [15]. The limitation of this technique is that the DCs had to be purified away from contaminating endothelial cells by magnetic bead selection before any functional analyses could be performed.

In this report we describe a simple, cost-effective and convenient Transwell-based culture method for the endothelial cell-mediated differentiation of human DCs from blood monocytes. This system generates APCs with a frequency and purity comparable to more traditional DC populations derived in vitro, but does so in only 2 days, in the absence of exogenous factors and without the need for a cumbersome matrix to support the growth of HUVECs. The transmigrated APCs derived from these cultures resemble classical in vitro DCs in their expression of MHC and costimulatory molecules and capacity to induce recall and primary antigen-specific T cell responses. Therefore, this system provides

an alternative means of generating human DCs in a manner that is more reflective of their development under physiologic conditions.

Materials and Methods

HUVEC Preparation and Transwell Seeding

Primary HUVECs were purchased from VEC Technologies (Rensselaer, NY) at the 2nd passage or Lonza (Allendale, NJ) at 8 doublings. The endothelial cells, as supplied by the vendors, were thawed and immediately applied at a concentration of 9×10^5/cm2 to 12-well Transwell buckets containing polycarbonate (PC) membranes with 5 μm pores (Corning, Lowell, MA). Alternatively, the cellswere thawed, expanded by 10 doublingsin EGM-2 media (Lonza), and refrozen prior to being used in Transwell assays. Within Transwell cultures, the primary HUVECs from VEC Technologies were grown in MCDB-131complete media containing 10% fetal bovine serum, 10 ng/ml endothelial growth factor, 1 μg/ml hydrocortisone, 0.2 mg/ml ENDOGRO, 0.1 mg/ml heparin and an antibiotic/antimycotic solution (all reagents from VEC Technologies) while the cells from Lonza were grown inM199 media (Lonza) containing 20% fetal bovine serum (HyClone, Logan UT), 2 mM L-glutamine, 100 U/ml penicllin and 0.1 mg/ml streptomycin (Sigma, St. Louis, MI). 85% of the media was exchanged every other day. HUVECs were cultured in Transwell buckets for 7 days prior to being used in monocyte migration assays (see Results section).

HUVEC Microscopy

The formation of tight-gap junctions in HUVEC monolayers was assessed by fluorescence microscopy. The staining process involved fixing and permeabilizing the endothelial cells with 3.2% paraformaldehyde (32% stock from Electron Microscopy Science, Hatfield, PA) for 10 min and −20 °C methanol for 5 min, respectively. The cells were labeled with an antibody against human CD31 (M89D3; BD Pharmingen, San Jose, CA) for 1 h at RT in a humidified chamber and then the nuclei were labeled with 1 µg/ml DAPI (Sigma) for 5 min. Next, the cells were fixed again with 3.2% paraformaldehyde for 10 min at RT and then covered with GelMount (Biomedia, Beaufort, SC). Extensive washes with PBS were included between each step. The labeled cells were examined on an Olympus IX81 fluorescence microscope.

Transendothelial Diffusion Assay

The permeability of the endothelial cell monolayer was measured in a standard diffusion assay (Nevo et al., 2001). HUVECs were cultured on PC membranes as described above, with minor modification. 24 h prior to the start of the experiment, the cells were switched into assay media (IMDM containing 5% heat-inactivated autologous plasma or human AB serum, 2 mM L-glutamine, 100 U/ml penicillin and 0.1 mg/ml streptomycin). Next, the cells were switched into diffusion media (IMDM supplemented with 1% BSA) for 1 h. FITC conjugated dextran (70 kDa; Sigma), diluted to 1 mg/ml in the same media, was added to the upper well. Thereafter, 100 µl aliquots were taken from the lower chamber at 30 min intervals. To avoid changes in hydrostatic pressure, an equal volume of fresh diffusion media was added to the lower chamber after each sample was removed. The fluorescence of

the media samples was measured with a Bio-Tek Synergy HT spectrophotometer containing a 480/520 nm filter set. A standard curve established by measuring the fluorescence of known amounts of FITC-dextran was used to calculate the concentration of dextran that permeated the HUVEC monolayer.

Trans-Endothelial Electrical Resistance

Transendothelial electrical resistance (TEER) was used as a second method to examine the integrity of the HUVEC monolayer. Endothelial cells were cultured in Transwell buckets, and 24 h before TEER was measured, the cultures were switched into assay media. TEER was measured using a voltohmeter (EVOM-ENDOHM-6,World Precision Instruments, Sarasota, FL) and resistance chamber that is compatible with the Transwell inserts. The voltohmeter was calibrated each day as described by the manufacturer and three individual readings were taken for each well. The TEER readings of the HUVEC monolayers on Transwell membranes were normalized against values collected from Transwell inserts alone (in the absence of endothelial cells).

Human PBMC Preparation

Enriched leukocytes or apheresis products were purchased from Florida's Blood Centers (Orlando, FL). All of the donors were in good health and all blood products were negative for common blood-borne pathogens, as detected by standard assays. PBMCs were enriched by density centrifugation; briefly, 45–50 ml leukocytes were diluted with 90 ml citrate buffer (PBS containing 0.1% BSA and 0.6% Na citrate). 35 ml of the diluted blood was layered onto 15ml Ficoll-Paque PLUS (GE Healthcare Bio-Sciences, Piscataway, NJ) in a 50 ml conical tube and centrifuged at 400 g for 25 min. The

interface cells were removed, washed twice with citrate buffer and resuspended in serum-free X-VIVO 15 media (Lonza). The PBMCs were used immediately, stored for up to 24 h at 4 °C, or frozen in liquid nitrogen for extended storage.

Monocyte Transmigration Assays

A range of 1-10 million ($1–10\times10^6$) PBMCs were applied to confluent endothelial cells in the upper Transwell chamber that had been transferred into X-VIVO 15 media 24 h earlier. After 1.5 h, the upper chambers were washed twice with the same media to remove non-adherent and loosely bound cells, and the Transwell plates were incubated for an additional 48 h to allow for leukocyte transmigration and differentiation. The upper chambers were then removed and the cells in the lower chamber were harvested for phenotypic or functional analyses. Standard tissue culture dishes were used; the nonadherent cells were collected with moderate washing while the adherent cells were lifted with Trypsin–EDTA.

DC Phenotyping

The tandem dyes PE-, APC-, or PerCP-Cy5.5-were conjugated to monoclonal antibodies specific for human CD1a (HI149), CD14 (M5E2), CD16 (3G8), CD40 (5C3), CD80 (L307.4), CD86 (2331), CD83 (HB15e) and HLA-DR (L243) were purchased from BD Pharmingen and diluted as suggested by the manufacturer. Isotype controls included MIgG2a (G155-178) and MIgG1 (MOPC-21), which were also purchased from BD Pharmingen. The transmigrated cells were collected at various times following PBMC seeding and labeled with specific antibody for 45 min at 4 °C, washed extensively and fixed with 2%

paraformaldehyde. The buffer used for cell labeling was PBS with 2% BSA and 0.05% sodium azide. Samples were acquired on an LSRII (BD Pharmingen) and FlowJo software (Treestar, Ashland, OR) was used for analysis.

T cell Stimulation Assay

Two days after PBMCs were applied to the HUVEC monolayer, the transmigrated cells in the lower chamber were pulsed with 1 μg/ml tetanus toxoid (TT; Calbiochem, San Diego, CA), recombinant protective antigen (rPA) from Bacillus anthracis (List Biological Laboratories, Campbell, CA) or the 42 kDa fragment of the Plasmodium falciparum merozoite surface protein-1 (MSP-1), which was a generous gift of Dr. E. Angov, Walter Reed Army Institute of Research, Silver Springs, MD. 1 day later, the cells were treated with 25 ng/ml TNFα to induce maturation, and 24 h later, the nonadherent fraction was collected, washed in X-VIVO 15 media and combined at a 1/60 ratio with autologous T cells in the same media. Cytokine-derived DCs were prepared using standard procedures [16, 17]. Briefly, monocytes were purified from total PBMC using anti-CD14 antibody-conjugated magnetic beads (Miltenyi Biotec, Auburn, CA) and cultured for 7 days at 1×106/ml in XVIVO 15 media containing 100 ng/ml GM-CSF (R&D Systems) and 25 ng/ml IL-4 (Pierce Biotechnology, Rockford, IL). The cells were pulsed with antigen and matured with 25 ng/ml TNFα using the timing described above. Frozen stocks of autologous PBMCs were used as a source of lymphocytes. CD4+ T cells were purified by negative selection using magnetic beads from Miltenyi Biotec. The purified T cells were plated at 2.5×106/well in 48-well flatbottom tissue culture plates (Corning) and the DCs were added at a 1/60 ratio to the T cells. Each well contained a final 800 μl volume. The leukocyte cocultures were incubated for 12 days at 37 °C and 5% CO2 and then the T cells were analyzed for intracellular cytokine production and surface CD154 (CD40L) expression using

standard procedures. Target APCs (cytokine-derived DCs) were prepared using the same approach to generate stimulator DCs (see above). These cells were pulsed with antigen for the final 24 h of culture. The target DCs were cultured with the activated T cells for 8 h at a 1/4 ratio; 1 μg/ml brefeldin A (Sigma), which blocks protein egress from the Golgi apparatus, was added during the final 6 h of culture. The cells were surface-labeled with an antibody specific for CD4 (SK3) and then labeled intracellularly with an antibody specific for human IFNγ (B27) and CD154 (TRAP1) using cytofix/cytoperm and perm/wash reagents from BD Pharmingen.

Phagocytosis Assays

Transmigratory non-adherent monocytes were collected 2 days following PBMC application and incubated overnight with 1 μm-diameter orange fluorescent beads or AlexaFluor 488-labeled zymosan particles at a ratio of 3/1 to the cells (both reagents from Invitrogen, Carlsbad, CA). Then, the cells were washed once in FACS buffer and analyzed by flow cytometry. In some cases, the APCs were treated with 20 μg/μl cytochalasin D for 2 h at 37 °C prior to incubation with the beads or particles to block phagocytic activity.

Results

This report describes a novel approach for the endothelial cell-driven development of human DCs from blood monocytes in the absence of any exogenous factors. A nonimmunogenic and biologically inert PC membrane, with 5 μm pores that permit cell transmigration, provides support for the growth of a confluent monolayer of HUVECs. The membrane is housed in an upper chamber that is suspended

over, and is separable from, a lower chamber (tissue culture well). When whole PBMCs are applied to the upper chamber, the confluent endothelial cells permit the selective passage of monocytes through the membrane and concomitantly regulate and promote their differentiation into functional APCs. 2 days after the Transwell is seeded with PBMCs, the upper chamber is removed and antigen, in the presence or absence of additional maturation stimuli, is added to the DCs in the lower chamber. See Fig. 1 for a diagrammatic representation of this method.

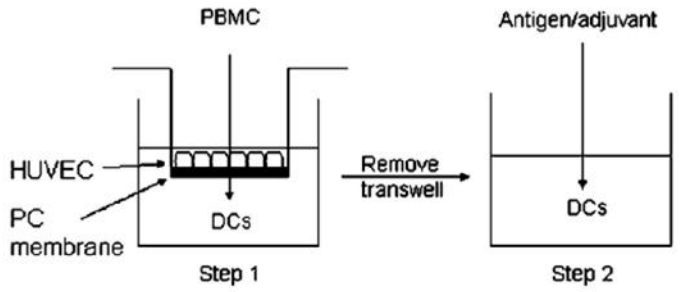

Figure 1. Schematic of the membrane device.

HUVECs cells are grown to confluency/quiescence on a PC membrane in a Transwell bucket and then total PBMCs are applied to the upper chamber for 1.5 h (step 1). The unbound cells are washed away and the remaining leukocytes are allowed to transmigrate for 48 h. Next, the upper chamber is removed and the DCs are collected for analysis or pulsed with antigen for an additional 2 days (step 2).

HUVECs Form a Confluent Monolayer with Tight-Gap Junctions on PC Membranes

`Primary endothelial cells were used directly from frozen stocks obtained from commercial sources or expanded by 10 doublings prior to being used in assays. The growth characteristics of endothelial cells on PC membranes were assessed by seeding 3×10^5 HUVECs per 24-well Transwell bucket (the area of the membrane is equivalent to the area of a well in a 96-well plate) and then examining the cells at several time points post-seeding for the formation of cell–cell junctions, which is indicative of a quiescent, confluent monolayer [18]. Although the cells were seeded at a density

sufficient to form a solid monolayer within 1–2 days (data not shown), the formation of CD31 (PECAM-1)-positive tight-gap junctions was not evident until 3–4 days post-seeding. (Fig. 2A shows an immunofluorescence image of confluent endothelial cells at 7 days post-seeding.) Increased electrical resistance (TEER) across the cell monolayer and decreased dextran diffusion through the confluent cells can also be used to confirm the formation of tight-gap junctions in cultured HUVEC [19, 20]. The results presented in Fig. 2B demonstrate that TEER increased about 6-fold between days 3 and 4 post-seeding and reached a plateau of 60–80 Ω thereafter. This increased electrical resistance was correlated with an increased ability of the HUVECs to block the diffusion of FITC-labeled dextran from the upper to lower Transwell chamber during the culture period. On day 2 of culture, the HUVECs were quite permeable, with greater than 80% of the labeled dextran passing through the monolayer in a 2-h assay. In contrast, the day 8 endothelial cells allowed less than 30% of the labeled dextran to pass through the membrane during the same timeframe (Fig. 2C). The kinetics of tight-gap junction formation, as evaluated by these methods, were consistent with previously published reports and demonstrate that endothelial cells can be cultured to confluence/quiescence on PC membranes [19, 20]. The inter-assay variation in HUVEC growth rates and kinetics of tight-gap junction formation was nearly zero when Transwell chambers were seeded with endothelial cells of the same lot. Therefore, a single evaluation of the HUVEC growth dynamics by TEER and diffusion analysis was sufficient to establish the appropriate timing of PBMC application for all subsequent experiments using the same batch of endothelial cells. For the studies outlined here, Transwells were seeded with HUVECs for 7 days prior to the application of PBMCs.

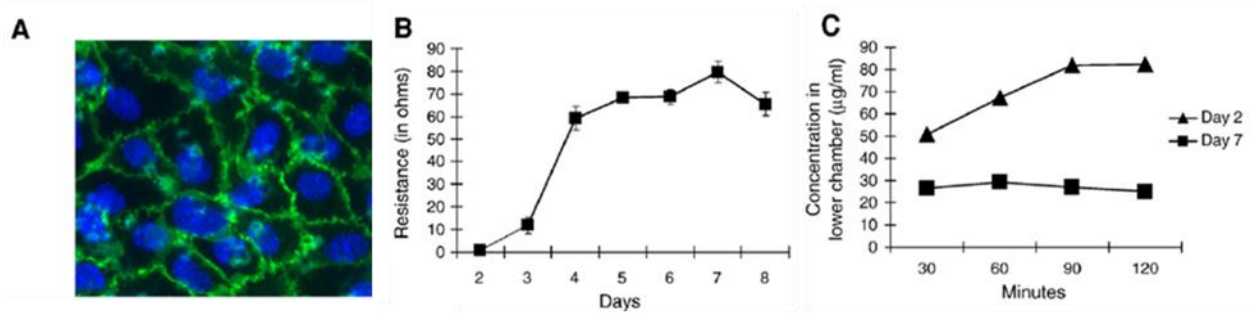

Figure 2. HUVECs form confluent/quiescent monolayers on Transwell-PC membranes.

Primary HUVECs were seeded in the upper chamber of Transwells and analyzed for confluency and the formation of tight-gap junctions. HUVECs were seeded at 3×105/well in 24-well Transwell-PC membrane buckets. After 7 days, the cells were fixed and surface-labeled with a FITC-conjugated antibody specific for CD31, and the nuclei were stained with DAPI. CD31 and DAPI labeling are shown in green and blue, respectively (A). At the indicated time points, transendothelial electrical resistance (TEER) readings were collected and normalized against the values for empty Transwells on the same day. The error bars represent 1 SD of triplicate readings in each well (B). On days 2 and 7, the same HUVEC cultures were incubated with 1 mg/ml FITC-dextran (70 kDa) for 120 min and the concentration of dextran in the lower chamber was determined by fluorescence at 30 min time points (C).

HUVECs Seeded on PC Membranes Provide a Selective Barrier to the Passage of Blood Monocytes

Previous studies have shown that HUVECs, when grown to confluency on a collagen support matrix, create a highly restrictive barrier for the migration of nearly all PBMC populations except monocytes [13]. Similarly, when 5×10^6 PBMCs were applied to confluent HUVECs on a PC membrane in the upper Transwell chamber for 1.5 h, nearly all of the transmigrated cells were uniform in size and morphology (Fig. 3, right panel), and when assessed by flow cytometry, were greater than 95% monocytes (see below). After 2 days of culture in standard tissue culture treated plastic dishes, about 50% of the transendothelial migrated monocytes were weakly/non-adherent, while the other half exhibited strong adherence and morphologically resembled macrophages. Most often, human DCs are generated in culture by differentiating purified blood monocytes with exogenous cytokines for about 1

week. In our hands, in more than 50 donors, 100×10^6 unfractionated PBMCs typically contained about 20% CD14+ monocytes. In turn, 20×106 purified monocytes cultured in the presence of GM-CSF and IL-4 for 1 week yielded approximately 20%, or $3–4\times10^6$, nonadherent DCs. (The remainder of the monocytes differentiated into tightly adherent macrophages.) By comparison, when 100×10^6 PBMCs were applied at a density of 5×10^6/ well to Transwell chambers, about 8×10^6 non-adherent APCs were harvested from the lower Transwell chamber after a 2- day culture period. We considered the possibility that a seeding density of 5×10^6 PBMCs, which was shown to be optimal in other endothelial cell-monocyte culture formats in our laboratory, might not be most suitable for the Transwell approach. However, this appeared to represent an optimal loading density since doubling the number of PBMC applied to the upper chamber of a Transwell-HUVEC well (from 5×10^6 to 10×10^6) did not significantly increase the number of transmigrated monocytes and decreasing the number of loaded PBMC only resulted in a proportional decrease in the number of cells recovered from the lower Transwell chamber. Likewise, altering the PBMC seeding density did not markedly impact the ratio of adherent to non-adherent cells harvested from the lower Transwell chamber. (This data is summarized in Table 1.) The importance of confluent HUVECs in permitting the selective migration of blood monocytes was most clearly illustrated in assays comparing PBMC migration through Transwell-PC membranes containing or lacking a confluent endothelial monolayer. As mentioned above, Transwells containing a confluent endothelial cell monolayer yielded a highly purified (greater than 95%) transmigrated monocyte/APC population from unfractionated PBMCs applied to the upper chamber. In contrast, the absence of HUVECs permitted a more heterogeneous population of cells, including erythrocytes and lymphocytes, to pass through the PC membrane into the lower Transwell chamber (Fig. 3, left panel). Phenotypic analysis revealed that this population consisted of, on average, 31% $CD14^+$ monocytes, 53% $CD3^+$ T cells and 13% $CD19^+$ B cells (Table 2). While non-confluent endothelial cells are not routinely used in PBMC transmigration assays,

we found that HUVEC monolayers not having fully developed tight-gap junctions, i.e., those with a suboptimal TEER reading, yielded a transmigrated population containing more contaminant cells than fully confluent endothelial cells (data not shown). Of note, the PBMC loading density had little effect on the purity of the transendothelial-migrated population harvested from the lower Transwell chamber.

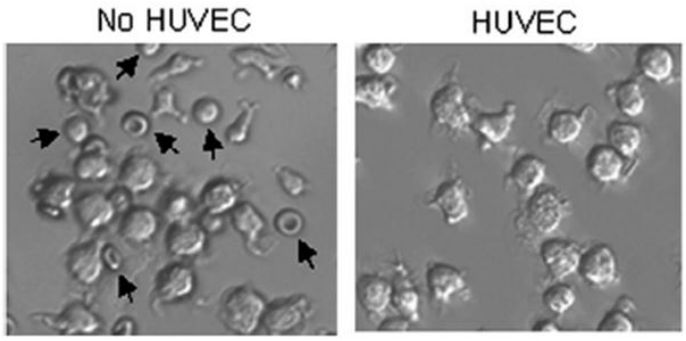

Figure 3. Endothelial cells permit the passage of a homogeneous population of cells through the Transwell device.

PBMCs were applied to the upper Transwell chamber. 48 h later, cells that passed through a PC membrane in the absence (left) or presence (right) of a HUVEC monolayer, and into the lower chamber of the Transwell, were imaged by phase microscopy, 20× magnification. Arrows indicate contaminating red blood cells or lymphocytes. A non-adherent plate was used for this assay.

Table 1. Analysis of PBMC seeding density on transmigrated cell recovery and phenotype.

# of PBMCs Seeded onto Transwell	Transmigrated Cells	
	Total Yield ($\times 10^5$)	Adherent/ Non-adherent
10.0×10^6	8.3 (0.34)[a]	52/48[b]
5.00×10^6	7.9 (1.01)	51/49
1.00×10^6	2.9 (0.12)	51/49

[a] Values represent an average yield, from 4 distinct donors, in the number of transendothelial-migrated cells harvested from the lower Transwell chamber 48 h after PBMCs were applied to confluent HUVECs in the upper Transwell chamber. The standard deviation is shown in parenthesis.

[b] Values represent the proportion of adherent and non-adherent cells in the transmigrated pool 48 h after HUVECs were seeded with PBMC.

HUVECs Trigger Phenotypic Changes Characteristic of DCs in Transmigrated Monocytes

It has been shown that monocytes which have migrated through a confluent HUVEC layer, and then reverse transmigrated back through the same endothelial cells, differentiate into APCs that resemble classical DCs in phenotype and function [12, 13]. We sought to determine whether a single migration of monocytes through a confluent HUVEC layer, as occurs in the Transwell approach, is sufficient to promote their differentiation towards DCs. To this end, the non-adherent transmigrated APCs were collected from the lower Transwell chamber 48 h after PBMCs were applied to the upper chamber and examined for characteristic features of DCs. For many of these analyses, the role of endothelial cells in regulating the differentiation state of monocytes was examined by comparing cells that had migrated through PC membranes in the presence of a HUVEC monolayer with those that had passed through a PC membrane alone. Immune cells, and the various activation/maturation states of

these populations, are often defined by their expression of a particular pattern of surface proteins. For this study, ligands important for APC phenotype and/or function were used to assess the role of HUVEC in promoting the differentiation of transendothelial-migrated monocytes. Specifically, the phenotypic profile of transmigrated (nonadherent) APCs that had contacted endothelial cells (shown in Fig. 4A) was compared with those that had passed through an empty Transwell bucket (Fig. 4B). Since it was possible that monocytes passing through a porous PC membrane in the absence of a HUVEC layer might also experience a change in their marker profile, non-migrated $CD14^+$ cells that had been cultured for 2 days in assay media absent of exogenous factors were used to establish a baseline expression level for each marker of interest. Thus, the median fluorescence intensity (MFI) of markers on the non-migrated monocytes was set at 100% and compared against the change in MFI of the same markers on monocytes that had transmigrated through the PC membrane, in the absence or presence of HUVEC, 48 h earlier (Fig. 4B).

Table 2. Phenotypic characterization of non-adherent transmigrated cells in Transwell cultures.

Transmigrated Cells[a]	Minus HUVEC			Plus HUVEC		
	Donor #1	Donor #2	Donor #3	Donor #1	Donor #2	Donor #3
$CD14^+$	37.0[b]	28.0	34.0	97.1	96.5	95.8
$CD3^+$	50.0	55.0	53.0	2.0	3.0	3.5
$CD19^+$	12.0	15.0	12.0	0.7	1.0	0.6

[a] 5×10^6 PBMCs were applied to Transwell chambers lacking or containing confluent endothelial cell. Excess cells were washed away 1.5 h later and then the transmigrated cells were harvested from the lower chamber and evaluated by flow cytometry for the specified markers at 48 h post-seeding.

[b] Numbers represent the percentage of leukocyte-gated events in the transendothelial-migrated population and are derived from 6 pooled Transwell cultures.

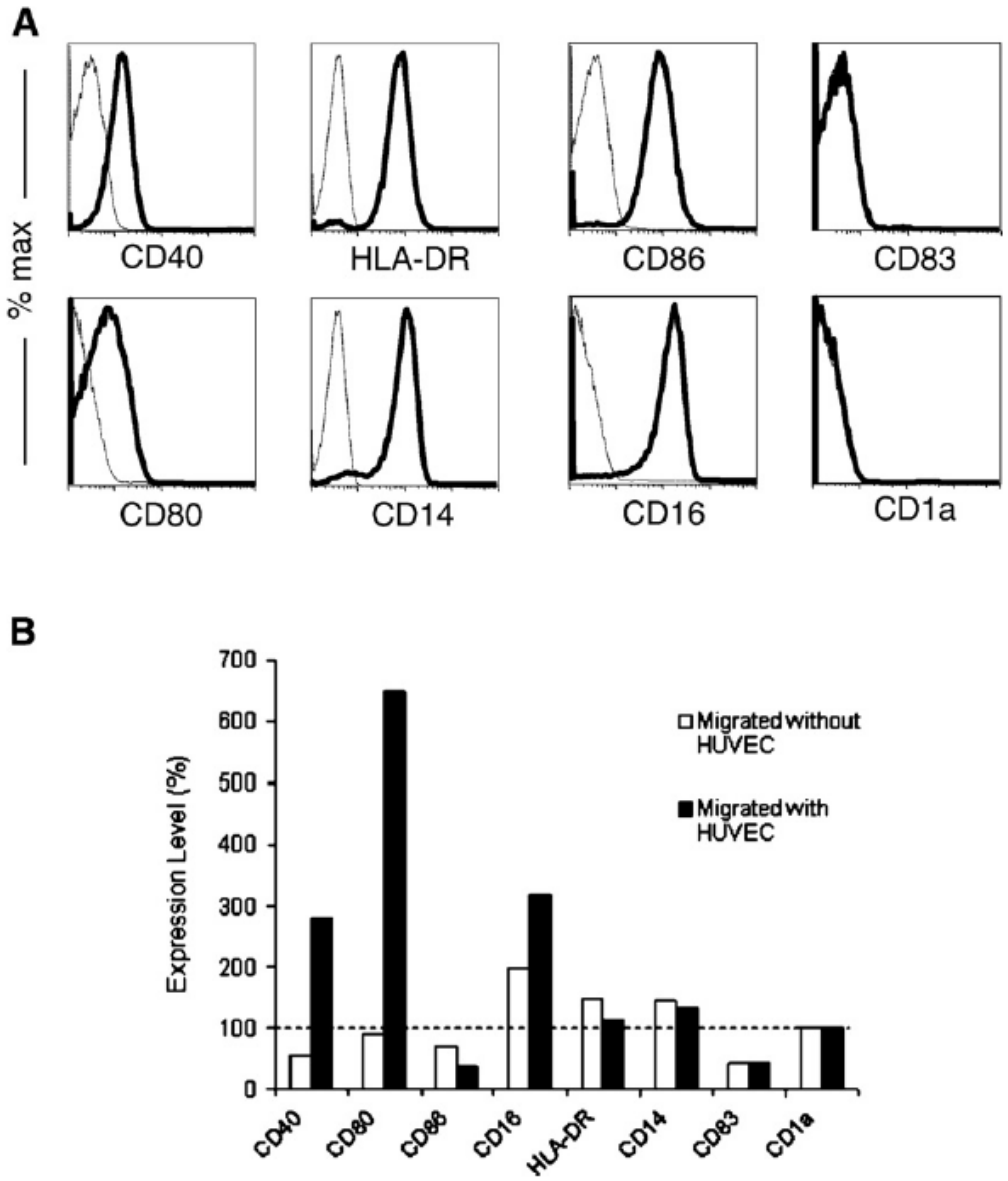

Figure 4. (A) Histograms and (B) MFI of marker expression reveal transmigration of monocytes through an endothelium is sufficient to trigger their differentiation towards a DC phenotype.

CD14+ monocytes were isolated and cultured in media. At the same time, PBMCs were applied to the Transwells the presence or absence of HUVEC. (A) Histograms of marker expression on monocytes that had transmigrated through an endothelial layer. The solid lines indicate the intensity of labeling with a specific antibody, while the dotted line indicates the background fluorescence with an appropriate isotype control. (B) The MFI of surface proteins on HUVEC-migrated monocytes, as shown in (A), or non-HUVEC-migrated monocytes, was plotted as a percent increase or decrease over the MFI of the same protein on non-migrated monocytes.

The presence of a HUVEC monolayer caused the transmigrated monocytes to experience a marked increase in expression of two molecules, CD40 and CD80, which provide critical costimulatory/activating signals to DCs and T cells, respectively. The low affinity IgG receptor, FcγRIII (CD16), which is important for the uptake of antibody-coated proteins, was upregulated on APCs that migrated through the HUVEC layer, though it was also elevated to a lesser extent on cells that passed through a PC membrane lacking an endothelial monolayer. The minimal increase in expression of CD86 and HLA-DR on transmigrated monocytes was not surprising since these proteins were already expressed at a high level on non-migrated monocytes (data not shown). Transwell-derived APCs were unlike traditional cytokine derived DC in their retention of the monocyte marker, CD14 (Fig. 4A and B), though these results are consistent with prior methods that utilized endothelial cells to drive the differentiation of DCs from monocytes [13]. In vivo and in vitro data indicate that monocytes can differentiate into either macrophages or DCs [13, 21, 22]. Correspondingly, it appeared that cells which had migrated through the endothelium could be divided into two populations that were unique in their morphology and capacity to adhere to tissue culture plates. Phenotype analysis, which is shown in Fig. 5, provided further confirmation that these were indeed distinct subsets of cells. The adherent monocytes expressed low levels of the DC marker, DC-SIGN, and high levels of CD68, suggesting that this population was macrophage-like. In contrast, the elevated expression of DC-SIGN on the non-adherent transmigrated monocytes implied that these cells had differentiated towards a DC phenotype.

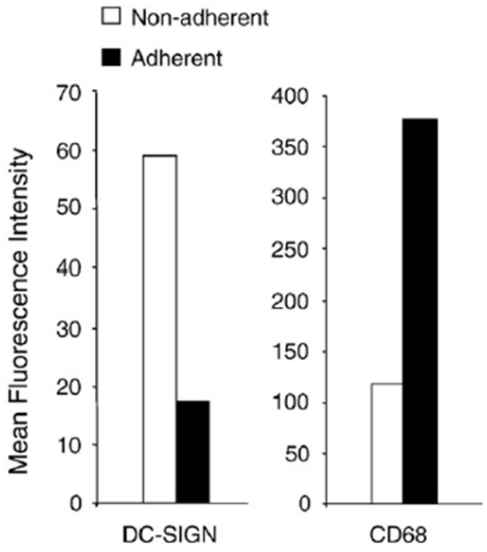

Figure 5. Adherent transmigrated monocytes phenotypically resemble macrophages.

PBMCs were applied to the upper chamber of a Transwell containing HUVECs and 48 h later the migrated, non-adherent and adherent cells were collected from the lower chamber. The cells were labeled with specific antibodies and analyzed by flow cytometry. The MFI for each marker on adherent and non-adherent cells is represented graphically.

Transmigrated DCs have Phagocytic Activity

The increased expression of costimulatory ligands on Transwell-derived cells suggested that a single transendothelial migration might be sufficient to trigger at least a fraction of the monocytes to differentiate into DCs. However, the fact that no surface protein has been identified which is unique to human DCs makes it difficult to characterize these cells based on marker expression alone. Therefore, additional experiments were performed to determine whether the Transwell-derived APCs possessed the functional attributes of DCs that are important for the induction of specific T cell responses. For instance, the capacity of APCs to ingest fluorescent latex beads or zymosan (yeast) particles was used to gauge their phagocytic activity, which is critical for processing and MHC presentation of exogenous

proteins [23, 24]. The results of Fig. 6 demonstrate that Transwell-derived APCs were capable of acquiring both materials, though the zymosan particles were engulfed with much greater efficiency than the 1 μm latex beads (Fig. 6, thin lines). Although both materials are captured via mannose receptors, it is possible that the increased efficiency of yeast particle uptake by the Transwell-derived cells was mediated by additional receptors, such as TLR2 [25]. The addition of cytochalasin D, an inhibitor of energy-dependent phagocytosis, yielded a partial reduction in the uptake of both materials by the Transwell-derived APCs (Fig. 6, thick line). Therefore, it appeared that the particles were ingested by an active mechanism.

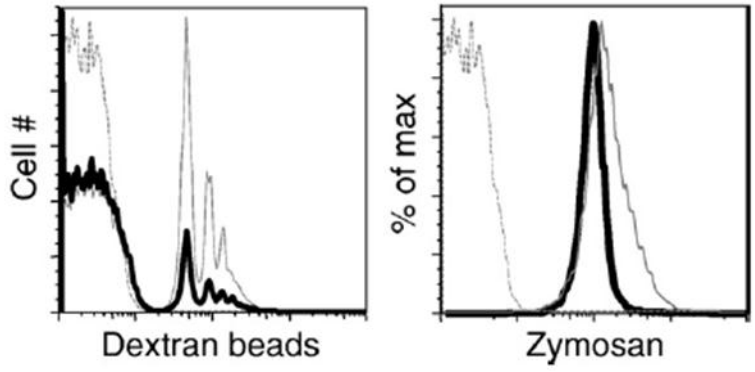

Figure 6. Transmigrated APCs have phagocytic activity.

The non-adherent transmigrated APCs were harvested from Transwells and incubated with FITC-labeled dextran beads (1 μm) or zymosan particles, in the absence (thin line) or presence (thick line) of 20 μg/ml cytochalasin D, for 24 h. The cells were analyzed by flow cytometry in the presence of trypan blue, which quenches any extracellular FITC fluorescence. This ensures that the only signal detected originates from material within the cell. The frequency of zymosanpositive cells was nearly 100%, while ~30% of the APCs acquired latex beads.

Transmigrated APCs Respond to DC Maturation Stimuli

Another hallmark feature of DCs is their ability to respond to various inflammatory stimuli by altering their expression of molecules associated with antigen presentation and T cell stimulation. To

assess the maturation potential of Transwell derived APCs, migrated non-adherent cells harvested from the lower chamber were stimulated for 24 h with TNFα and analyzed by flow cytometry for changes in their surface marker profile (Fig. 7). Markers associated with antigen uptake, such as the low affinity Fc receptor, CD32, decreased on activated DC, while others, such as CD40, CD80 and CD86, that serve critical costimulatory functions for the induction of adaptive immunity, were elevated on the TNFα-treated cells. The fact that MHC class II (HLA-DR) and CD14 were unaffected by the maturation stimuli further highlights the unique phenotype of Transwell-derived APCs since cytokine-derived DCs in vitro typically experience increased MHC class II and decreased CD14 expression following stimulation (data not shown). Importantly, the loss of CD14 is not a defining characteristic of DCs in vivo, as its expression can be variable depending on the differentiation state and anatomical location of the DC population being evaluated [26, 27].

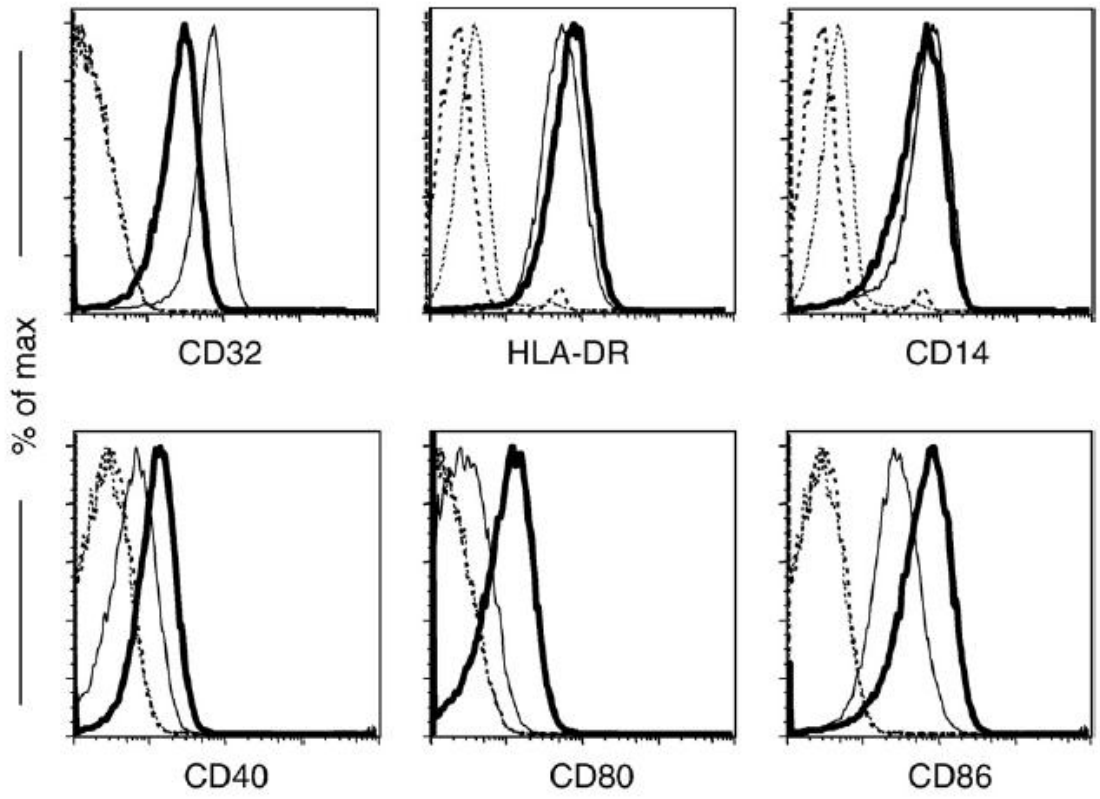

Figure 7. Transmigrated APCs respond to maturation stimuli (heavy line) as compared to mock (thin line) or isotype control (broken line).

Two days after PBMC application to the Transwells, the transmigrated cells were harvested and incubated for an additional 48 h in the absence or presence of TNFα. Thereafter, the cells were incubated with the antibodies specific for the indicated markers and analyzed by flow cytometry. Thin solid lines = non-matured cells; Thick solid line = matured cells; dotted lines = isotype controls. All analysis plots include only gated monocytes.

Transmigrated DCs induce specific T cell responses against recall and primary antigens

The critical feature that distinguishes DCs from other APC populations is their ability to stimulate naive antigen-specific T cell responses in vivo and in vitro. Therefore, transendothelial-migrated APCs from the Transwell device were evaluated for their ability to induce autologous $CD4^+$ T cell responses against primary and recall antigens. For this purpose, Transwell-derived APCs were pulsed overnight

with 1 μg/ml soluble antigen, matured for 24 h with TNFα, and then cultured for 12 days with autologous T cells in a serum-free media (X-VIVO 15) that is optimized for the culture of lymphocytes. The cultured T cells were evaluated for antigen specificity by the production of cytokines and upregulation of CD40L/CD154 following a short-term (7-h) restimulation with autologous cytokine-derived DCs that had been pulsed with antigen and matured with TNFα, as described above [28, 29]. Controls in these assay included stimulator and target DCs that had been loaded with an irrelevant protein or no antigen at all. The quality of the Transwell-derived DCs as stimulators of T cell responses was gauged against traditional cytokine-derived DCs prepared from the same donor. As well, the role of HUVEC in promoting the differentiation of monocytes into functional DCs was assessed by including APCs that had transmigrated through a PC membrane lacking a HUVEC monolayer.

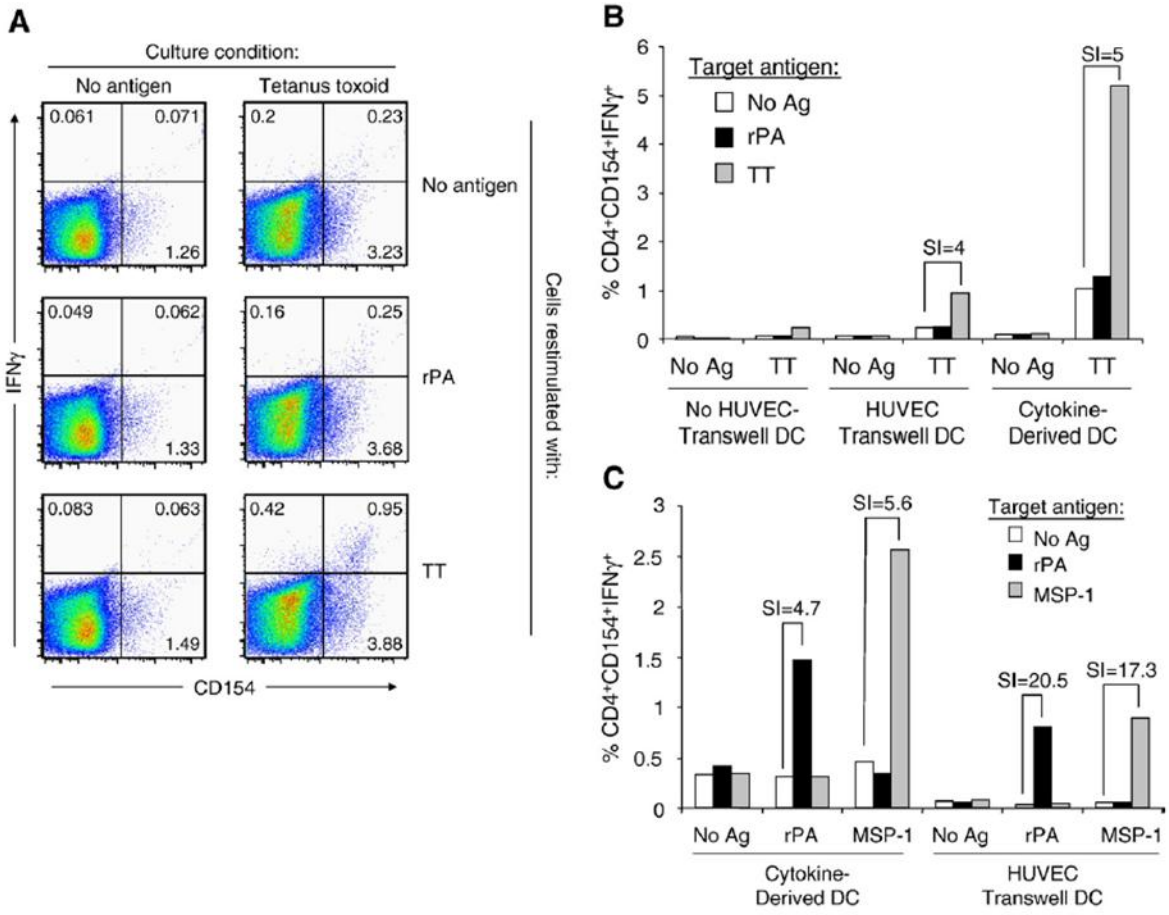

Figure 8. Transwell-derived APCs are potent stimulators of recall and naive T cell responses.

Transwell- or cytokine-derived APCs were pulsed overnight with antigen, as indicated, and then cultured with autologous T cells at a ratio of 1/60 for 12 days. Thereafter, the cultured cells were restimulated with autologous antigen-pulsed cytokine-derived DCs (at a 1/4 ratio to the T cells) for 7–8 h and then assayed for cytokine production and CD154 upregulation by intracellular staining. Unpulsed DCs, or those pulsed with irrelevant antigen, were included as negative controls. (A) Dot plots showing representative staining patterns of CD154 and IFNγ on CD4- gated lymphocytes specific for the recall antigen, TT. The capacity of Transwell (HUVEC and non-HUVEC) and cytokine-derived DC to stimulate recall TT (B) or naïve rPA and MSP-1 (C) T cell responses were evaluated.

Since the signaling requirements of memory antigen specific T cells are not as stringent as primary (naïve) lymphocytes, we first evaluated the capacity of Transwell derived DCs to stimulate a tetanus toxoid (TT)-specific recall response in $CD4^+$ T cells from a donor with a high TT sero titer (180

μg/ml). The results of Fig. 8A clearly demonstrate the ability of HUVEC-positive Transwell-derived DCs to promote the expansion of memory TT-specific T helper cells since 12 day-cultured lymphocytes were capable of eliciting effector function (upregulation of CD154 and expression of IFNγ) following a 7-h restimulation with TT-pulsed targets. The specificity of the lymphocytes is highlighted by the fact that target DCs pulsed with TT, but not those pulsed with a control protein, elicited IFNγ and CD154 expression by 0.95% of the $CD4^+$ T cells in cultures stimulated with antigen for 12 days. T cells cultured for 12 days in the absence of antigen were unable to elicit a TT-specific response when stimulated with antigen-pulsed target DCs for 7 h (Fig. 8A). A comparison of the capacity of different DC populations to induce TT-specific $CD4^+CD154^+IFN\gamma^+$ effector cells is shown graphically in Fig. 8B. The importance of HUVECs in promoting the differentiation of monocytes into functional DCs is underscored by the lack of expansion of antigen-specific T cells in cultures containing APCs that traversed a Transwell in the absence of endothelial cells (Fig. 8B). The increased T cellstimulatory capacity of transendothelial-migrated monocytes, as compared to monocytes that transmigrated the PC membrane in the absence of HUVEC,may be related to the increased expression of costimulatory ligands, such as CD40 and CD86, on the Transwell-derived APCs (Fig. 4B). The cytokine-derived DCs were more potent stimulators of antigen-specific T cell activity than either population of Transwell-derived DCs, though it appeared there was a concomitant increase in background (non-antigen-specific) T cell activity in cultures containing this APC population. As a result, the fold-increase in antigen-specific response over background (standard index, SI) was quite similar between cytokine-derived and Transwell-derived DCs (approximately 5-fold vs. 4-fold, respectively). While a single DC/T ratio was used for this comparison experiment, other assays assessing recall T cell responses using Transwell-derived and cytokine-derived DC stimulators over a range of DC/T cell ratios (1/30,1/60 and 1/120) failed to show a marked distinction between the two APC populations (data not shown). Having documented the ability of Transwell-

derived APCs to stimulate recall T cell responses, we next sought to determine whether these cells were capable of generating competent T cell effectors from fully naïve precursors. For this study, we chose as model antigens the malarial protein, MSP-1, and recombinant PA from B. anthracis. DCs were pulsed with antigen and cultures were established for 12 days using protocols described above. The cytokine-derived DCs were capable of inducing an rPA-specific T helper cell population that represented about 1.5% of the total pool, while the MSP-1-specific response peaked at approximately 2.5%. Although the Transwell-derived APCs stimulated a smaller-magnitude T cell response (just under 1% for both MSP-1 and rPA), the background $CD4^+$ T cell effector activity in these cultures was notably lower than observed in parallel cultures containing cytokine-derived DCs. For this reason, the SI in Transwell-DC cultures was about 3–5-fold higher than in cytokine-derived DC wells. This result was not surprising given that similar observations were made in experiments shown in Fig. 8B.

Discussion

There has been tremendous interest in developing a better understanding of the biology of DCs because of their specialized role in orchestrating primary cellular and humoral immune responses. The paucity of DCs in the body, combined with the limited availability of tissue samples from humans, make it difficult to evaluate these cells ex vivo. The study of cytokine-derived DCs, i.e., purified blood monocytes that have been cultured in exogenous growth factors (GM-CSF and IL-4), has contributed greatly to our understanding of this unique cell population and provided a source of APCs for clinical applications. The utility of cytokine-derived DCs is limited, however, because this culture method fails to replicate the physiology involved in the development of DCs from circulating monocytes in the body. As well, some researchers suggest that this DC population lacks full functionality and may not accurately represent the

varied DC populations found under physiologic conditions [16, 17, 30, 31]. We report in this study a convenient Transwell-based method that utilizes endothelial cells to drive the development of DCs in 2 days, in the absence of any exogenous growth factors and without the pre-selection of monocytes from bulk PBMCs. This technique, which loosely replicates the process of blood monocyte extravasation through vessel walls, allows for the generation of a highly purified APC population that resemble classical DCs in morphology, phenotype and function. While others have developed tissue constructs to generate human in vitro DCs in a similar manner [5, 6, 12-14], this protocol is unique in its simplicity. It requires no 3-dimensional support matrix for the culture of endothelial cells, as has been done previously, and unlike other methods, is amenable to the use of fast-growing endothelial cell lines that are advantageous because of their consistency and rapid growth rates. Regarding this last point, the use of the long-term endothelial cell line, EA.hy926 [32], which was a generous gift of Cora-Jean Edgell (University of North Carolina at Chapel Hill, Chapel Hill, NC), in the Transwell system generated DCs that were comparable in phenotype and function to APCs derived from cultures containing primary endothelial cells (data not shown). Finally, the use of a Transwell device ensures that the HUVEC monolayer cultured in the upper chamber, which is allogeneic to the donor PBMC applied to the system, is segregated from the transmigrated APCs in the lower chamber. This is important when the APCs are used in subsequent assays to stimulate autologous lymphocytes. Circulating monocytes that traverse the vasculature into tissues can differentiate into either DCs or macrophages [21, 22]. Likewise, the collagen-based construct described in earlier reports also supports the differentiation of blood monocytes into both cell types; cells that reverse-transmigrate out of subendothelial collagen resemble immature DCs whereas those that remain in the matrix appear to be macrophages [6, 12, 13]. The geometry of the Transwell device is such that both monocytes-derived populations are collected in the lower chamber. Conveniently, the non-adherent/loosely adherent DCs are readily isolated from the

strongly adherent macrophages by gently washing the wells with warm media. A key role for endothelial cells in promoting the differentiation of monocytes into DCs in this Transwell based system was highlighted by the finding that cells which had transmigrated through a PC membrane in the presence of HUVECs were markedly better at stimulating antigen-specific T cell responses than monocytes that had traversed a PC membrane in the absence of endothelial cells. These results are consistent with a previous observation that monocytes having contacted HUVECs were more adept than un-manipulated monocytes at stimulating T cell activity [12, 13, 15]. Past studies have suggested that the differentiation program is driven by direct cell:cell contact between the endothelial cells and monocytes, though the specific interactions mediating this differentiation program remain undefined. While some previous studies suggest that endothelial cells are not sufficient to promote APC function in blood monocytes, the disparity between our results and those of past reports are likely explained by differences in the model systems. For instance, Seguin et al. (2003) observed that monocytes transmigrating through an endothelial cell layer on a porous membrane were actually worse than non-migrated monocytes in regards to APC functionality, but these results were obtained with brain derived endothelial cells rather than the HUVECs used in our experiments [33].

Because DCs are a heterogeneous population, with phenotypes that are reflective of the tissue micro-environment in which they are found, it has thus far been difficult to identify a single phenotypic marker that is common to all DC populations [34, 35]. For this reason, it is critical to use several criteria to accurately discriminate DCs from other cell types. The non-adherent APCs harvested from the Transwell system had many of the functional attributes of DCs derived from other in vivo and in vitro sources. For instance, the cells had long processes, or dendrites, extending from the cell body that have been shown to aid antigen presentation by increasing the surface area of the cell [36]. As well, they efficiently acquired antigen, as demonstrated by their ability to phagocytose latex beads and yeast

particles, and were capable of triggering functional T cell responses against recall and primary antigens. This latter feature of the Transwell-derived APCs provides the most compelling argument that these cells are indeed DCs since no other APC population is thought to be capable of stimulating the proliferation and differentiation of naïve T cells into competent effectors [1, 2, 37]. While the Transwell-derived APCs had all the functional traits of DCs, they expressed a unique surface profile that differed from other in vitro DC populations. Cytokine-derived human DCs, i.e., those generated from monocytes that have been cultured in GM-CSF and IL-4, are usually negative for the monocyte marker, CD14, and positive for the DC marker, CD1a [38]. In contrast, the Transwell-derived DCs had a marker profile that included the expression of CD14 and a lack of CD1a. These opposing results might be explained simply by differences in culture conditions specific to each method. For example, the lack of CD1a on Transwell-derived APCs is not unexpected since it has previously been demonstrated in our laboratory that DCs derived in serum-free culture media containing GM-CSF and IL-4 also lack expression of this particular surface protein (data not shown). As well, we and others have shown that human serum is similarly unable to promote CD1a expression on human monocytes-derived DCs in culture [39]. We would anticipate that APCs derived from Transwells containing fetal bovine serum would express CD1a since this culture condition supports CD1a expression on other cultured human DC populations. If compared solely against cytokine-derived DCs, the retention of CD14 on Transwell-derived APCs might suggest that these cells have not fully differentiated into DCs. However, these results are consistent with other reports suggesting that monocytes triggered to differentiate into DCs via contact with endothelial cells do not lose CD14 expression [13, 40]. In fact, Li et al. (2003) demonstrated that endothelial cells may actively promote the expression of CD14 on these cells, since monocytes cultured on plate-bound P selectin (an endothelial cell ligand), in addition to IL-4 and GMCSF, gave rise to DCs that retained CD14 [40]. Finally, $CD14^{+}$ DC populations have been identified in vivo [41]. The flexibility of the Transwell system makes

itwell-suited to address the effect of different endothelial cell types on monocyte migration and the resultant DC populations. While the system described here relied on the use of HUVECs to drive the differentiation of monocytes into DC, the use of other endothelial cell populations within the Transwell system might preferentially drive the differentiation of monocytes into other tissue-specific DC subpopulations. For instance, a previous report showed that intestinal epithelial cells cultured in a Transwell bucket gave rise to a unique DC population that lacked costimulatory and MHC class II molecules and were poor stimulators of T cell responses. This in vitro population resembled tolerogenic DCs found in the intestinal mucosa in vivo [42]. As noted earlier, monocytes having migrated through Transwells containing brain endothelial cells had lower functionality than non-migrated monocytes [33], a result that contrasted our finding with Transwells containing HUVEC. The modular design of the Transwell device allows for multiple configurations that would permit a greater dissection of the DC development/differentiation pathways in vivo. For instance, transmigrated APCs harvested from a Transwell could be passed through a second Transwell chamber containing a monolayer of lymphatic cells, a process that might more closely recapitulate the migration of matured/activated tissue-resident DCs through the lymphatics in vivo. Additional cell types that might be necessary to promote the differentiation or function of DCs could also be introduced into the system. For example, fibroblasts contained in the lower chamber of the Transwell device could serve as a source of inflammatory signals and act as an antigen depot during the application of certain adjuvants or pathogens. In summary, we have described a novel and convenient approach for generating large numbers of highly purified human DCs from blood monocytes. Using a flexible and well characterized Transwell device as a support structure for the culture of endothelial cells and transmigration of monocytes through this confluent monolayer, a population of nonadherent APCs was generated that resemble other in vitro DC populations in phenotype and function. The use of a transformed endothelial cell line, or pre-expanded

primary HUVEC, to promote the development of DCs vastly improved the cost-effectiveness and practicality of this approach. This method provides a simple means to generating human DCs in a manner that more closely mimics their development in vivo, and thus could provide new insight into the biology of this unique immune cell population.

Acknowlegments

I am grateful to Dr. Cora-Jean Edgell for providing the EA.hy926 cell line and Dr. Conan Li and David Moe for providing excellent scientific and technical advice and support. I appreciate the generosity of Dr. E. Angov, at the Walter Reed Army Institute of Research, for supplying MSP-1 protein. This work was funded by the DARPA/Defense Sciences Office RVA Phase II Program.

CHAPTER TWO: COUPLING SENSITIVE *IN VITRO* AND *IN SILICO* TECHNIQUES TO ASSESS CROSS-REACTIVE CD4$^+$ T CELLS AGAINST THE SWINE-ORIGIN H1N1 INFLUENZA VIRUS

Abridgment

Having developed a reasonable approach for investigating DCs and innate immunity, we extended the utility of the system using a DC-based approach to investigate adaptive immune responses. Here, we interrogated immunodominate peptides conserved between the seasonal influenza virus HA protein and the novel H1N1 pandemic strain as immunogens capable of driving a multifunctional immune response using the DC-based approach. The overall sweeping goal of this approach was to identify novel immunogens capable of eliciting antigen-specific immunity for their potential use as targets for influenza vaccine development, replacing costly and time consuming traditional methods.

The outbreak of the novel swine-origin H1N1 influenza in the spring of 2009 took epidemiologists, immunologists, and vaccinologists by surprise and galvanized a massive worldwide effort to produce millions of vaccine doses to protect against this single virus strain. Of particular concern was the apparent lack of pre-existing antibody capable of eliciting cross-protective immunity against this novel virus, which fueled fears this strain would trigger a particularly far-reaching and lethal pandemic. Given that disease caused by the swine-origin virus was far less severe than expected, we hypothesized cellular immunity to cross-conserved T cell epitopes might have played a significant role in protecting against the pandemic H1N1 in the absence of cross-reactive humoral immunity. In a published study, we used an immunoinformatics approach to predict a number of CD4$^+$ T cell epitopes are conserved between the 2008-2009 seasonal H1N1 vaccine strain and pandemic H1N1

(A/California/04/2009) hemagglutinin proteins. Here, we provide results from biological studies using PBMCs from human donors not exposed to the pandemic virus to demonstrate that pre-existing $CD4^+$ T cells can elicit cross-reactive effector responses against the pandemic H1N1 virus. As well, we show our computational tools were 80-90% accurate in predicting $CD4^+$ T cell epitopes and their HLA-DRB1-dependent response profiles in donors that were chosen at random for HLA haplotype. Combined, these results confirm the power of coupling immunoinformatics to define broadly reactive $CD4^+$ T cell epitopes with highly sensitive in vitro biological assays to verify these in silico predictions as a means to understand human cellular immunity, including cross-protective responses, and to define $CD4^+$ T cell epitopes for potential vaccination efforts against future influenza viruses and other pathogens.

Introduction

The recent pandemic swine-origin influenza A virus (S-OIV1; H1N1) presented a major worldwide public health threat during the 2009/2010 influenza season. Fears over this unique virus were fueled, in part, by its strong propensity to replicate and cause more severe disease in naïve laboratory animals than other seasonal H1N1 viruses [43]. Additionally, scientists predicted herd immunity would provide minimal protection against the S-OIV because its envelope hemagglutinin (HA) and neuraminidase proteins, which are the primary targets of influenza-specific antibody, were derived from a classical swine lineage that evolved pronounced antigenic variations following its split from the human seasonal H1N1 viruses during the 1918 pandemic [44-46]. This supposition was confirmed by a series of studies showing most individuals (those under 60 years of age) lack pre-existing cross-protective humoral immunity against the S-OIV and vaccination with the 2008/2009 seasonal trivalent

influenza vaccine (TIV) rarely elicited neutralizing antibody responses against this unique H1N1 virus [45, 47].

Despite research studies suggesting the S-OIV is highly pathogenic in laboratory animals and shares few B cell epitopes with most seasonal H1N1 viruses [48], it triggered only mild symptoms in many patients and failed to evolve into a major global pandemic [49]. A potential explanation for this unexpected observation was that pre-existing (memory) influenza-specific T cells generated cross-reactive effector responses against the S-OIV capable of limiting disease severity and virus spread in individuals lacking pre-existing cross-protective antibody. A recent study in support of this theory showed ferrets immunized with the seasonal trivalent influenza vaccine (TIV) were protected from S-OIV-induced disease, but lacked sterilizing immunity against this novel virus [50]. This claim was further substantiated by an *in silico* evaluation and meta-analyses performed by our group [51] and Greenbaum et al. [48], respectively, demonstrating the pandemic and seasonal H1N1 viruses share highly conserved T cell epitopes.

While our computational tools provided strong evidence for the existence of shared T cell epitopes between the S-OIV and seasonal H1N1 strains, we sought a practical (biological) assessment of these predictions. This was accomplished in the current study by using a highly sensitive in vitro DC-based $CD4^+$ T cell culture assay developed at sanofi pasteur – VaxDesign campus [52, 53] to examine the capacity of human influenza-specific T helper cells from donors not previously exposed to S-OIV to generate cross-reactive effector responses against these immunogens. Though our published *in silico* study provided a comprehensive evaluation of potentially cross-reactive H1N1 $CD4^+$ and $CD8^+$ T cell epitopes derived from both the influenza HA and NA proteins, we specifically focused the current evaluation on $CD4^+$ T cells against the HA protein of the virus since we were interested in understanding whether vaccination with the seasonal TIV (comprised principally of the HA protein and poorly able to

elicit $CD8^+$ T cells) might be capable of generating cross-reactive $CD4^+$ T cell responses against the S-OIV. As such, the target epitopes chosen for the biological evaluation included a series of synthetic HA peptides that are highly conserved between the pandemic H1N1 virus, A/California/07/2009, and the 2009/2010 seasonal H1N1 vaccine strain, A/Brisbane/59/2007, and were predicted by us to generate strong T cell responses by binding promiscuously to eight HLA-DRB1 alleles that cover 99% of the population [51, 54].

Using this approach, we readily generated effector T helper cells against ten HA epitopes that are highly conserved between S-OIV and other H1N1 viruses. Furthermore, we demonstrated the EpiMatrix T cell epitope algorithm was 80-90% accurate in predicting $CD4^+$ T cell epitopes and their HLA-DRB1-dependent response profiles in donors that were chosen at random for HLA haplotype. As a whole, these results strongly support the hypothesis that pre-existing, cross-reactive $CD4^+$ T cell immunity limited the spread and severity of disease resulting from the S-OIV pandemic. As well, this study highlights the utility of coupling robust in vitro immunoassays with computational techniques to better understand human immunity, including cross-protective responses, and to define $CD4^+$ T cell epitopes for potential vaccination efforts against future influenza viruses and other pathogens.

Materials and Methods

Human Donors and PBMC Isolations

PBMCs used in the assays were acquired from normal healthy donors who provided informed consent and were enrolled in a sanofi pasteur – VaxDesign Campus apheresis study program (protocol CRRI 0906009). Blood collections were performed at Florida's Blood Centers (Orlando, FL) using

standard techniques approved by their institutional review board. Within hours following their harvest from the donor, the enriched leukocytes were centrifuged over a ficoll-paque PLUS (GE Healthcare, Piscataway, NJ) density gradient [52, 53]. PBMCs at the interface were collected, washed, and cryopreserved in IMDM media (Lonza, Walkersville, MD) containing autologous serum and DMSO (Sigma-Aldrich, St. Louis, MO). All PBMCs used in this assay were collected from subjects in our donor program prior to the outbreak of the S-OIV in Florida in May of 2009. The ages of the donors (in years) follows: 1142 (25), 1010 (21), 940 (25), 923 (25), 720 (46), 548 (23), 208 (39), and 182 (40).

Peptides and Reagents

Synthetic peptides matching sequences of the HA protein from S-OIV were generated by BioSynthesis, Inc. (Lewisville, TX) to a purity of at least 95%. (The sequences can be found in Table 3.) The tetanus toxoid P30 peptide (TT947-967; FNNFTVSFWLRVPKVSASHLE) was synthesized by Elim Biopharmaceuticals (Hayward, CA) to a purity of at least 95%. The influenza A/Brisbane/59/2007 (H1N1) hemagglutinin (Brisbane HA) protein and influenza A/California/07/2009 (H1N1) hemagglutinin (California HA) protein were purchased from Protein Sciences (Meriden, CT). The Fluvirin 2008-2009 TIV and influenza A H1N1 2009/2010 monovalent S-OIV vaccine were procured from Novartis International AG (Basel, Switzerland).

Generation of Cytokine-Derived Dendritic Cells

Dendritic cells (DCs) were prepared using our published methodology [52]. Briefly, monocytes were purified from total PBMCs by positive magnetic bead selection (Miltenyi Biotec, Cologne,

Germany), cultured for 7 days in X-VIVO 15 (Lonza) serum-free media supplemented with GM-CSF (R&D Systems, Minneapolis, MN) and IL-4 (R & D Systems), and then harvested for assay usage. In all assay conditions described below where vaccines or purified proteins were used as antigens, the DCs were pulsed for at least 2 hrs with the immunogen and washed prior to being used in the assay. In cases where synthetic peptides were used to stimulate T cell responses, the epitopes were added directly to the assay wells (the DCs were not pre-pulsed).

IFNγ ELISPOT

$CD4^+$ T cells were enriched from frozen PBMCs by negative magnetic bead selection (Miltenyi Biotec) and cocultured with autologous DCs at a 10:1 ratio in 96-Well Multiscreen HTS plates (Millipore, Billerica, MA) that had been pre-coated with anti-human IFNγ Ab (BD Pharmingen). As noted above, some DCs were pre-treated with a 1:500 dilution of the 2008/2009 seasonal TIV (which contained the Brisbane H1N1 virus) or S-OIV vaccine formulation or 1.8 µg/ml Brisbane HA or California HA proteins. Otherwise, the DCs were added to the T cells in the presence of 1.0 µg/ml pooled or individual S-OIV HA peptides or the negative control tetanus (TT947-967) epitope. After a 24-hr coculture, the plates were processed using the IFNγ ELISPOT kit (BD Pharmingen) and quantified by colorimetric evaluation using hardware and software analysis from AID EliSpot (Strassberg, Germany).

$CD4^+$ T cell Stimulation Assay

$CD4^+$ T cell stimulation assays were performed using protocols established at sanofi pasteur – VaxDesign Campus [52, 53]. Briefly, autologous $CD4^+$ T cells were enriched from frozen PBMCs by

negative magnetic bead selection (Miltenyi Biotec) and then co-cultured with autologous DCs that either had been untouched (control wells) or pre-pulsed for at least 2 hrs with 1.8 μg/ml Brisbane HA protein. After a 12-day incubation period, the lymphocytes were harvested and evaluated for effector activity in an intracellular cytokine staining assay (ICCS) where fresh autologous DCs served as APCs. For the readout/ICCS assay, the DCs were pre-pulsed with the Brisbane HA protein or cultured with the T cells directly in the presence of 1 μg/ml synthetic peptide. The T cells and target DCs were co-cultured for 7 h; 1 μg/ml brefeldin A (Sigma-Aldrich) was added to the wells during the final 5 h of culture to prevent protein egress from the Golgi apparatus. Following the incubation period, the cells were labeled with the Live/Dead Fixable Stain Kit (Invitrogen, Carlsbad, CA), treated with cytofix/cytoperm and perm/wash reagents from BD Biosciences (San Jose, CA), and then labeled with eBioscience (San Diego, CA) antibodies specific for human CD4 (SK3), IFNγ (B27), and CD154 (TRAP1). The samples were acquired on an LSRII flow cytometer (BD Biosciences) and analyzed using FlowJo software (Tree Star, Ashland, OR).

Immunoinformatics Analyses

EpiMatrix, a T-cell epitope mapping algorithm developed by EpiVax, screens protein sequences for 9–10 amino acid peptide segments predicted to bind to one or more MHC alleles [55, 56]. EpiMatrix uses the pocket profile method, which was first described by Sturniolo and Hammer [57], to make these predictions. For reasons of efficiency and simplicity, the predictions are limited to the eight most common HLA-DRB1 class II alleles [58]. Raw EpiMatrix values are normalized with respect to a score distribution derived from a large set of randomly generated peptide sequences. Any peptide/MHC allele scoring above 1.64 on the EpiMatrix "Z" scale (the top ~5% of the distribution of a random peptide set) has a significant chance of binding to the MHC molecule for which it was predicted; peptides scoring

above 2.32 on the scale (the top ~1%) are extremely likely to bind. The scores of most well-known T cell epitopes fall within this range [51, 58]. After screening for putative MHC class II epitopes, we used the ClustiMer algorithm to identify protein segments with high T cell epitope density. 93% of these epitope predictions have proven to be accurate in prospective biological evaluations [51, 58, 59].

Individualized T cell Epitope Measure (iTEM)

The iTEM, or individualized T cell epitope measure, predicts how individuals will respond to specific T cell epitopes. Our original method for calculating iTEM scores was published and validated [60]; here, we used an improved algorithm, which produces even better predictions of subject-specific immune responses, to predict S-OIV HA epitope immunogenicity. Briefly, an iTEM score is generated by first evaluating a peptide for predicted binding to a subject's HLA-DRB1 alleles using the EpiMatrix system (see above). Combining the EpiMatrix scores for each peptide-HLA-DRB1 allelic combination in the haplotype yields an iTEM score for a particular individual. This is achieved by ranking EpiMatrix scores for each allele by magnitude: the highest 9-mer score is weighted 100% and each subsequent positive score for the same allele is underweighted by a factor of 1/n, where n is the rank. This discount factor addresses the fact that a given HLA class II molecule's ability to bind only one 9-mer peptide at a time, which results in lower-affinity peptides occupying a given peptide binding groove for comparatively less time than higher-affinity peptides.

In a series of retrospective studies completed during the development of the iTEM formula, a value of 2.06 gave the best balance between sensitivity and specificity [60]; as such, iTEM responses of 2.06 or higher in the current study were considered positive. The iTEM scores calculated for each of the peptide-HLA-DRB1 pairs were then compared to the in vitro T cell assay results generated using

methods described above. (Specific $CD4^+$ T cell responses 2-fold greater than the background (no antigen) condition were considered responsive in the in vitro stimulation assay.) Based on this evaluation, the peptide-HLA pairs were divided into one of four categories (true positives, true negatives, false positives, and false negatives). In this context, true-positive peptides were predicted and in vitro-validated as immunogenic, while true-negative peptides were predicted and biologically validated to be non-immunogenic. False-negative peptides were predicted to be non-immunogenic, yet produced a positive response; false-positive peptides were predicted to be immunogenic but produced no response in the in vitro T cell assay.

Results

In an effort to better understand whether pre-existing cellular immunity might have generated protective responses against the S-OIV, we examined the capacity of human influenza-specific T helper cells to elicit cross-reactive effector responses against highly conserved epitopes from this novel virus. We specifically chose for this evaluation frozen PBMCs from our stock that had been collected from eight subjects prior to the emergence of the S-OIV in Florida in May of 2009 to try to eliminate the possibility they had been exposed to this virus. The T cell epitopes chosen for this study met two criteria: First, they contained one or more MHC class II-restricted core epitopes that are highly conserved between the S-OIV and Brisbane H1N1 viruses and were predicted to bind strongly to HLA-DRB1 molecules [51]. Second, they share sequence homology with $CD4^+$ T cell epitopes identified in various seasonal influenza H1N1 viruses [48, 51]. This evaluation also included one additional published MHC class II peptide, HA359-376, that is cross-conserved between the pandemic and seasonal H1N1 viruses [48], but was not predicted by us to contain any core HLA-DRB1-restricted epitopes [51]. The

sequences and corresponding promiscuous core 9-mer MHC class II-binding sequences are shown in Table 3.

Table 3. A/California/07/2009 HA peptide sequences included in this evaluation.

A/California/07/2009 HA region	Peptide epitope sequence	Predicted HA HLA-DR epitopes[a]
36-53	VLEKNVTVTHSVNLLEDK	VTHSVNLLE
43-60	VTHSVNLLEDKHNGKLCK	VTHSVNLLE
113-132	IDYEELREQLSSVSSFERFE	LREQLSSVS
359-376	TGMVDGWYGYHHQNEQGS[b]	
394-411	NKVNSVIEKMNTQFTAVG	IEKMNTQFT
436-453	WTYNAELLVLLENERTLD	YNAELLVLL; LVLLENERT
441-460	ELLVLLENERTLDYHDSNVK	LVLLENERT
461-480	NLYEKVRSQLKNNAKEIGNG	YEKVRSQLK; VRSQLKNNA
527-549	LYQILAIYSTVASSLVLVVSLGA	ILAIYSTVA; IYSTVASSL; LVLVVSLGA
530-541	ILAIYSTVASSL	ILAIYSTVA; IYSTVASSL

[a] Lines are used to highlight core 9-mer regions within the peptides.

In an attempt to directly quantify the frequency of circulating influenza-specific $CD4^+$ T cells capable of cross-reacting against S-OIV in eight donors, we stimulated purified lymphocytes with DCs for 24 hr in an IFNγ ELISPOT assay. (The DCs were either pre-pulsed with purified protein or peptides were added directly to the assay well.) By design, this short 1-day antigen encounter is intended to trigger cytokine production by antigen-specific T cells without inducing any cell divisions that would otherwise alter the precursor frequency determination. Using the seasonal 2008/2009 seasonal TIV (Brisbane H1N1) as a benchmark in this analysis, we were not surprised to find the frequency of the responding T cell population varied by as much as 10-fold (20-200 TIV-specific $CD4^+$ T cells/600,000 total $CD4^+$ T cells)

since each donor's unique genetic background and immune history with influenza would impact the magnitude of the responding population (Figure 9). The S-OIV vaccine also generated a detectable $CD4^+$ T cell response in all but one donor, though in most cases this vaccine elicited a lower-magnitude response than the TIV. The purified Brisbane and S-OIV HA proteins elicited even weaker, but reasonably equivalent, $CD4^+$ T cell populations in only a subset of the donors (Figure 9). (This might reflect a strong potential for T cell cross-reactivity between the Brisbane and pandemic H1N1 viruses.) Taken as a whole, this hierarchy of responses is perhaps not surprising since the three-component (H3N2, influenza B, and seasonal H1N1) seasonal TIV offered a broader complement of antigens for T cell recognition than the single-component S-OIV prophylactic and the purified proteins lack the inflammatory potential of the formulated vaccines. Despite our observation of positive and detectable $CD4^+$ T cell responses in ELISPOT wells stimulated with vaccines and purified proteins, the T helper cell responses elicited by the single or pooled synthetic peptides were modest at best, with only two donors generating populations with measurable significance over the background (no antigen) control (Figure 9).

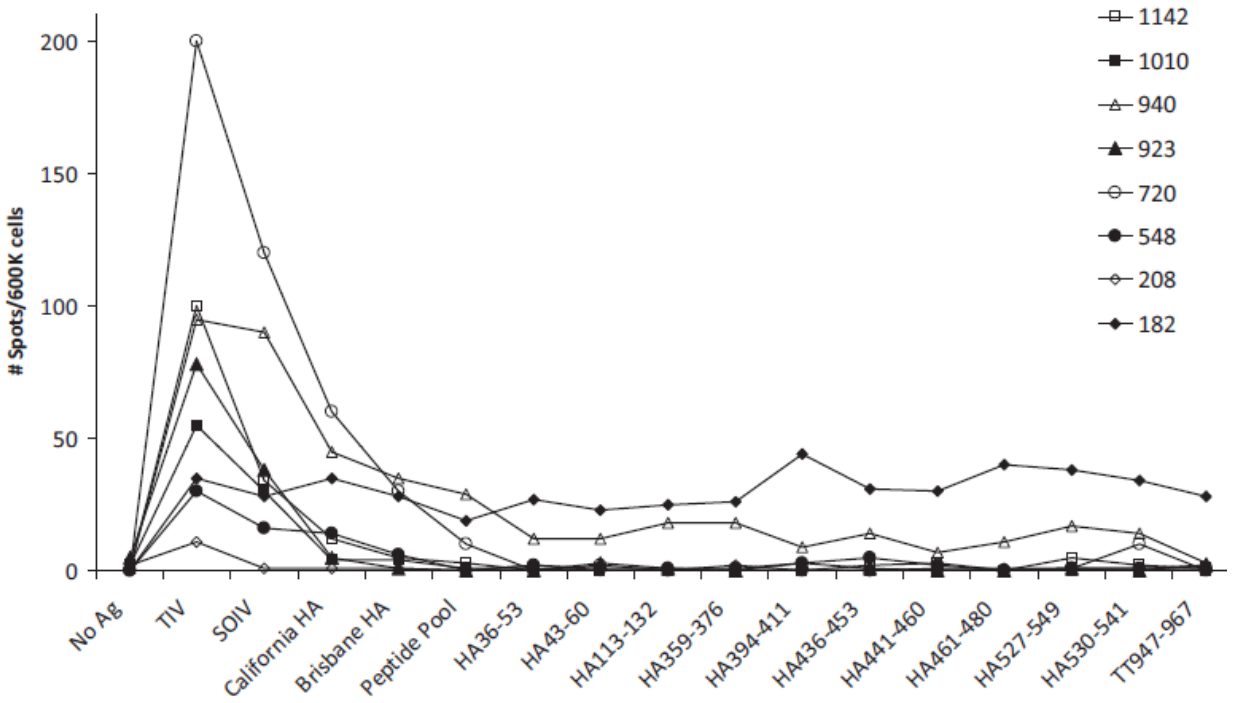

Figure 9. Demonstration of influenza-specific CD4$^+$ T cell cross-reactivity against the S-OIV.

CD4$^+$ T cells were isolated from frozen PBMCs and cultured with purified autologous DCs for24h.Where indicated, the DCs were left untouched or pulsed overnight with vaccine or protein. Peptides, individually or together as a pool, were added directly to the DC/T cell co-culture well. Thereafter, antigen-specific T cells were detected by IFNγ ELISPOT assay. Eight donors were included in this evaluation.

We believe the ELISPOT results described above provide compelling evidence that pre-existing influenza-specific CD4$^+$ T cells can generate cross-reactive T helper cell responses against the novel S-OIV. However, we were unable to use this approach to examine the fine specificity of the circulating T helper cells on a single-epitope basis because of the low frequency of influenza-specific CD4$^+$ T cells in PBMC samples evaluated directly ex vivo. To circumvent this issue, we performed a highly sensitive DC-based T cell coculture assay developed at sanofi pasteur – VaxDesign campus [52, 53] to amplify the influenza-specific population prior to evaluating the fine epitope specificities of the virus-specific lymphocytes. Briefly, purified CD4$^+$ T cells from the same eight donors described in Figure 9 were stimulated for 12 days with autologous DCs that had been pre-pulsed with the Brisbane HA protein.

(DCs not pulsed with the foreign protein served as a negative control.) Thereafter, the cultured T cells were harvested and evaluated for their potential to respond to the same HA protein or individual S-OIV HA peptide epitopes in a short-term (7-hr) ICCS assay. In this way, we could readily address whether the 2009/2010 seasonal TIV Brisbane H1N1 strain could amplify T helper cells against specific peptide epitopes derived from the S-OIV HA protein.

Focusing on donor 940 as a representative example of the datasets generated with this approach, we found the T helper cells from this subject were highly active against the Brisbane HA protein, eliciting a $CD4^{+}CD154^{+}IFN\gamma^{+}$ T cell population against the matched target that was more than 8-fold over background in the no-antigen control target (Figure 10). (Of note, we use the dual expression of CD154 and IFNγ as a stringent readout of antigen specificity in the ICCS assay.) Likewise, this donor also responded vigorously against several of the pandemic H1N1 peptides, but not a universal T cell epitope from tetanus toxoid (TT947-967), which served as a negative control in these experiments (Figure 10). This latter result indicates the in vitro proliferative response was specific to the influenza protein and not global/non-specific in nature.

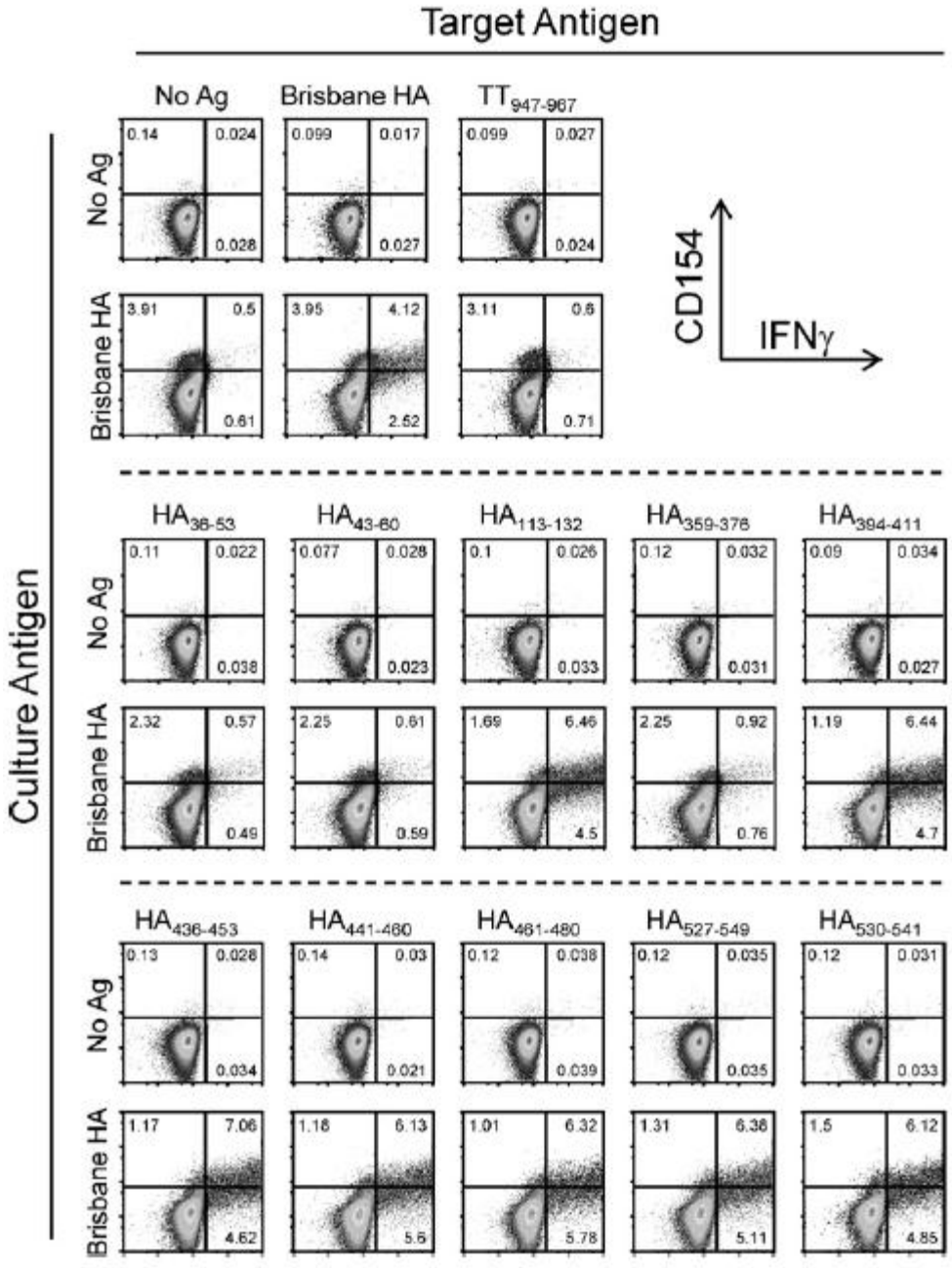

Figure 10. Demonstration of robust cross-reactive influenza-specific CD4$^+$ T cell effector responses against predicted S-OIV HA epitope sequences.

DCs were pulsed with Brisbane HA and then cultured with autologous CD4+ T cells. After 12 days, the cultures were harvested and restimulated with fresh autologous DCs that had, been pulsed overnight with Brisbane HA. Some assay wells were pulsed directly with S-OIV HA peptides or the negative control TT peptide, TT947–967. After 7h, the lymphocytes were evaluated by intracellular flow cytometry.

Table 4. Predicted binding of the S-OIV HA peptide sequences to particular HLA-DRB1 alleles.

A/California/07/2009		5% HLA-DR Binding Restriction							
HA region	Peptide epitope sequence	101	301	401	701	801	1101	1301	1501
36-53	VLEKNVTVTHSVNLLEDK		X	X		X		X	
43-60	VTHSVNLLEDKHNGKLCK		X	X		X		X	
113-132	IDYEELREQLSSVSSFERFE	X	X	X		X	X	X	X
359-376	TGMVDGWYGYHHQNEQGS								
394-411	NKVNSVIEKMNTQFTAVG	X		X	X		X		X
436-453	WTYNAEL*LVLLENERT*LD	X	X	X	X	X	X	X	X
441-460	ELLVLLENERTLDYHDSNVK	X		X	X	X	X		X
461-480	NLYEK*VRSQLKNNA*KEIGNG	X	X	X	X	X	X	X	X
527-549	LYQILA*IYSTVASSL*VLVVSLGA	X	X	X	X		X	X	X
530-541	ILA*IYSTVASSL*	X		X	X			X	X

[a] Whole-peptide binding predictions for HLA-DRB1 alleles are shown. Peptides are scored according to their potential to bind a particular allele. Scores in the top 5th percentile are marked with an X: a large X denotes binding of the peptide is enhanced by the core 9-mer binding peptides shown in Table 1; a small X indicates predicted binding without the contribution of a core 9-mer peptide.

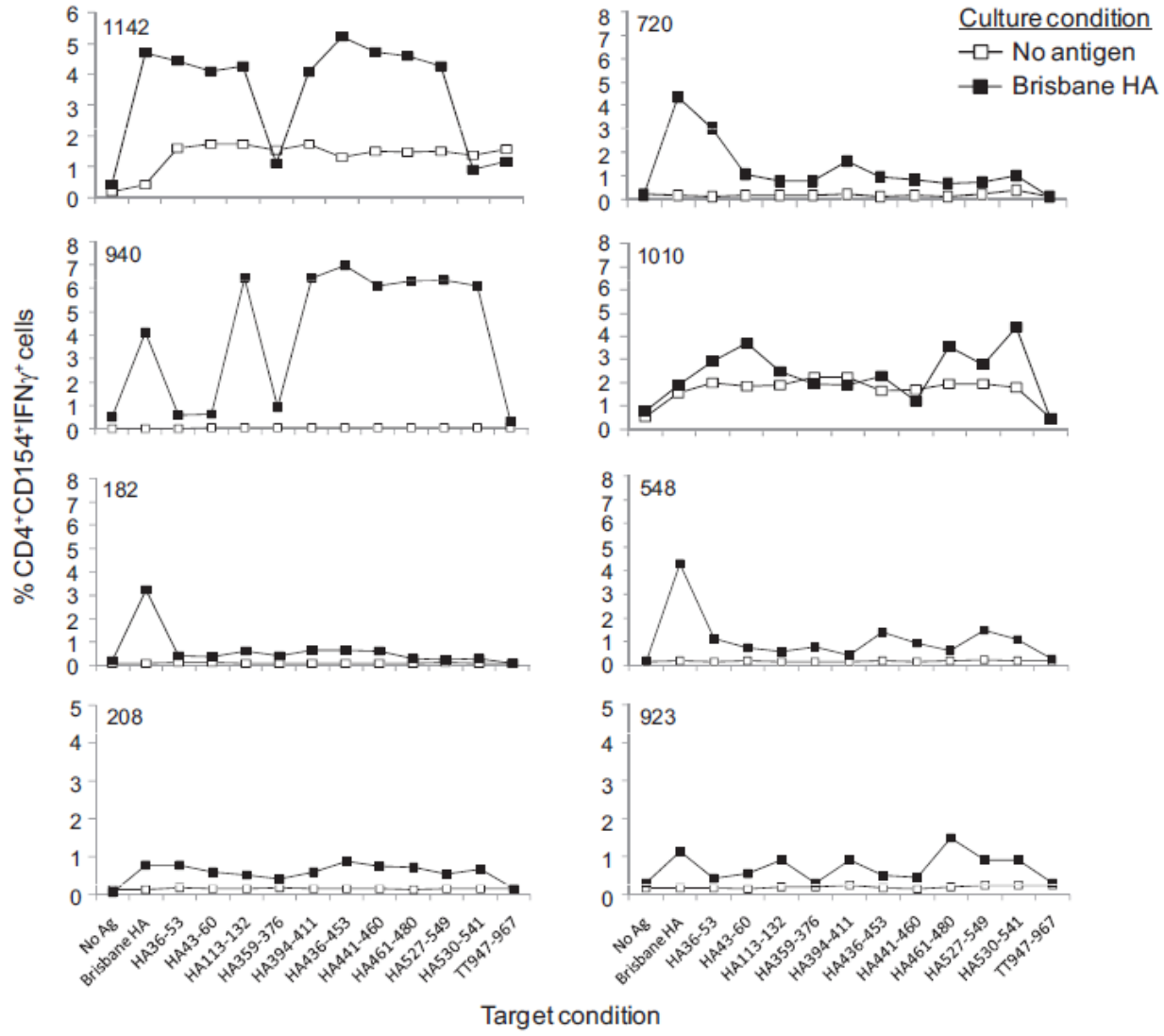

Figure 11. Highly conserved S-OIV HA peptides elicit strong CD4$^+$ T cell responses from donors not previously exposed to the pandemic H1N1 virus.

CD4$^+$ T cells and autologous DCs were co-cultured and assessed by ICCS using the method described in Fig. 10. The raw data, as generated in Fig. 10, was plotted as line graphs for all eight donors.

Extending this evaluation to include all eight donors, which are shown graphically in Figure 11, we found a considerable (up to 14-fold) increase in the frequency of Brisbane HA-specific CD4$^+$ T cells in the antigen-stimulated cultures (closed symbols) in seven out of eight donors, which clearly illustrates

the capacity of the lymphocytes to respond to specific antigen stimulation in the in vitro $CD4^+$ T cell assay. As well, the fact that the S-OIV HA peptides could be used to elicit strong T helper cell responses from cultures stimulated with the Brisbane HA protein suggest these highly conserved epitopes are generated during the natural processing of the full-length HA for MHC class II presentation since the whole protein was used as an antigen source in the original 12-day stimulation assay. Similar to what we showed for donor 940 (Figure 10), the universal tetanus peptide generated no response over background in any subjects included in this evaluation (Figure 11). This point, taken together with our observation that not all influenza peptides elicited T cell activity in all donors, suggests the virus-specific $CD4^+$ T cell responses are valid. It is notable that nine of the S-OIV HA peptide sequences included in this study were predicted to have a strong capacity to induce potent $CD4^+$ T cell responses via their capacity for high-affinity and promiscuous interactions with multiple HLA-DRB1 alleles [51]. Therefore, we were not surprised to find most of the peptides elicited positive (2-fold over background/no-antigen control) responses in the majority of donors shown here (Figure 11). Given that these peptide sequences were chosen because of their strong homology between the Brisbane H1N1 and pandemic H1N1 viruses, these results suggest vaccination with the 2009/2010 seasonal TIV could have elicited potentially cross-protective $CD4^+$ T cell responses against the S-OIV.

Table 5. Comparison of predicted and actual S-OIV HA peptide immunogenicity.

	A/California/7/2009 HA Peptide Sequences											
1st percentile	Donor ID	HLA DRB1	HA_{36-53}	HA_{43-60}	$HA_{113-132}$	$HA_{359-376}$	$HA_{394-411}$	$HA_{436-453}$	$HA_{441-460}$	$HA_{461-480}$	$HA_{527-549}$	$HA_{530-541}$
	1010	1301, 1302	X[a]	X	X	X	X	X		X	X	X
	720	0101, 0701	X	X	X	X	X	X	X	X	X	X
	1142	0301, 0407	X	X	X	X	X	X	X	X	X	X
	182	0101, 0901			X	X	X	X	X			
	940	1201, 1501			X		X	X	X	X	X	X
	923	0101, 0103			X		X			X	X	X
	208	0401, 0701	X	X	X	X	X	X	X	X	X	X
	A/California/7/2009 HA Peptide Sequences											
5th percentile	Donor ID	HLA DRB1	HA_{36-53}	HA_{43-60}	$HA_{113-132}$	$HA_{359-376}$	$HA_{394-411}$	$HA_{436-453}$	$HA_{441-460}$	$HA_{461-480}$	$HA_{527-549}$	$HA_{530-541}$
	1010	1301, 1302	X	X	X	X	X	X		X	X	X
	720	0101, 0701	X	X	X	X	X	X	X	X	X	X
	1142	0301, 0407	X	X	X	X	X	X	X	X	X	X
	182	0101, 0901			X	X	X	X	X			
	940	1201, 1501			X		X	X	X	X	X	X
	923	0101, 0103			X		X			X	X	X
	208	0401, 0701	X	X	X	X	X	X	X	X	X	X

[a] Epitopes predicted to elicit a positive response in a particular donor in either the top first, fifth, or tenth percentile are indicated by gray shading. Those peptides that generated positive T helper cell responses at least 2-fold over background in the biological assays are indicated by an X.

To examine the fidelity of the computational tools used by Epivax to map T cell epitopes and MHC class II restriction profiles, we directly compared the human T cell data shown in Figure 11 with our published S-OIV HA peptide binding predictions [51]. To begin, each core 9-mer sequence was evaluated for its capacity to engage the HLA-DRB1 alleles expressed by the donors in this study; those sequences expected to have a high probability of inducing a response (binding potential ranked in the top 5th percentile) were marked with a large X in Table 4. We also assessed the HLA-DRB1 binding potential of each full-length peptide, with 5th percentile values indicated by a small X in Table 4. It is notable that peptide HA359-376, which is not predicted to have any promiscuous core 9-mer peptides (Table 3), nevertheless might have the potential to induce responses by engaging four predominant HLA-DRB1 molecules (Table 4).

Table 6. Correlation between *in silico* prediction of donor responsiveness and *in vitro* biological assay results.

Peptide	Cluster Score	Donor ID (HLA DRB1*-)													
		1010 (1301,1302)		720 (0101,0701)		1142 (0301,0407)		182 (0101,0901)		548 (0701,1302)		940 (1201,1501)		923 (0101,0103)	
		SI	iTEM	SI	iTEM	SI	iTEM	SI	iTEM	SI	iTEM	SI	iTEM	SI	iTEM
HA_{36-53}	11.24	3.95	4.36	23.23	4.93	10.26	5.26	1.95	1.72	5.38	5.39	1.14	1.75	1.40	3.44
HA_{43-60}	1.9	5.01	4.36	8.15	0.00	9.53	5.15	1.75	0.00	3.67	2.18	1.22	0.00	1.83	0.00
$HA_{113-132}$	10.11	3.31	4.88	5.92	2.11	9.86	4.15	3.05	2.11	2.86	2.44	12.92	3.09	3.00	4.22
$HA_{359-376}$	1.29	2.64	0.00	6.00	1.70	2.56	1.68	2.00	0.00	3.76	1.70	1.84	0.00	1.00	0.00
$HA_{394-411}$	5.29	2.57	3.76	12.46	4.13	9.42	2.98	3.10	2.31	2.14	3.70	12.88	1.83	3.00	4.62
$HA_{436-453}$	19.41	1.65	3.64	7.00	7.44	12.09	4.26	3.10	3.35	6.71	5.91	14.00	1.84	1.67	6.69
$HA_{441-460}$	8.61	1.59	0.00	6.23	5.09	10.95	4.75	3.00	2.36	4.43	2.73	12.26	1.84	1.50	4.72
$HA_{461-480}$	30.69	4.81	8.89	4.85	5.09	10.65	5.90	1.40	2.04	2.76	7.49	12.64	3.06	4.93	4.08
$HA_{527-549}$	53.09	3.77	7.72	5.62	11.29	9.88	6.94	1.15	5.10	7.19	10.05	12.76	5.55	3.00	10.20
$HA_{530-541}$	15.71	5.92	6.01	7.46	6.77	2.16	2.22	1.35	3.19	5.33	6.59	12.24	4.11	3.00	6.38
Correlation			0.66		-0.07		0.74		-0.09		0.60		0.67		0.36

[a] For each donor/peptide combination, the actual T helper cell response stimulation indices (SI) and corresponding predicted immunogenicity values (iTEM) are shown.

Next, we directly correlated these *in silico* predictions with the in vitro biological data shown in Figure 11. When compiled together into Table 5, we found a strong correlation between the 5th percentile binding predictions (gray shading) and the true capacity of the peptides to induce specific T helper cell responses at least 2-fold over background (marked with an X). In fact, 95% (62 out of 65) of the total positive biological responses were predicted accurately at the 5th percentile ranking. As well, it is clear from this analysis that a 1% cutoff provides a very conservative prediction of influenza-specific $CD4^+$ T cell epitopes since it markedly underestimated positive responses in the T cell assays. Increasing the number of predictions to include those in the 10th percentile slightly increased the number of hits (64 out of 65), but also introduced additional false-positives (Table 5). Of note, the fact that 8 of the 9 S-OIV HA peptides included in this evaluation were predicted to induce positive $CD4^+$ T cell responses in the majority of the eight subjects included in this study reflects our interest in choosing peptides with highly promiscuous core 9-mer sequences that should be able to interact with most individuals in a population.

Table 7. Analysis of the efficacy of *in silico* predictions of T helper cell responsiveness against the S-OIV.

HA	Donor ID							
	1010	720	1142	182	548	940	923	208
36-53	P	P	P	N	P	N		P
43-60	P		P	N	P	N	N	
113-132	P	P	P	P	P	P	P	P
359-376						N	N	
394-411	P	P	P	P	P		P	P
436-453		P	P	P	P			P
441-460	N	P	P	P	P			P
461-480	P	P	P	N	P	P	P	P
527-549	P	P	P		P	P	P	P
530-541	P	P	P		P	P	P	P

Item 2.06 Cutoff - SI 2.0 Cutoff

SI

iTEM		Pos	Neg		
	Pos	54	6	0.90	PPV
	Neg	11	9	0.45	NPV
		0.83	0.60		
		Sensitivity	Specificity		

P	True Positive (Prediction of response confirmed)
N	True Negative (Prediction of no response confirmed)
	False Positive (Prediction of response, none observed)
	False Negative (Prediction of no response, response observed)

Broadening this *in silico* evaluation, we also used the iTEM algorithm (described in the Materials and Methods section) to calculate the probability that a given peptide sequence will elicit a $CD4^+$ T cell immune response in a particular donor. This approach provides a more comprehensive forecast of T cell epitope immunogenicity since it takes into account the binding profile of all the predicted epitopes within a particular peptide sequence against the collective whole of an individual's HLA-DRB1 haplotype. For this study, iTEM scores were calculated for each peptide-donor combination, and those yielding values greater than 2.06 (a pre-determined threshold for this technique [60]) were evaluated for correlation with positive $CD4^+$ T cell responses (2-fold over background) in the in vitro assays (Tables 6

and 7). Of the 80 peptide-HLA-DRB1 (8 donors X 10 peptides) combinations derived from this study, 65 of these yielded a significant CD4+ T cell response (SI =>2). Of these 65 combinations, 54 (83%) had iTEM scores > 2.06, which meant they were predicted to elicit significant T cell responses (Tables 6 and 7). In the 15 instances where the peptide-HLA combination did not generate a significant T cell response in the in vitro assay, 9 of these (60%) were also predicted to fail to generate responses in the iTEM analysis (score <2.06). One interesting outlier is HA359-376, a confirmed MHC class II peptide [48] that was not predicted to contain any core 9-mer binding motifs (Tables 3 and 4). While the *in silico* binding scores for this peptide fall below the threshold of significance, it did produce a modest response in vitro that was responsible for 6 of 11 false negative predictions. Upon further evaluation, we noted the strongest-scoring 9-mer within this sequence, YHHQNEQGS, contains a glutamic acid at position 6 that negatively impacts the Epimatrix scores since it is typically highly disfavored in this position. In this case, however, the adverse effect of the glutamic acid must be outweighed by the positive effects related to the surrounding amino acids. Taken together, the results of this study confirm an iTEM score greater than 2.06 provides a strong indicator of the capacity of a particular peptide to elicit a specific $CD4^+$ T cell response. While it is possible for peptides with iTEM scores less than 2.06 to trigger responses, setting a high/conservative cutoff value reduces the chance the algorithm will be used to generate false-positive predictions. Indeed, the fact that 54 out of 60 (90%) predicted positive responses were confirmed by the biologic assessments provided in this analysis (Table 7) is perhaps the most important metric of success since one would not want to overestimate the capacity of the population to respond to a peptide vaccine.

Discussion

In light of the fact that pre-existing antibodies offered only limited protection against the pandemic S-OIV of 2009, we and others postulated cross-reactive T lymphocytes elicited by the 2009/2010 seasonal TIV or prior exposure to other H1N1 viruses might have played an important role in limiting disease and the spread of this novel virus by generating direct anti-viral effector functions or accelerating the induction of naïve virus-specific B cell responses against novel S-OIV antigens upon subsequent infection. Shortly after the emergence of this virus in 2009, we used in silico techniques to define T cell epitopes that are highly conserved between the S-OIV and the seasonal vaccine strain, Brisbane H1N1, and were predicted to bind promiscuously to the most prominent HLA-DRB1 alleles [61]. In the current study, by performing a biological evaluation of cross-reactive S-OIV-specific $CD4^+$ T cells in the circulation of eight donors chosen at random for HLA-DR genotype, we demonstrated that the computational methods were highly accurate in defining CD4+ T cell epitopes that were broadly reactive, i.e., capable of eliciting responses from nearly all the donors included in this evaluation. In the process of completing this evaluation, we also confirmed that pre-existing $CD4^+$ T cells can generate cross-reactive effector responses against the S-OIV virus, which bolsters the argument that cellular immunity might have engendered some protection against disease resulting from pandemic H1N1 infection.

Our demonstration of cross-reactive T helper cells against S-OIV is consistent with a series of studies that have evaluated potentially cross-protective influenza-specific cellular immunity against this novel virus. For example, two independent studies demonstrated CTLs and CD4+ T cells raised against the seasonal H1N1 viruses, A/Brisbane/59/2007 and A/New Caledonia/20/99, respectively, were capable of responding against whole protein antigens from the S-OIV [62, 63]. In addition, a study by Ge

et al. [64] provided evidence of cross-reactive human T helper cell responses against defined epitopes from the HLA-DR4 molecule. Our study was complementary to these prior reports, but differed from them in two ways. First, we were particularly interested in addressing whether vaccination with the conventional seasonal TIV might elicit protective immunity against S-OIV, so we focused our evaluation on cross-reactive T helper cells specific for the primary vaccine antigen, HA. Second, we too were interested in assessing peptide-specific T cell responses, but did not limit our evaluation to any particular HLA-DR haplotype. In fact, as mentioned above, we targeted our evaluation of cross-reactive T helper cell epitopes against a panel of eight HLA-DR allele supertypes that cover 99% of the population [51].

While there is a long history of research examining cross-reactive T cells against influenza, most of these studies targeted the non-structural/more conserved proteins of the virus, such as NP, M1, and PB1, since they offer the greatest potential for eliciting long-lived cross-protective immunity against influenza. For example, recent studies have provided evidence for the existence of T cells reactive against several non-structural proteins from seasonal virus strains that can generate cross-protective responses against avian influenza (H5N1) [65, 66]. As well, individuals not previously exposed to H5N1 viruses were shown to exhibit cross-reactive T cell against both the structural and non-structural proteins from an avian (Hong Kong H5N1) influenza strain [67]. As mentioned above, we specifically focused our evaluation on the structural HA protein of the S-OIV because it is the primary component of the seasonal influenza vaccine and, thus, is likely the primary target of T cell immunity following immunization with a split virus vaccine. While HA is not a dominant target of cellular immunity during natural infection, recent studies with a DR1-transgenic mouse model and tetramer staining of human peripheral blood leukocytes suggest the presence of shared HA T cell epitopes between seasonal H1N1 viruses and the S-OIV [68-70].

Although $CD8^+$ T cells are considered a key player in anti-influenza cellular immunity, we limited our investigation to $CD4^+$ T cells because we were specifically interested in whether the 2009/2010 seasonal TIV, which is poor at generating $CD8^+$ T cell immunity, had the capacity to elicit a T helper cell response against the S-OIV. Though we cannot make definitive statements from our data regarding the role of virus-specific $CD4^+$ T cells in limiting S-OIV infection, a strong body of experimental evidence suggests influenza-specific T helper cells can limit influenza disease, particularly in the absence of an efficacious humoral response. A number of conclusions can be drawn from these published studies [50, 71-80]: (1) the rate of viral clearance upon secondary infection slows considerably, beyond that seen during the primary infection, in the absence of functional memory $CD4^+$ T cells, (2) T cell help is required for the generation of high virus-specific IgG antibody titers, (3) vaccine efficacy is improved when cross-reactive helper T cell populations are present from prior infection and/or vaccination, (4) memory T helper cells specific for a previous influenza strain contribute to cross-strain antibody responses and confer direct protection against heterologous infection, and (5) effective vaccination can elicit protective cellular immune responses capable of secreting cytokines and cytolytic activity. For these reasons, we believe pre-existing $CD4^+$ T cells elicited against the 2009/2010 seasonal TIV could have the capacity to limit S-OIV disease severity.

Our goal, as we embarked on this study, was to employ a short-term (24-hr) IFNγ ELISPOT assay to evaluate the frequency of circulating human T cells capable of responding against the novel S-OIV in donors with no prior exposure to this novel virus. Though we were quite successful using this highly sensitive assay to evaluate T cell responses when the autologous DC targets were pulsed with vaccine formulations or intact viral HA protein (each contain a multitude of potential T cell epitopes), we failed to detect specific T cell effectors in five of eight donors when single peptide antigens were added to the assay wells (Figure 9). While this result might be taken to suggest the peptides do not represent

dominant HA epitopes, we do not think it is possible to broadly judge the relative strength of the peptides in this evaluation because the sum of the individual epitopes also exceeded the whole protein and pooled peptide responses by at least 10-fold for donors 182 and 208 (Figure 9). Furthermore, these results are consistent with our observations in other experimental systems that the sum of individual peptide-specific responses often does not match the total T cell response (A. DeGroot et al., unpublished results). Notwithstanding these observations, it is very likely the ten peptides included in this evaluation represent only a subset of the potentially cross-reactive peptides that are shared between Brisbane and California HA proteins. In fact, we chose for this evaluation only those peptides that contained sequences we had predicted were the most broadly cross-reactive (amongst multiple HLA class II alleles) and highly conserved between the Brisbane and California H1 viruses [61].

Our inability to detect individual peptide-specific responses by ELISPOT is not surprising given other researchers have experienced similar difficulties using this technique to evaluate direct ex vivo T cell responses in humans [81, 82]. In fact, past studies aimed at evaluating individual peptide-specific T cell responses from humans have resorted to long-term in vitro stimulation periods (up to 10 day) to trigger the proliferation/accumulation of the specific lymphocytes to a number where they could be detected by ELISPOT assay [67]. In a similar approach, we employed a highly sensitive T cell stimulation/challenge assay developed in our laboratory to evaluate S-OIV peptide-specific $CD4^+$ T cell responses. This technique has been successfully employed to evaluate primary and recall T cell responses against a variety of protein antigens and a formulated yellow fever vaccine [52, 53]. As well, we believe this was a critical component of the study presented here because it addresses one of the limitations of *in silico* epitope-mapping techniques, namely, that they predict epitopes based on the capacity of a peptide sequence to bind MHC, but do not evaluate the capacity of the MHC machinery of cells to yield that particular sequence for MHC presentation. To this point, the two-stage stimulation

technique – where one round of DCs are pulsed with the HA protein (12-day coculture), and then the second round of DCs present the individual peptides (ICCS analysis) – provides direct evidence that the native protein was processed through the DCs machinery to give rise to the peptide epitopes of interest in this evaluation. It is notable that sum of the T cell responses elicited by the individual peptides often exceeded the response elicited by the native HA protein in the ICCS assay (Figures 2 and 3), though this observation is perhaps not surprising since pulsing DCs with the native HA protein may be inefficient compared to directly loading the APCs with high concentrations of individual peptides. Nevertheless, given the strength of the peptide-specific responses in the ICCS assay against either the whole protein or individual epitopes, we think it is safe to conclude the DCs did efficiently process the HA protein to generate the peptide epitopes included in this evaluation.

As demonstrated here, bioinformatics offers a powerful approach for predicting T cell epitopes, though the critical step for epitope-driven vaccine design remains the in vitro and in vivo validation of such predictions. Towards this goal, the algorithm used here has been successfully applied to the analysis of previously published epitopes and in the prospective selection of peptides from HIV, Mycobacterium tuberculosis, Tularemia, and vaccinia virus [83-87]. In the current study, we sought to comprehensively assess the reactivity of influenza $CD4^+$ T cell epitopes as a function of individuals' specific HLA haplotypes, which can be predicted via iTEM calculations. Here, we utilized a refined methodology in which iTEM scores more closely correlate with in vitro responses to successfully model the wide spectrum of HLA haplotypes found in eight randomly chosen donors. In this case, we were able to predict immune responses using iTEM with high sensitivity and minimal false-positive predictions. The refined iTEM method may afford us an improved capacity to predict immune responses in the context of larger antigen sets; this would need to be investigated in future studies involving multiple protein antigens.

An epitope-driven approach towards vaccine design shows great promise with influenza and other infectious diseases and could overcome challenges facing both subunit and poly-epitopic vaccines. Indeed, merging *in silico* and in vitro strategies to define potential epitopes has led to the discovery of immunogenic tuberculosis specific T-cell epitopes which may have application in vaccines against this pathogen. So as to improve current influenza vaccine strategies, future pandemic epitope-based formulations could (1) expand the generation of cross-reactive T cell epitopes, (2) exploit sequence conservation within circulating influenza strains, and (3) expand HLA population coverage of cross-reactive epitopes. To improve the immunogenicity of this type of formulation, we feel it would be important to choose peptides that induce multi-functional T cell responses in human PBMCs. As well, we believe the successful implementation of this strategy would require a careful selection of vaccine delivery vehicle, route, and formulation strategy.

Conclusions

In summary, this study confirmed the capacity of circulating $CD4^+$ T cells to generate cross-reactive effector responses against the S-OIV and validated our previous predictions of highly immunogenic HA-derived T cell epitopes that are shared between seasonal and pandemic H1N1 viruses. The implication of these results are clear, namely, that priming with the 2009/2010 seasonal TIV might have generated cross-conserved T helper cells capable of providing enhanced protection against subsequent S-OIV infection via direct anti-viral effects or accelerating the induction of naïve antibody responses against the novel virus. Going a step further, we think these observations lends support to the notion that vaccines which “arm the immune system” via cellular/T cell-dependent defenses against influenza virus might provide an alternative to current prophylactic strategies [88] since vaccines that

stimulate effective antibody response must be developed on a seasonal basis in a costly and sometimes inefficient process. This hypothesis is supported by the study of Ellebedy et al. [50] demonstrating a correlation between the strength of T cell responses against cross-reactive epitopes and attenuation of influenza symptoms in H1N1-infected humans, ferrets, and mice. Finally, these observations lend support to the integration of *in silico* and sensitive in vitro testing methods for defining and assessing cross-reactive T cell response in preparation for the next influenza virus pandemic and other infectious diseases.

Acknowledgment

I am thankful to T. Kamala and J. Moser for critically reviewing the manuscript. As well, I appreciate the contribution of F. Terry in performing computational analyses. This work was funded by a DARPA/DSO(BAA09-310) project (#70023) entitled, “Immune Analysis of Brisbane and California H1N1 in Human Sera and the MIMIC® System.”

CHAPTER THREE: EXPOSURE TO TITANIUM DIOXIDE NANOMATERIALS PROVOKES INFLAMMATION OF AN IN VITRO HUMAN IMMUNE CONSTRUCT

Abridgment

Coinciding with our investigation of novel biological agents, such as the use of peptides for vaccination, a major gap in the literature and our understanding of how novel non-biological materials like nanoparticles interact with human immunity had become a strong point of interest in the scientific community at large. However, a dilemma existed that stood in the way of filling this void; an absence of accurate models or systems for performing such evaluations considering testing directly in humans is impossible. This venture into interrogating the effects, if any, that NPs would impart upon human immunity expanded the capability of the system and our understanding of such novel small immunogens.

The overwhelming expansion of nanoparticle technology is largely due to its promise to enhance a wide array of applications and has led to its pervasive presence in the consumer market. Significant potential lies in research exploring the utility of nanoparticles as biomaterials, drug delivery vehicles, cancer therapeutics, and immunopotentiators. Understanding the fate of nanoparticles *in vivo* is critical to their development and subsequent suitability for therapeutic purposes. Incorporation of nanoparticle technologies for tissue engineering applications has exemplified the urgency to characterize nanomaterial immunogenicity. This study explores TiO_2, one of the most widely manufactured nanomaterials, synthesized into three nano-architectures: anatase (7-10 nm); rutile (15-20nm); and nanotube (10-15 nm diameter, 70-150 nm length). The autologous human MIMIC™ immunological model was utilized as a predictive, non-animal alternative, to diagnose nanoparticle immunogenicity.

Peripheral blood mononuclear cells and endothelial cells were exposed to TiO_2 nanoparticles for 48 h and evaluated for viability. MIMIC™ derived monocytes were incubated with the nanoparticle preparations for 48 h and evaluated for phenotypic maturation markers and costimulatory molecule upregulation as well as cytokine secretion. In addition, B cells cultured with the nanoparticles were evaluated for antibody secretion by ELISPOT. Cumulatively, the TiO_2 nanoparticle treated cultures revealed overall elevated levels of proinflammatory cytokines, increased maturation and costimulation molecules as well as increased antibody expression as compared to cultures treated with micron-sized (>1 μm) TiO_2. Little difference was noted between different phases of TiO_2 preparations (rutile, anatase, or nanotube structure). In brief, exposure of the MIMIC™ platform to these nanoparticle formulations generated an enhanced immunogenic response characteristic of an inflammatory response which was absent in the micron- TiO_2 as well as untreated cultures.

Introduction

Nanomaterials (defined as particles with diameters less than 100 nm) have been rapidly assimilated into the consumer market because of their unique physiochemical properties and tunable characteristics. Nanoscale TiO_2, one of the most widely manufactured nanoparticles, has been incorporated into pigments, cosmetics, sunscreens, and is at the frontier of nanotechnology with its application as a biomaterial. For instance, nanostructured TiO_2 has been utilized in dental implant technology and is being widely studied for various biomedical applications including scaffolds, coatings, and implants [89, 90]. TiO_2 has gained significant interest in the field of tissue engineering; it is thought to have the potential to profoundly change the field by providing researchers a material to repair, replace, or even enhance normal tissue function.

Despite all their promise, there are conflicting reports on the exposure risk of nanoparticles and their degradation products to humans. For example, nanostructured TiO_2 is reported to be a biocompatible coating for grafts and shows great promise as a suitable bone substitute [91, 92], yet culture, animal, and epidemiological studies suggest that these materials promote pulmonary disease and the development of cancer [93-98]. A catalog of similar hazardous findings has led to the classification of nanoscale TiO_2 as a potential carcinogen by the International Agency for Research on Cancer (IARC) [99-102]. Nanoscale TiO_2 might be expected to elicit inflammation through the release of innate triggers, such as reactive oxygen species, or otherwise being recognized as a foreign entity by the host [101, 103]. However, a scarcity of information on the interaction of these agents with cells of the human immune system exists, likely a result of the current deficit of appropriate assays to evaluate human immunity in the laboratory. These inconsistencies underline the importance of novel approaches that use predictive assay models focused on the inflammatory response to determine the impact on biological systems and are necessary to protect human health.

We undertook an extensive set of studies to develop a sensitive and reliable model to evaluate human immunity in the laboratory. This system, termed Modular IMmune In vitro Construct (MIMIC™), is comprised of several components that permit the interrogation of innate (short-term inflammation) and adaptive (long-term memory) responses in separate or longitudinal studies. The peripheral tissue equivalent (PTE) component of the MIMIC™ system is principally comprised of blood vein endothelial cells, which participate in inflammatory reactions by secreting soluble factors and regulating the flow of immune cells from the vasculature into tissues, and monocyte-derived dendritic cells, a critical antigen presenting cell population that bridges innate and adaptive responses and stimulates naïve T cell responses. The synergistic effect of the cell types comprising the PTE permit the evaluation of early immune responses associated with foreign body encounter and acquisition, and has been shown to

support the induction of inflammatory responses against a variety of immunostimulators and immunosuppressants [5, 13, 14, 53].

Here, we employed the PTE construct of the MIMIC™ system to enumerate and characterize the capacity of TiO_2 formulations (anatase, rutile, and nanotubes) to induce inflammation. We have chosen to study multiple crystal phases of nanoscale titanium dioxide because of conflicting biocompatibility reports despite widespread incorporation into the consumer market [89, 91, 92, 104-110]. These assays revealed that treatment with these nanosized TiO_2 formulations generate ROS production, increase proinflammatory cytokine expression from the endothelium and DC population, increase DC maturation, and have the capacity to induce an antibody response as compared to the micron-sized titanium. This study has emphasized the utility of MIMIC™ for testing efficacy and immunotoxicity of nanomaterials and finds these TiO_2 nanoparticle formulations to induce inflammation.

Materials and Methods

Materials

Bacterial Lipopolysaccharide (LPS) and pokeweed mitogen (PWM) were obtained from Sigma (St. Louis, MO). The tetrazolium dye, 3-[4,5-dimethylthiazol-2-yl]-2,5-diphenyl tetrazolium bromide (MTT) was obtained from Invitrogen (Carlsbad, CA). Silicone dioxide nanoparticles (used as a comparative control in some experimental models) were obtained from Sigma. Reactive oxygen species (ROS) levels were determined using 2′,7′-dichlorodihydrofluorescein diacetate (DCF; Sigma).

Synthesis of Titania Nanoparticles

Nanoparticles were synthesized by wet chemical synthesis. At first a 50:50 mixture of ethanol (99.8% Sigma Aldrich) and deionized water (18.2 M) was boiled to reflux. At this point the pH of the boiling solution was adjusted to pH 3.0 by addition of 1N HCl. Titanium isopropoxide (Sigma Aldrich) was added slowly to this refluxing mixture which precipitates immediately to a white solution. The solution was then stirred at 85^{o}C for 4 hours. The white solution was then cooled to room temperature and washed several times with ethanol until dry. The as prepared sample was mostly anatase (partially amorphous) and was used as such. For obtaining rutile nanoparticles the anatase nanoparticles were calcined at 800º C for 2 hours and the crystalline structure was conformed using X-ray diffraction.

Synthesis of Titania Nanotubes

Titania nanotubes were prepared by hydrothermal procedure previously established [111-113]. In a typical synthesis 0.5 gm of anatase titania from above synthesis was mixed with 20 ml of 10 M sodium hydroxide solution. The mix was then poured in an autoclave and heated at various temperatures from 120- 150º C for 20-24 hrs. The final solution was cooled to room temperature and washed several times to remove additional sodium hydroxide. A final wash of 1N HCl to neutralize was carried out and titania nanotubes (partially amorphous) were subsequently washed again several times, filtered and dried at 120° C. Nanoparticles were dispersed in Dulbecco's phosphate buffered saline (DPBS; Lonza, Basel, Switzerland) by sonication and vortexing followed by immediate delivery to the cultures.

Transmission Electron Microscopy

The samples were analyzed using high resolution transmission electron microscopy (HRTEM) (Philips 300 TECNAI operated at 300 kV) to confirm the shape, size and morphology of the nanoparticles. The samples were prepared by dipping a holy carbon coated copper grid into a dilute suspension of nanoparticles dispersed in acetone.

Evaluation of Endotoxin Contamination

All nanoparticles samples were analyzed for the presence of endotoxin contamination using a quantitative kinetic chromogenin Limulus Amoebocyte Lysate method (Lonza-BioWitthaker, Walkersville, MD). *Escherichia coli* 055:B5 endotoxin (Lonza BioWitthaker) was used as a standard.

Human Peripheral Blood Mononuclear Cell Isolation

Aphaeresis was performed at Florida's Blood Center (Orlando, FL) using a COBE® Spectra Apheresis System (Gambro, Lakewood, CO). The study was reviewed and approved by the Chesapeake Research Review Inc. (Columbia, MD). All donors were in good health and were negative for blood-borne pathogens as detected by standard blood bank assays. The aphaeresis product was processed to enrich the peripheral blood mononuclear cell (PBMC) fraction by using ficoll-hypaque (Amersham, Piscataway, NJ) density gradient separation according to standard protocols as previously described [53]. PBMCs were cryopreserved in DMSO-containing media for extended storage in liquid nitrogen vapor phase until needed.

Cell Culture

The two primary cell types were used in this study are human umbilical vein endothelial cells (HUVEC; Lonza) and PBMCs. HUVECs have been shown to be intimately involved in orchestrating the inflammatory cell response via transendothelial cell trafficking, making them a suitable choice for this co-culture model. HUVEC were cultured as previously described [114]. PBMC aliquots were thawed in Iscoves Modified Dulbecco's medium (Lonza) supplemented with 10% autologous donor serum, 100 IU/mL Penicillin and 100 μg/mL Streptomycin. Cells were washed and cultured in X-VIVO-15 (Lonza) seeded into 24 well dishes at 2.5 x 10^6 cells per well. All cultures were incubated at 37°C in a humidified incubator with 5% CO_2.

Cell Viability Assay

To determine cytotoxicity levels of nanoparticles, HUVEC and PBMCs cultures were prepared at approximately 2,000 and 20,000 cells per well, respectively, in 96-well flat bottom tissue culture plates. The HUVEC monolayer was approximately 70-80% confluent after 24 hours of culture. Serial dilutions of rutile, anatase and titania nanotubes were added and incubated 24 hours. MTT was added to each well (1.2 mM) and incubated for 4 hrs at 37°C with 5% CO_2. To solubilize the dye, a cell lysis solution (10% SDS, 5 mM HCl) was added and incubated for 14 hours at 37°C. Absorbance of the soluble dye was determined at 570 nm in using a Spectramax 190 UV-visible spectrophotometer (Molecular Devices, Sunnyvale, CA). To validate the use of this assay on these cell types as a representative measure of cell viability, we used a standard curve of known concentration of cells (established by counting trypan blue stained cells with a heamocytometer). In addition, HUVEC and PBMCs cultures were prepared at

approximately 2,000 and 20,000 cells per well, respectively, in 96-well flat bottom tissue culture plates as described above. LDH release was monitored using a Spectramax 190 UV-visible spectrophotometer (Molecular Devices, CA) as described by the manufacturer (Roche, Basel, Switzerland) to acquire additional information about the cytotoxicity of the nanoparticle treatment

ROS Determination

HUVECs were cultured in 24-well flat bottom tissue culture plates until 70-80% confluent. PBMCs were cultured into 24-well dishes at a density of 2 x 10^6 cells per well. The cultures were then treated with serial dilutions of rutile, anatase and titania nanotubes for 72 hours. Subsequently, cultures were treated at room temperature for 30 minutes with DCF at a final concentration of 10 μM. Cells were washed of excess dye with DPBS, harvested using cell dissociation solution (Sigma), and washed again in DPBS. Fluorescence of the oxidized DCF (indicative of peroxide levels) was analyzed by flow cytometry using LSR II (BD Pharmingen, San Diego, CA). FlowJo software (Treestar, Ashland, OR) was used for data analysis.

Allogeneic Naïve $CD4^+$ T cell Proliferation

DCs were derived from the HUVEC-based model and were stimulated with the TiO_2 particle preparations (micron TiO_2, rutile, or nanotubes) (6.25 μM) for 48 hours. The DCs were harvested and added at an optimized ratio of 1:400to allogeneic naïve $CD4^+$ T cells previously isolated by magnetic separation (Miltenyi Biotec) and labeled with carboxyfluorescein succinimidyl ester (CFSE) following the instructions of the manufacturer (Molecular Probes, Invitrogen). As a positive control of proliferation

and activation, phytohemagglutinin and phorbol 12-myristate 13-acetate (PHA/PMA) (1 µg/mL each) was added to wells containing only the $CD4^+$ cells and as a negative control the $CD4^+$ were unstimulated. After 5 days the cultures were harvested and stained following the manufacturers instruction for CD25, CD3, CD4, (eBioscience) and Live/Dead Aqua for viability (Invitrogen) and then acquired by FACS using BD Pharmingen's LSR II.

Dendritic Cell Phenotyping

*Phycoerythrin (*PE), allophycocyanin (APC), Peridinin chlorophyll protein (PerCP-Cy5.5)-conjugated monoclonal antibodies specific for human CD14 (M5E2), CD86 (2331), CD83 (HB15e), CCR7, and HLA-DR (L243) (all from BD Pharmingen) were used to determine the cell surface receptors expressed on the reverse transmigratory DCs. Isotype control antibodies included MIgG2a (G155-178) and MIgG1 (MOPC-21) were also purchased from BD Pharmingen. DCs from the PTE module were collected and labeled with the above mentioned specific antibodies for 45 min at 4°C in PBS containing 2% bovine serum albumin (BSA) and 0.05% sodium azide, washed extensively, and cells were subsequently fixed with 2% paraformaldehyde. Flow cytometry was used to determine the abundance of each cell type (sub-population) expressing markers using LSRII (BD Pharmingen) and FlowJo software (Treestar) as described above.

Bioplex Cytokine Quantification Assay

Supernatant samples collected from the PTE – MIMIC™ module were analyzed for cytokine production by means of the BIOPLEX Multiplexing array system (Bio-Rad, Hercules, CA) as previously

described [115]. Samples were harvested after 48 hours of treatment with nanoparticles or positive control antigens.

Peripheral Tissue Equivalent Module

The peripheral tissue equivalent (PTE) was prepared as previously described [13]. HUVEC monolayers were seeded with 5 x 10^5 PBMCs per well in a 96-well format. After a 90 minute migration period, the excess PBMCs were washed from the module. Treatments of TiO_2 nanoparticles (6.25 μM) or LPS (10 ng/mL) were immediately applied and allowed to incubate for 48 hours. The RT APC were then harvested at the 48 hour time point and analyzed by DC phenotyping while the supernatants were examined for cytokine production using the BioPlex system.

Statistical Analysis

Each experiment was confirmed at least three times using cells isolated from at least three separate donors. All results were analyzed using analysis of variance (ANOVA). Statistical significance was considered at $p<0.05$.

Results and Discussion

Particle Characteristics

Titanium dioxide for commercialization or tissue engineering applications is commonly prepared as nanotubes or either of two crystal phases (rutile and anatase). As such, nanostructures of these three

types were prepared for use in this study. Consistent and optimal material architecture began with the controlled synthesis of titania nanotubes and nanoparticles using simple wet chemical and hydrothermal synthesis. The structure and diameter of each material was verified using high resolution transmission electron microscopy (HRTEM) (Figure 12). Anatase nanoparticles were between 7-10 nm wide while the rutile nanoparticles were 15-20 nm in diameter. The hydrothermally synthesized titania nanotubes shown in Figure 12c were approximately 10-15 nm in diameter and 70-150 nm in length. The nanomaterials were prepared in a single batch to provide confidence in material consistency throughout all the experiments shown here. Since these preparations were being used in immunoassays (see below), great effort was taken to ensure they were free of contaminating lipopolysaccharide (LPS); all samples were confirmed negative for endotoxin (EU<0.6) using the quantitative kinetic chromogenin Limulus Amoebocyte Lysate method.

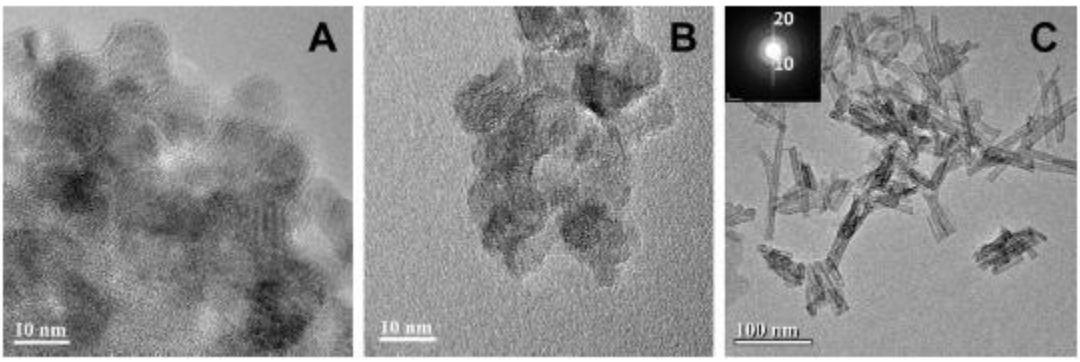

Figure 12. HRTEM image of titania nanoparticles (A) anatase, (B) rutile, and (C) nanotubes.

Partially amorphous character of particles is observed in case of anatase nanoparticles, while the aspect ratio of nanotubes was around 1:10 to 1:15. Captures by Ajay S. Karakoti.

Particle Dosing

Because many of the current applications of titanium dioxide nanomaterials are placed in vivo or otherwise encourage human exposure, it is important to understand the impact of these materials on

human health. As a first gauge of the impact of titanium dioxide nanoparticles on human physiology, we evaluated the cytotoxicity of these products on cell types (HUVECs and PBMCs) comprising the PTE construct over a 2-fold concentration of nanoparticles from 0.05 μM to 100 μM. This analysis was carried out using a 3-(4,5-Dimethylthiazol-2-yl)-2,5-diphenyltetrazolium bromide (MTT) reduction assay, which relies on the colorimetric detection of enzymatically modified MTT that takes place only in viable cells. Viability is measured as percent of control, were the average unstimulated control viability value was set as 100%. Figure 13a shows an average cell viability of 44 ± 6.24% in HUVEC treated for 48 hrs with 100 μM anatase, rutile or nanotubes. This data was consistent with our preliminary studies using the human adenocarcinoma line, A549, and keratinocyte line, HaCaT (data not shown). Contrary to the endothelial cells, PBMCs had enhanced resistance to titanium dioxide nanoparticles, as treatment with equivalent concentrations of nanoparticles resulted in an average cell viability of 83 ± 5% (Figure 13b). When examined, the MTT data suggests these nanomaterials act as metabolic toxins, even at lower doses (0.05 μM – 6.25 μM), sharply reduce cell viability. However, cell viability begins to plateau after 50 μM treatment, where the dose-dependant loss of viability is not as dramatic. This suggests both cell populations are extremely sensitive to low-dose titanium dioxide nanomaterials. In an effort to confirm these observations, we evaluated the same particle-dosing panel with a lactate dehydrogenase (LDH) assay that relies on a colorimeteric readout of the release of LDH from the cell cytosol into the culture supernatant following disruption of the plasma membrane. Surprisingly, the cell loss/membrane disruption remained below 15% for both HUVEC and PBMCs in all dosing regimens (Figure 13c-d), which suggests that titanium nanoparticles reduce cellular metabolic activity (MTT data) but do not trigger overt cell destruction/necrosis (Figure 13c-d).

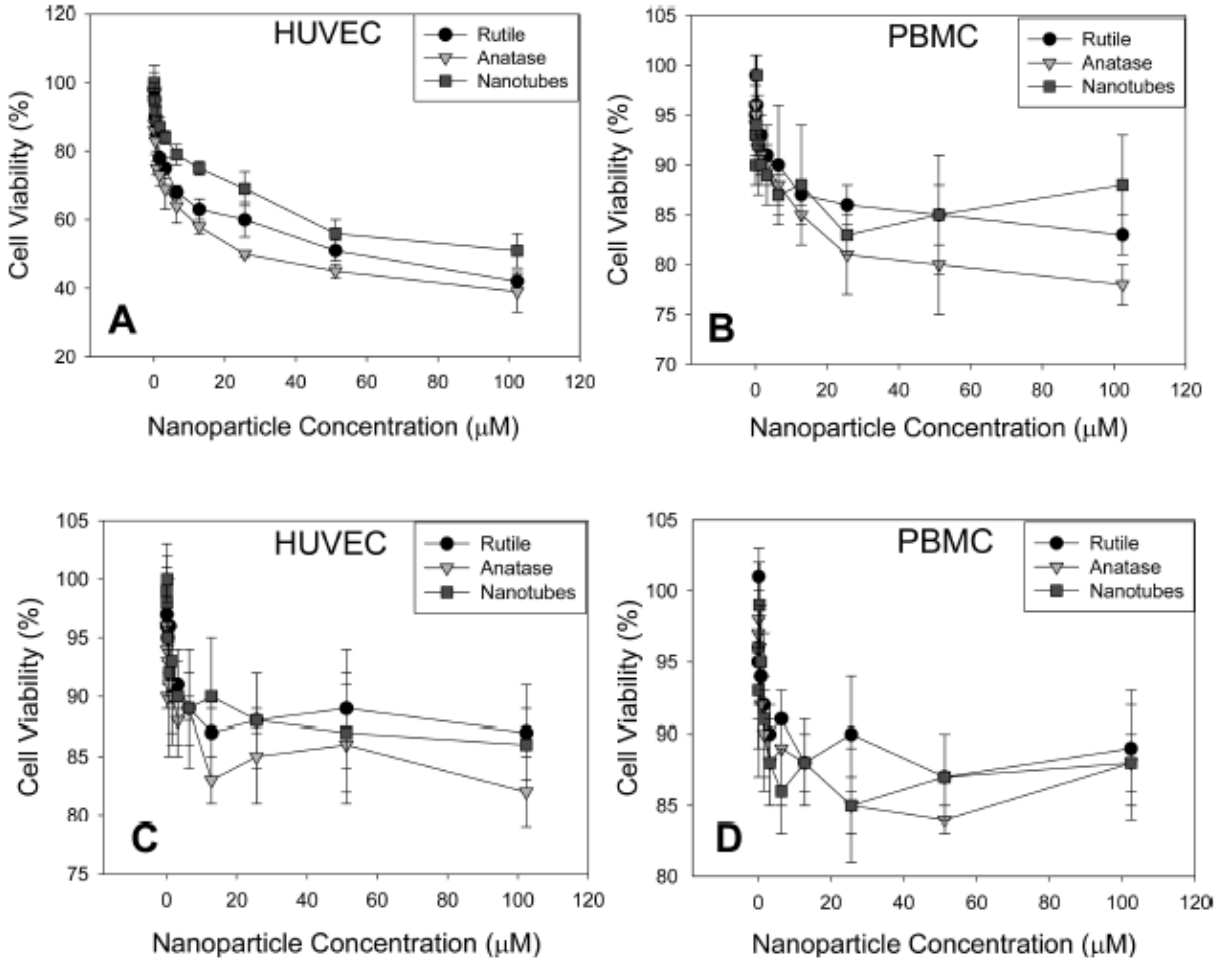

Figure 13. Toxicity of TiO_2 nanomaterials in HUVEC (A and C) and PBMC (B and D) primary culture models.

(A) HUVEC cells cultured in medium 199 containing 20% serum and (B) PBMCs cultured in X-VIVO 15 were exposed to TiO_2 nanoparticles at concentrations indicated in the plot. MTT dye reduction was assessed after incubating the cells with the nanomaterials for 24 h, and the absorbance collected was compared to untreated cells to determine the relative percent cell viability. LDH release by loss of cell membrane integrity after 24 h nanoparticle treatment was investigated for (C) HUVEC cells and (D) PBMCs Error bars represent mean ± SD for at least three independent experiments.

Similar to the MTT data, the LDH data set corroborates the level of sensitivity the cells have to the nanoparticles with the prominent loss of membrane integrity in the lower dose range, and then plateaus in the upper dose range. Because this study aimed to investigate the potential inflammatory

effect of titanium dioxide nanomaterials, and thus required intact, metabolically active cells, we felt it critical to choose a nanoparticle dose that increased cell death no more than 15%. As such, we concluded that titanium dioxide could be delivered to the target cell populations at a dose of 6.25 μM.

Innate Response Induced by Nanoparticle Treatment

The innate immune system is comprised of a number of cell types that respond to insult or infection of the host by releasing a variety of pro-inflammatory factors in a rapid and non-antigen-specific manner [116-118]. Because nanomaterials lack the classical pathogen-associated molecular recognition patterns, their immunogenicity may be limited to innate inflammatory responses. The PTE construct provides us with a physiological environment to examine these inflammatory signals produced by the resident endothelium and phagocytes, both cell populations are critical for orchestrating innate immune responses in vivo. The secretion of pro-inflammatory cytokines like IL-1α, IL-1β, IL-6, and TNFα direct the innate response by recruiting and activating neighboring immune cells. These cytokines may be accompanied by anti-inflammatory cytokine like IL-8 and IL-10, as well as maturation signals like IFNγ, acting to balance the response and lead to activate adaptive immunity.

In the current study, supernatants collected from the PTE were analyzed using the Bioplex cytokine array. The levels of certain cytokines in the media can be directly correlated to the immuno-stimulatory effects of the treatments. When treated with nanoparticles of varying size and crystal structure, rutile (15-20nm), anatase (5-7nm), and nanotubes, we observed alterations in cytokine expression, suggesting that all of the titanium dioxide nanoparticle preparations inflame the PTE construct (Figure 14). The increase in secretion of pro-inflammatory cytokines IL-1α, IL-1β, IL-6, and TNFα was seen across a panel of at least 5 donors with little variation (p<0.05). The secretion of anti-

inflammatory cytokines like IL-8 and IL-10 was also observed. This is not surprising considering the HUVEC monolayer has been characterized to be a major producer of IL-8. In addition to IL-8, the HUVEC also produce IL-6, a pleiotropic cytokine that plays an important role in host defense through immune and inflammatory regulation. The production of the immunosuppressive cytokine IL-10 by the resident phagocytic population in the PTE is likely a response to the increasing levels of IL-1 and TNFα [119, 120]. The accumulation of this data illustrates that nanoscale titanium dioxide of different structures and associated surface chemistries induce an inflammatory response in the PTE construct. This data is corroborated by previous studies reporting ultrafine titanium dioxide particles cause an increase in tissue inflammation and alter macrophage chemotactic response [121]. Together this data concludes that titanium dioxide nanoparticles are reactive enough to initiate an inflammatory response.

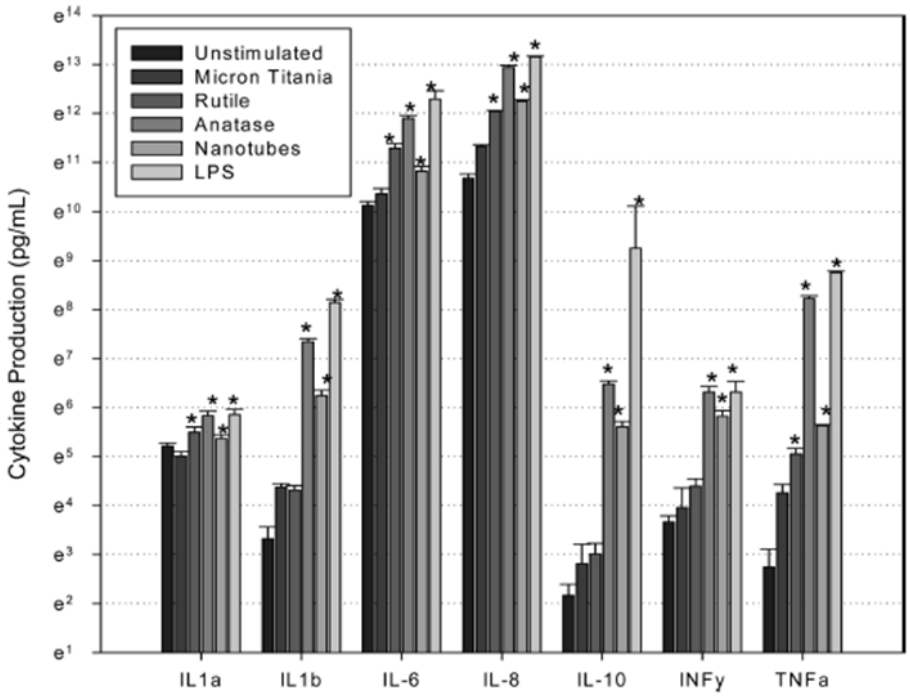

Figure 14. Nanoparticle treatment induces inflammatory cytokine production.

The PTE was treated with NPs or LPS (10 ng/mL) for 24 h and supernatant were examined. Increased proinflammatory cytokines in nanoparticle treatments over micrometer-sized titania was visualized across three donors with great consistency ($p \leq 0.05$ as compared to micrometer titania). Error bars represent mean ± SD for at least three donors.

Reactive Oxygen Species as a Component of Inflammation.

Having shown that nanoparticles induce inflammatory responses within the PTE construct, we questioned which mechanisms of inflammation might be triggered by the materials. While it is unlikely that nanoparticles interact with toll-like receptors because they lack the conserved patterns found on viral and bacterial pathogens that trigger this pathway of the inflammatory response, TiO_2 is highly photoreactive and has the potential to generate reactive oxygen intermediates in biological systems. These intermediates have damaging effects upon cell viability and function, and, in turn, stimulate innate immune responses [122]. To detect the presence of reactive oxygen species (ROS) in the PTE after 48 h treatment with the nanoparticle preparations, we used a 2,7-dichlorofluorescein (DCF) assay.

Briefly, nonfluorescent fluorescein derivatives (reduced dichlorofluorescein, DCFH) are placed into the culture medium, and after being oxidized by ROS, these compounds fluoresce. By quantifying total fluorescence, we were able to quantify the total ROS by flow cytometry. Figure 15 clearly shows a 10-20 fold increase in the ROS levels in PBMCs and HUVECs following 48-h treatment with the TiO_2 nanoparticles distinct from the micrometer titania, which resembles the untreated control profile. In addition, we investigated the constituent cell lineages of PBMCs (CD3, CD4, CD8, CD19, and CD14) to determine if any single subpopulation was biased toward production of ROS. Antibodies to the cell surface markers listed above were used to stain the nanoparticle-treated PBMCs that were subsequently analyzed by flow cytometry. We found that the greatest ratio of ROS producers were $CD14^+$ (monocytes), with over 80% of the total $CD14^+$ population positive for DCF expression (data not shown). Thus, it should be noted that the resulting increased ROS production is likely coming primarily from a cellular source (such as NADPH oxidase) and not directly from the chemical reactivity of titanium dioxide. However it is not yet clear whether low level ROS production, mediated through the chemistry or crystal structure of the nanoparticle is responsible for triggering the ROS response by the monocytes. Nonetheless, this is consistent with previous findings that phagocytes are responsible for the majority of ROS generation in mounting an inflammatory response in vivo [123-125]. While the ROS generation between different nanoparticle architectures was not equivalent, it is difficult to state any correlation of ROS production linked to particle dimension. However, it is clear that the material properties of nanotitanium dioxide invoke a more pronounced level of ROS in both HUVEC and PBMCs beyond the null and micrometer titanium dioxide treated cultures, as previously reported in other culture models [126]. The absence of an increase in both proinflammatory cytokines and ROS in the micrometer titania treated cultures suggests the behavior of nanotitanium mediates a proinflammatory effect as previously reported with other nanomaterials [127]. However, ROS generation is not the only pathway to consider

for the induction of an immune response to nanomaterials, it is likely that ROS participates in a conglomerate of steps that lead to innate immune activation. It is believed that activation of the inflammasome is a central feature to activating the innate immune system prior to the initiation of an effective adaptive immune response. Recent reports have concluded that nanoparticles may have the capacity to activate the inflammasome pathway via signaling both TLR and NLRP3 in antigen-presenting cells leading to the increased production of proinflammatory cytokine IL-1β [128, 129]. The authors have observed such an increase in IL-1β (Figure 14) upon treatment with nanoparticles and propose to include in future studies an assessment of inflammasome activation in response to ROS and other "danger signals" as an alternative mechanism of innate immune activation by nanomaterials.

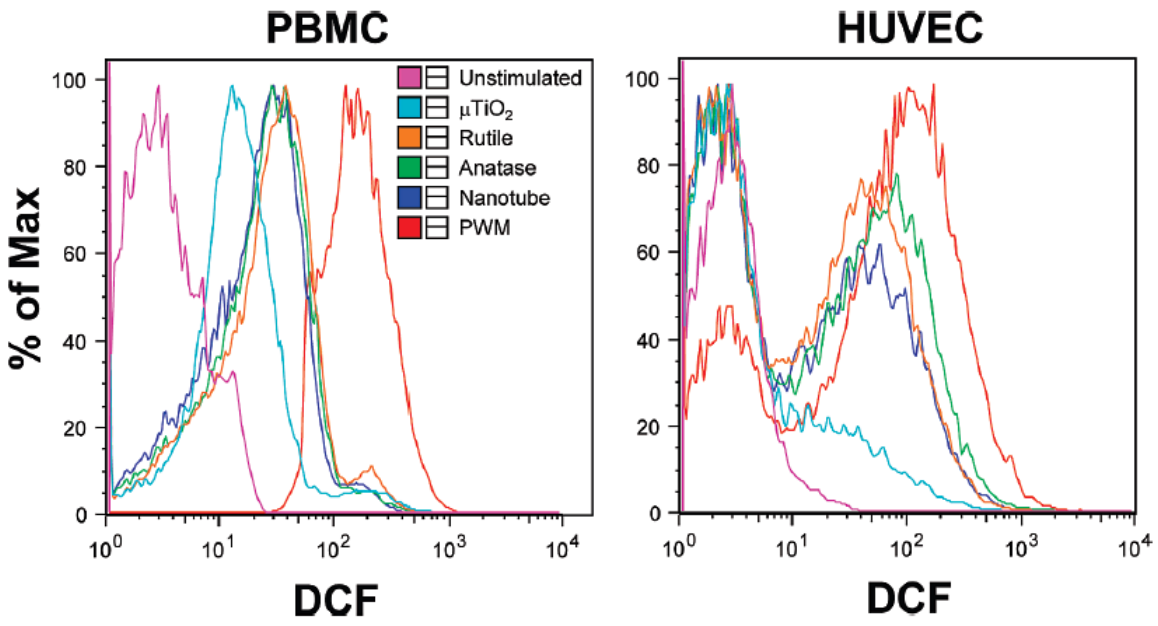

Figure 15. Nanoparticles induce ROS production in primary tissue culture models.

HUVEC cells and PBMCs were exposed to TiO2 nanoparticles or PWM at concentrations. ROS production was assessed with DCF-DA after a 24 h NP exposure and acquired by flow cytometry. Analysis is gated on live cells only. Plots are representative of several independent experiments.

Effect of Nanoparticles on DC Maturation and Function

DCs are a unique antigen-presenting cell (APC) population that can both participate in inflammatory reactions, by producing a variety of inflammatory mediators, and directly respond to the product of these innate pathways by undergoing a process of maturation that allows them to become more potent inducers of the adaptive arm of the immune response. In the absence of stimuli, the vast majority of DCs are immature. Uptake and processing of antigen in combination with the aforementioned inflammatory signals matures them into potent DCs capable of initiating antigen-specific primary and secondary immune responses when combined with lymphocytes. It is unclear whether or not treatment with nanoparticles can trigger DC maturation, but the ability of nanoscale TiO_2 to induce ROS in phagocytes suggests the possibility that these materials might activate this potent APC population. Previous reports have described nanoparticle uptake by APCs, supporting the pathway of APC activation [130].

DCs for research and clinical applications are typically derived from purified blood monocytes and are cultured in a cocktail of cytokines for a week or more [131]. The caveat being that these DCs are harvested as a highly synchronized and uniform population of cells, uncharacteristic of the DC populations found in vivo [132]. An asset of the PTE model is its ability to generate DCs without the use of exogenous factors, in a HUVEC driven system, recapitulating their growth and diversity in vivo [13]. Within this construct, DC maturation can be tied to the increased expression of the activation markers, CD1a and CD83, similar to what is observed in vivo. Additionally, the expression of chemokine receptor complex CCR7 is associated with the control of immature and mature DC migration in vivo, and has been shown to increase on PTE-derived DCs following treatment of the construct with known inflammatory stimuli [5, 6, 37].

Treatment of the PTE with nanoparticles generated a population shift from a precursor DC phenotype, traditionally CD14and HLA-DR, to an increased number of immature and mature DC phenotype CD14/HLADR^{low}, CD14/HLA-DR^{high}, respectively [13]. Analysis of the nanoparticle TiO_2 stimulated CD14/HLA-DR population demonstrated significantly enhanced expression of mature DC-specific marker CD83, secondary lymphoid tissue-directing chemokine receptor CCR7 and the costimulatory molecule CD86 compared to unstimulated and micrometer controls and was similar to cultures stimulated with LPS (Figure 16). There is an approximate 3-fold increase in DC-specific maturation marker CD83 expression on DCs treated with anatase, rutile, and nanotubes over those given micrometer- sized titania ($p<0.05$). This shift can be explained by inflammation of the resident DC population from phagocytosis and exposure to soluble nanoparticles and perhaps synergy with the inflamed endothelial cells in the PTE. The increase in CD86 and CCR7 indicate the DCs maturing ability for the costimulation of lymphocytes, triggering their subsequent activation and proliferation as seen in vivo, further suggesting the potential to drive such an adaptive response.

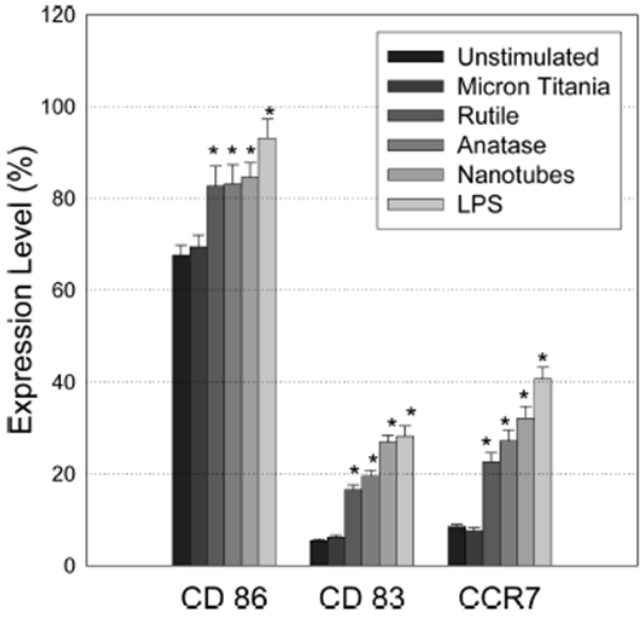

Figure 16. DCs increase expression of maturation markers upon stimulation with nanoparticles.

The PTE was loaded with PBMCs which were incubated for 90 min to allow migration of the APC population. Nonmigrated cells were then removed and the cultures were incubated for 24 h. Nanoparticles were then applied and subsequently incubated for 24 h. The reverse transmigratory (RT) DC fraction was then harvested and labeled with specific antibodies against DC surface receptors. Treatment with nanotubes resulted in approximately 15% increase in maturation marker expression as compared to the micrometer titania treated cells ($p \leq 0.05$ as compared to micrometer titania). Bars indicate expression level, MFI, of surface proteins from the migrated RT fraction. Analysis includes only live gated monocytes. Error bars represent mean ± SD for at least three donors.

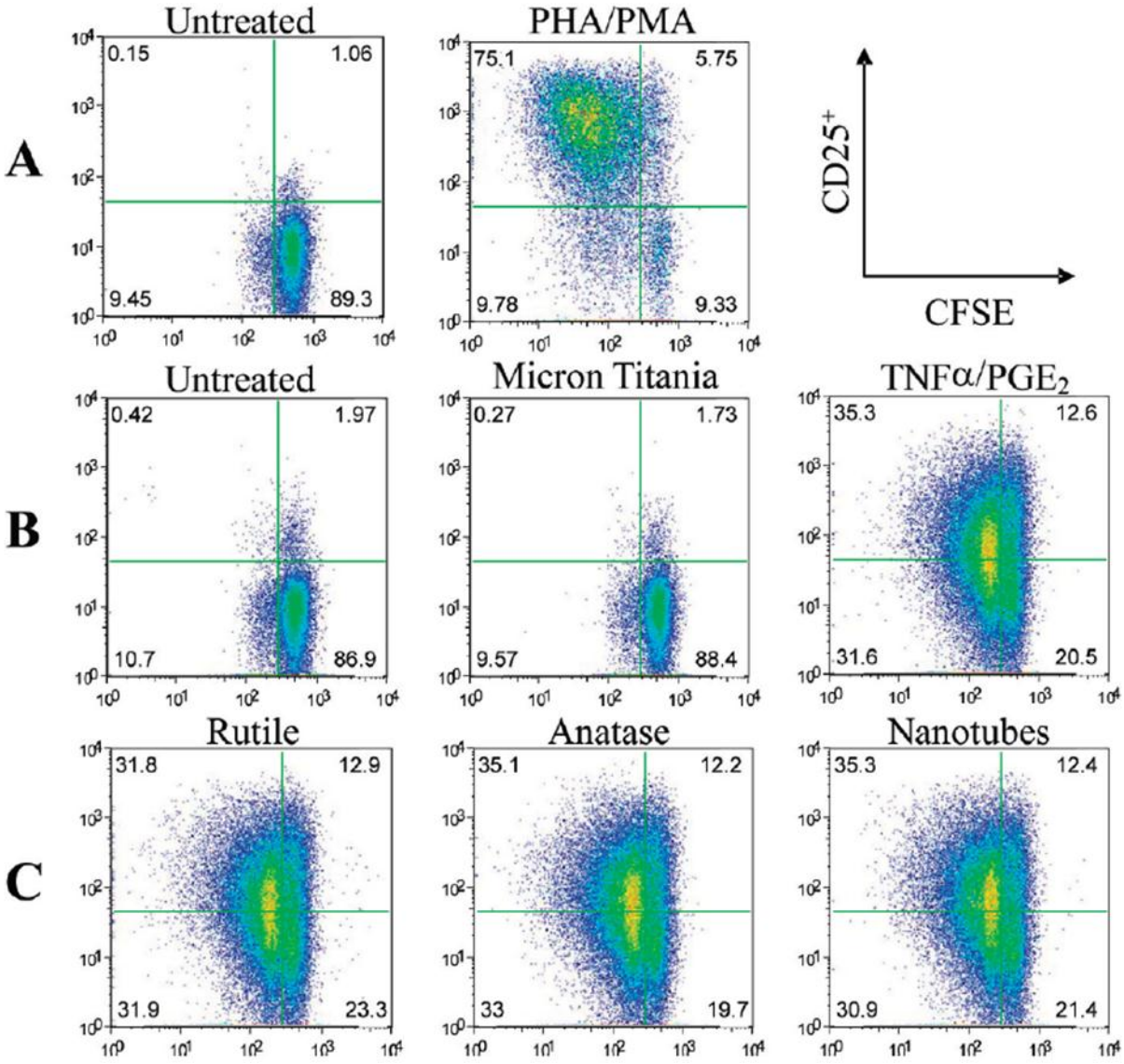

Figure 17. Nanoparticle-treated DCs induced proliferation of allogeneic naive CD4$^+$ T cells.

(A) Naïve CD4$^+$ T cells were untreated or stimulated with PHA and PMA in the absence of DCs. (B) Control conditions. (C) Naïve CD4$^+$ T cells, primed with HUVEC-derived DCs pulsed with nanomaterials for 24 h, were cultured for 5 days. Proliferative response and T-cell activation were determined by FACS as a measure of CFSE dilution and CD25 expression, respectively. Data are representative of five donors

Nanoparticle-Pulsed DCs Efficiently Prime Allogeneic Naïve $CD4^+$ T Cells

The capacity of nanoparticle-pulsed DCs to activate allogeneic naïve $CD4^+$ T cells ($CD45RA^+CD45RO^-$) was assessed by carboxyfluorescein succinimidyl ester (CFSE) dilution and $CD25^+$ expression (Figure 17). Activation of T cells will lead to the upregulation of CD25 surface expression and to proliferation of these cells as measured by CFSE diminution. Indeed, DCs treated with nanoparticles were powerful stimulators of naïve $CD4^+$ T cell proliferation and CD25 expression. Panel A shows the basal level of activation in the untreated control compared to those treated with phytohemagglutinin/phorbol myristate acetate (PHA/ PMA) in the absence of DCs. Panels B and C both show the proliferative response with the addition of DCs to the T cells. DCs were either unpulsed or pulsed with nanomaterials or given a maturation cocktail of TNFα and PGE_2. The proliferative activation of the T cells primed with nanomaterial pulsed DCs mimics the response of the T cells primed with matured DCs. Thus, TiO_2 nanomaterials are powerful inducers of naïve $CD4^+$ T-cell proliferation.

This investigation assessed the immunogenicity of nanostructured TiO_2 through the use of a model of human immunity, the MIMIC system. Currently, the literature is divergent on the biocompatibility of nanostructured TiO_2. Previous studies suggesting the biocompatibility of these particles have been established through growth and viability assays of primary or cancer lines where nanostructured TiO_2 provides a biomemetic support as a film or other coating. Indeed, physical analysis of nanostructured TiO_2 films revealed a granularity and porosity that mimics the natural extracellular matrix; such nanotopography has repeatedly been shown to enhance cell adhesion making TiO_2 films a suitable substrate for cell-based and tissue-based applications as mentioned in the introduction [89, 92]. However, the behavior of nanostructured TiO_2 as a thin film may be vastly different than that of free particulate nanostructured TiO_2. This study adds to previous reports that have shown TiO_2 nanoparticles

to be cyto/genotoxic and immunogenic when delivered into animal or cell culture models [102, 133, 134]. Cumulatively, these studies represent a schism in nanostructured TiO_2 biocompatibility. We have investigated nanoparticles using an alternative approach focused on human immunity that we believe has illuminated some of the controversy of TiO_2 biocompatibility. Our data has shown TiO_2 nanoparticles generate an immune response through the confluence of increased proinflammatory cytokine production and ROS generation. These precursory steps of activation assist in DC maturation upon exposure to these nanoparticles and facilitates the functionality of the nanoparticle pulsed DCs to activate naïve $CD4^+$ T cells and initiate lymphoproliferation. The lack of response above unstimulated control from the micrometer-sized TiO_2 particles coupled with the data from studies on nanostructured film suggest that larger particles, or those that have been cluster-assembled, remain inert and biocompatible while free TiO_2 nanoparticles may represent a health hazard.

Utilization of the MIMIC system has shown that nanoscale TiO_2 can initiate a cascade of events from activation of the endothelium to produce proinflammatory cytokines which lead to the maturation of resident DCs that, in turn, can regulate effector cell responses. This may seem confounding when compared to previous studies which have shown cells cannot specifically target materials that lack a protein recognition motif [135]. However, it has been shown more recently that TiO_2 antigens may be formed based on protein binding to TiO_2 nanoparticles, potentially influencing their activity in vivo [111]. The data above display that nanomaterials can activate DCs, even if only in a nonspecific inflammatory manner, which has major implications for autoimmune induction and instigating allergic reactivity. However, our studies also demonstrate that these nanomaterials may perform as effective adjuvants for use in vaccines because they have the capacity to not only stimulate the innate response but also initiate the adaptive arm through their interactions with DCs. The use of the in vitro human immune model (MIMIC system) on these sets of TiO_2 nanomaterials has revealed their inflammatory potential;

and may provide an immunological platform with broad application capable to rapidly evaluate a wide range of chemicals and materials in a physiologically relevant manner. This tool may find applications for the broader nanoscience and environmental science community to accurately address potential concerns over the immunotoxicology of nanomaterials.

Acknowledgments

I greatly appreciate Dr. Anthony Byers' careful review of the document. Vaxdesign's contribution was funded by the DARPA/Defense Sciences Office RVA Phase II Program and the work performed at UCF was funded by NSF grant CBET-0711239 to S.S. and W.S.

CHAPTER FOUR: CeO_2 AND TiO_2 NANOPARTICLES: DIVERGENT CATALYTIC BEHAVIOR DRIVES T_H1/T_H2 RESPONSE POLARIZATION

Abridgment

The previous work had annotated that small NP-size was responsible for inducing the pro-inflammatory effects to the cells of the human immune system. While this observation is now widely accepted, at the time of publication size-induced effects were a point of contention. This work prompted us to further investigate how other physicochemical features might influence the immune system. Namely, little remains known about the effect of material surface reactivity towards the status of the immune system. Since our previous work was established using TiO_2 as a model NP, we chose to use a material with opposite catalytic potential, namely CeO_2 NPs. Examining these materials in parallel offered us a unique opportunity to explore the effect nanocatalysts have on immunity.

Examination of catalytic nanoparticle-induced human immunomodulation has been scarcely explored. We investigated in parallel the effects of two catalytic nanoparticles, TiO_2 (oxidant) and CeO_2 (antioxidant), towards innate and adaptive immunity. We focused on the effect these nanoparticles had on human dendritic cells and T_H cells as a strategy towards defining their impact to cellular immunity. Combined, we report that TiO_2 nanoparticles potentiate DC maturation inducing the secretion of IL-12p70 and IL-1B, while treatment with CeO_2 nanoparticles induced IL-10, a hallmark of suppression. When delivered to T cells alone TiO_2 nanoparticles induced stronger proliferation in comparison to CeO_2 which also stimulated T_{Reg} differentiation. When co-cultured in allogeneic T cell assays, the materials directed alternate T_H polarization whereby TiO_2 drives largely a T_H1 dominate response, whereas CeO_2 drove a T_H2 bias. Combined, identifying immunomodulatory nanoparticles can provide researchers directions for nanomaterial development to specifically target or avoid immune consequences.

Introduction

Nanoparticles (NPs) are a ubiquitous staple of modern life, yet many questions remain as to how these materials affect human physiology. For instance, CeO_2 NPs have shown great promise at protecting tissues from oxidative stress and have been proposed as a modality to alleviate damage to surrounding healthy tissue following cancer radiation therapy [136-138]. However, some NPs have also been revealed to negatively impact human health, such as metallic NPs inducing acute toxicity to pulmonary and renal tissues [139]. Similar to foreign substances captured within the bloodstream or mucosa, NPs are likely to encounter a parallel fate where they will ultimately interact with the immune system since it functions as the principal responder to exogenous threats against human health. This has led to growing interest in understanding how these materials will interact with cells of the immune system considering observations that immune cells act to eliminate or interact with NPs in the bloodstream [140]. Adding concern to this interest is the fact that nanoparticles have many different and tunable physicochemical properties, including size, shape, chemical composition, solubility, and surface chemistry that can influence their interaction with the immune system.

Despite multiple studies detailing the influence of size, solubility, and surface modification on the biocompatibility of nanoparticles and their use in biological applications[141], only a limited number of studies have directly examined how the varied physical characteristics of NPs affect their interaction with the human immune system. Published studies from our laboratory and other groups have concluded that the inflammatory potential of NPs was inversely proportional to NP size [142-144]. Additionally, the surface charge of NPs has been shown to facilitate their binding to proteins or other macromolecules, leading to macromolecular complex formation or changes in protein conformation that can alter their immunogenicity or give rise to other potentially deleterious consequences [145].

Finally, studies have also suggested that the catalytic physicochemical properties (redox-active surface groups) are paramount to NP functionality. For example, preliminary studies on oxidizing catalytic NPs reveal their tendency to be proinflammatory [146, 147], yet the impact of these studies is dampened because these catalytic NPs were not directly compared against NPs with an opposite redox potential. In fact, few studies to date have examined whether antioxidant catalytic NPs impact immune function. Of all the physiochemical properties that could most profoundly modulate immunity, we think is perhaps most important since catalytic NPs have a unique capacity to directly modulate reactive oxygen species (ROS), which are well-established through a variety of mechanisms to regulate immune reactions [148].

To address the limitations in our understanding of how the oxidant properties of NPs affect their capacity to influence the immune system, we performed a study to examine the immunomodulatory effects of two particles with opposing redox potentials. Specifically, we utilized two NPs which can couple either oxidative (TiO_2) or reductive (CeO_2) reactions to provide us insight into how these disparate redox chemistries may impact the cellular redox environment and lead to immunomodulation. We examined viability, phenotype, uptake, ROS production, and functional influence on DC-T_H cell interaction and T cell proliferation following NP exposure in an in vitro model of human immunity. Intriguingly, we noted that CeO_2 NPs were uniquely capable of stimulating DCs to produce IL-10 and when co-cultured with T cells were capable of inducing T_H2 cytokines while TiO_2 NPs induced DCs to produce IL-12 and pushed a T_H1 polarized T cell program. We report these redox-active NPs can potentiate innate immunity and arm distinct adaptive responses producing distinct T cell subset polarization outcomes perhaps attendant to their contrasting catalytic activity (TiO2 NPs. Oxidant; CeO2 NPs, antioxidant). These data provide evidence towards NP-induced immunomodulation of both human DCs and T helper cells with a directionality we believe remains linked to surface reactive

physicochemical properties, suggesting a novel basis for modulating immunity through tuning NP surface chemistry.

Materials and Methods

Reagents

Bacterial lipopolysaccharide (LPS), phytohaemagglutinin (PHA), and phorbol 12-myristate 13-acetate (PMA) were obtained from Sigma (St. Louis, MO). ROS levels were determined using 2-,7-dichlorodihydrofluorescein diacetate (DCF; Sigma). The NLRP3 inhibitor glybenclamide was purchased from Sigma.

Synthesis of NPs

TiO_2 NPs were synthesized by wet chemical synthesis as previously described (Schanen 2009). Briefly, a 50:50 mixture of ultrapure ethanol (Sigma) and deionized water (18.2 M) was boiled to reflux. The pH of the boiling solution was adjusted to 3.0 with the addition of 1 N HCl. Titanium isopropoxide (Sigma) was added slowly to this refluxing mixture which precipitates immediately to a white solution. The solution was then stirred at 85 °C for 4 hours. The white solution was then cooled to room temperature and washed several times with ethanol until dry. The final preparation was mostly anatase (partially amorphous) TiO_2. CeO_2 NPs were synthesized using wet-chemical synthesis as described previously [149]. Briefly cerium nitrate hexahydrate was dissolved in deionized water (18.2 MΩ). A stoichiometric amount of hydrogen peroxide was added as an oxidizer and immediately resulted in the formation of cerium oxide NPs. The NP powder was obtained by washing the precipitate of CeO_2 NPs

several times with acetone and water to remove the surfactant used in the synthesis process. The solution was aged further to allow the slow reduction of surface cerium from 4^+ oxidation state to 3^+ oxidation state in acidic medium by maintaining the pH of the suspension below 3.5 with nitric acid.

Characterization

The NPs were analyzed using high resolution transmission electron microscopy (HRTEM) (Philips 300 TECNAI operated at 300 kV) to confirm the shape, size, and morphology of the NPs. The HRTEM samples were prepared by dipping a polycarbon-coated copper grid into a dilute suspension of NPs dispersed in acetone. Surface area of the NPs were measured based on physical adsorption of ultra-high purity nitrogen gas at liquid nitrogen temperature on 100 mg of NPs using a Brunauer-Emmett-Teller (BET) Nova 4200e instrument manufactured by Quantachrome (Boynton Beach, FL). The samples were prepared in quartz tube and degassed at 240°C in vacuum for 3 hours before actual measurement. The size of the NPs was determined by dynamic light scattering method using the Zetasizer Nano manufactured by Malvern Instruments (Worcestershire, UK). The physical characterization of the materials is reviewed in table 8.

Evaluation of Endotoxin Contamination

All NP preparations were confirmed negative for the presence of endotoxin contamination using the FDA-approved Endosafe LAL colorimetric and turbidimetric assay systems (Charles River Laboratories, Wilmington, MA).

Human Donors and PBMC Isolations

The assays used PBMCs from healthy donors who provided informed consent and were enrolled in a sanofi pasteur – VaxDesign Campus apheresis study program (protocol CRRI 0906009). Blood collections were performed at Florida's Blood Centers (Orlando, FL) using standard techniques approved by their institutional review board. Within hours following their harvest from the donor, the enriched leukocytes were centrifuged over a Ficoll-plaque PLUS (GE Healthcare, Piscataway, NJ) density gradient [52, 53]. PBMCs at the interface were collected, washed, and cryopreserved in IMDM media (Lonza, Walkersville, MD) containing autologous serum and DMSO (Sigma-Aldrich, St. Louis, MO).

Generation of Cytokine-Derived DCs

DCs used throughout the assays of this study were prepared using our previously published methodology [52]. Briefly, monocytes were purified from total PBMCs by positive magnetic bead selection (Miltenyi Biotec, Cologne, Germany) and cultured for 7 days in X-VIVO 15 (Lonza) serum-free media supplemented with GM-CSF (R&D Systems, Minneapolis, MN) and IL-4 (R & D Systems). In all assay conditions described below, treatments were delivered on day 6 followed by harvesting on day 7 for incorporation into the various assays.

ROS Determination

DCs were cultured into 12-well dishes at a density of $2.5x10^6$ cells per well in 2.5mL. The cultures were then treated with serial dilutions of TiO_2 NPs and CeO_2 NPs for 24 h. Subsequently, cultures were treated at room temperature for 30 min with DCF at a final concentration of 10 µM. Cells were washed

of excess dye with DPBS, harvested using cell dissociation solution (Sigma), and washed again in DPBS. Fluorescence in the FITC channel from absorbed and oxidized DCF (indicative of peroxide levels) was analyzed by flow cytometry using an LSR II (BD Pharmingen, San Diego, CA). FlowJo software (Treestar, Ashland, OR) was used for data analysis.

DC Phenotyping

For flow cytometry analysis of surface molecule expression, DCs were washed in fluorescence-activated cell sorting buffer (FACS, 0.1% sodium azide and 0.1% bovine serum albumin in phosphate buffer saline). Fc receptors were blocked with 10% mouse serum (Jackson ImmunoResearch, West Grove, PA) for 10 minutes at 4°C to prevent nonspecific binding. DCs were then stained with a vital dye and incubated at 4°C for 20 minutes. After washing away excess viability dye with PBS, the cells were then incubated with the appropriate antibody cocktail for 20 minutes on ice. The antibodies used in the staining panels include allophycocyanin-Cy7-labeled HLA- DR (LN3), eFluor 450-labeled CD14 (61D3), fluorescein isothiocyanate-labeled CD40 (5C3), phycoerythrin-labeled CD80 (2D10.4), allophycocyanin-labeled CD83 (HB15e), fluorescein isothiocyanate-labeled CD86 (IT2.2), Peridinin chlorophyll protein (PerCP)-Cy5.5 -labeled CD19 (SJ25C1), Peridinin chlorophyll protein (PerCP)-Cy5.5 -labeled CD3 (OKT3), allophycocyanin -labeled CD209 (LWC06), and phycoerythrin-Cy7-labeled CCR7 (3D12). CD14, CD11c, HLA-DR, CD40, CD19, CD3, CD80, CD83, CD86, CCR7 were purchased from eBioscience (San Diego, CA). CD209 was purchased from BD Pharmigen. Following staining, cells were washed in FACS buffer and immediately acquired on a BD LSRII flow cytometer (Becton Dickinson), and data analyzed using FlowJo software V9.2 (Tree Star).

Cellular Uptake

Samples treated for 24 hours with TiO_2 or CeO_2 NPs were harvested, washed and were placed in 70% nitric acid overnight to start the digestion process. Samples were then microwave digested. The temperature was steadily increased to 200°C over a 20 minute period and held for 20 minutes at 200°C. Samples were then boiled down to less than 1 ml each and reconstituted in water to an exact volume of 10 ml. Titanium and cerium levels were assessed using inductively coupled plasma mass spectroscopy (ICP-MS).

Luminex Cytokine Quantification Analysis

Supernatant from the treated DC culture wells and DC:T cell co-cultures were collected and analyzed for cytokine production by means of the BIOPLEX Multiplexing array system (Bio-Rad, Hercules, CA) as previously described [144].

$CD4^+$ T Cell Proliferation and induction of T_{regs}

Human $CD4^+$ T cells were isolated from human peripheral mononuclear cells (PBMC) of healthy blood donors by positive selection using EasySEP $CD4^+$ T cell isolation kit II (Stem Cell Technologies, Vancouver, Canada). Purified $CD4^+$ T cells were then carboxyfluorescein succinimidyl ester (CFSE)-labeled to follow proliferation and incubated either in the presence of the described NPs with or without PHA/PMA or without stimulation and left in culture for 5 days. For Treg analysis the T cells were co-cultured with DCs matured with TNFα and PGE_2 for 7 days as previously described [150]. The cells were

harvested, and examined by flow cytometry using LIVE/DEAD AQUA (PACIFIC ORANGE; Invitrogen), $CD4^+$ (Pacific Blue; eBioscience), CD25 (APC; eBioscience), Foxp3 (PE; BioLegend) and CFSE (FITC; Invitrogen) using a BD LSRII flow cytometer (Becton Dickinson), and data analyzed using FlowJo software V9.2 (Tree Star).

Naïve $CD4^+$ T Cell Allogeneic Stimulation Assay

DCs were either untouched, matured with a cocktail of TNFα and PGE_2 as a positive control, or were exposed to various doses of NPs for 24 hours prior to being harvested. The treated DCs were harvested and added at an optimized ratio of 1:400 to allogeneic naïve $CD4^+$ T cells isolated using EasySEP $CD4^+$ T cell isolation kit II (Stem Cell Technologies) and labeled with CFSE (Invitrogen). Here, PHA/PMA (1 μg/mL; 50 ng/mL) was used not only as a positive control for T cell proliferation, but also added in combination with NPs additionally added to the co-culture wells where described. After five days the cultures were harvested and stained for CD25, CD3, CD4, (eBioscience) and Live/Dead Aqua for viability (Invitrogen) and then acquired by flow cytometry using BD Pharmingen's LSR II as described above. Supernants were collected and examined for cytokine analysis.

Data Plotting and Statistical Analysis

Each experiment was repeated with at least three donors or more where described in the figure legend. Analyzed statistical results were determined using a paired students t-test. Statistical significance was considered at $p<0.05$. All graphs were produced using GraphPad Prism software V5 (La Jolla, CA).

Results

NP Characteristics

While it is well-established that NPs can affect human physiology, including the immune system, many questions remain as to how they mediate these effects. Of particular interest to us was to determine whether catalytic physicochemical properties of NPs, such as surface reactivity, impact their potential to modulate the immune system. For this purpose, we performed a parallel evaluation of the capacity of TiO_2 and CeO_2 NPs, which have opposite catalytic activities, to stimulate immune cell activation in an in vitro model of the human immune system. Since it is also possible other features of the NPs, such as agglomeration potential and purity can affect immune function [151], we were careful to first perform a variety of assessments to fully characterize the particles before initiating immunoassays (Figure 18). (See the *Materials and Methods* section for a detailed description of this process.) Fortuitously, we found both NPs had a low agglomeration tendency after 24 hours of incubating the NPs in X-VIVO 15 serum-free culture media that was used in all of the biological assays discussed below.

Table 8. Physical properties of nanomaterials investigated.

Particles	Preparation Method	Diameter (nm)	BET Surface (m^2/g)	Zeta Potential (mV)*	Surface Reactivity	Crystal Structure
TiO_2	HT-WCS[1]	7-10[†]	239	-9.84	Oxidative	Anatase
CeO_2	RT-WCS[2]	3-5[†]	90	-10.01	Reductive	Fluorite

[1]High temperature wet chemical synthesis. [2]Room temperature wet chemical synthesis. *Zeta potential after 24 hrs in X-VIVO 15 culture media. [†]Average diameter of NPs, expressed as mean size ± SD nm. Data gathered by Soumen Das.

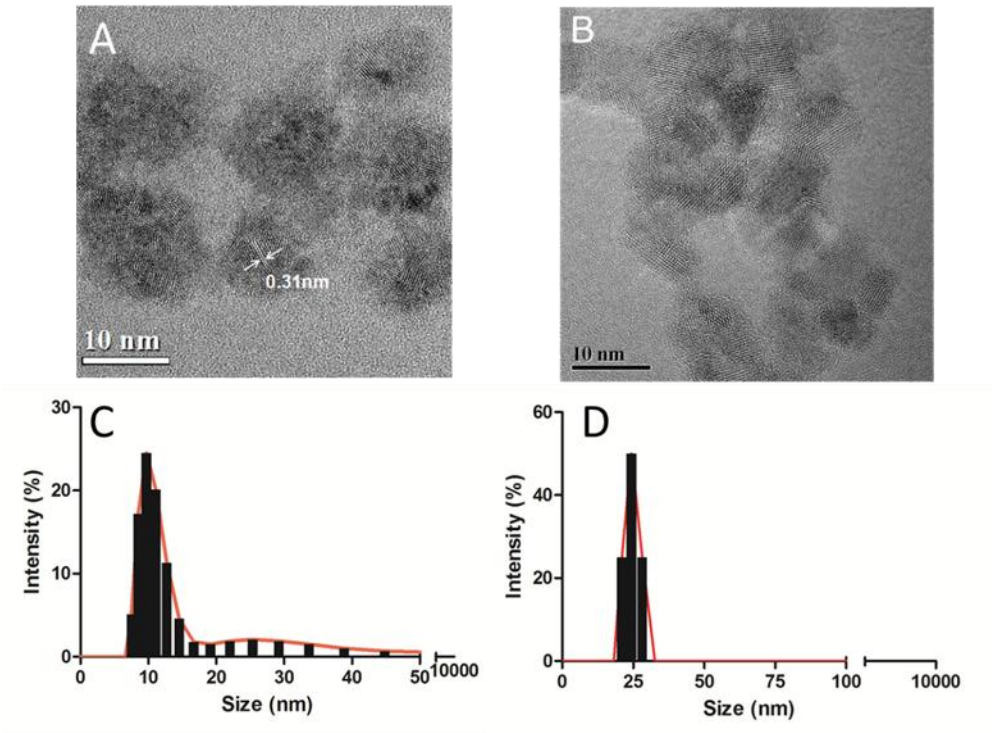

Figure 18. HRTEM of TiO_2 and CeO_2 NPs and their agglomeration status in X-VIVO 15 culture media determined by DLS.

High resolution transmission electron micrographs illustrate (A) freshly prepared CeO_2 NPs and (B) TiO_2 NPs and depict their formation into soft agglomerates of 10-15 nm. CeO_2 NPs composed of individual 3-5 nm nanocrystallites and 7-10 nm TiO_2 (anatase) NPs. Size distribution of 500 mM solution of (C) CeO_2 and (D) TiO_2 using dynamic light scattering. Figure captures by Soumen Das.

NP cytotoxicity to human DCs

We recognize NPs can interact with the immune system through a variety of mechanisms, but focused our evaluation principally on DCs since they are involved in many facets of innate and adaptive immunity. Although we had previous experience with the dosing range for TiO_2 NPs in our immune cell model [144], we felt it was necessary to establish these parameters for CeO_2 since they can provide a first-pass assessment of whether catalytic activity can affect the biological impact of the NPs in a dose-

dependent manner. Following a short-term treatment of the DCs with NPs, the cells were assessed with the fluorescent apoptotic dye (PO-PRO) in combination with a vital dye (7-AAD) to discriminate between live, dead, and apoptotic cells. Increased cell death or apoptosis was not observed in DCs exposed to CeO_2 NPs for 24-hours, while DCs treated with TiO_2 NPs for the same time period had an appreciable increase in the number of apoptotic and dead cells in a dose-dependent manner (Figure 19A). While our findings on TiO_2 NPs cytotoxicity in human DCs are consistent with our previous work and the observations of others using cell lines [144, 151-153], we are unaware of other studies demonstrating a high tolerance of human DCs for CeO_2 NPs.

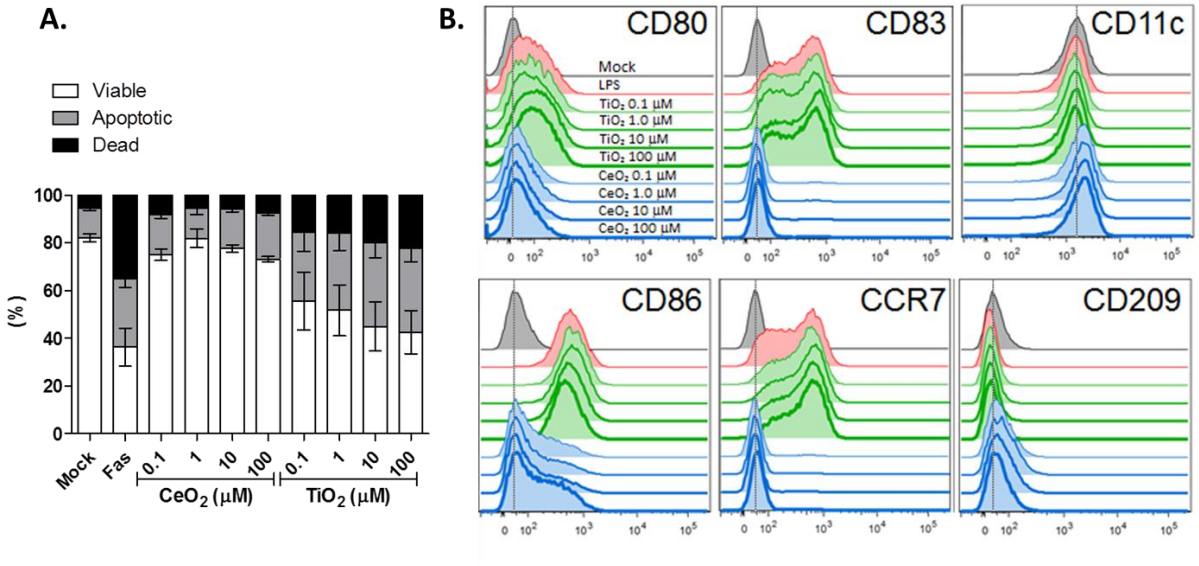

Figure 19. CeO_2 NPs have little cytotoxic or maturation effect to human DCs.

(A) Dendritic cells were exposed to the indicated concentrations of nanomaterials for 24 hrs and assessed for viability using 7-AAD. Apoptosis was assessed in human DCs by Po-Pro staining following 24 hour exposure with the indicated nanomaterials. As negative and positive controls, DCs were left untouched (mock) or were treated with 1μg/ml of Fas ligand (FAS), respectively. Bar graph data are plotted as mean (±SD) of viable, 7-AAD viability dye, or Po-Pro fluorescence. (B) Dendritic cells were exposed to the indicated concentrations of nanomaterials for 24 hours and assessed for phenotypic expression of appropriate human DC markers. DCs were stained with antibodies against the various markers and acquired by flow cytometry and analyzed using FlowJo software.

Phenotypic Maturation of DCs

NPs have previously been shown to have the capacity to activate DCs to undergo an innate maturation process, including altered surface marker profiles, that enhances their function [144, 154], in an effort to determine whether this immunostimulatory potential was driven, at least in part, by the oxidative activity of the TiO_2 particles, we directly compared DC activation/maturation triggered by TiO_2 with the anti-oxidant CeO_2 particles. As shown in Figure 2, DCs treated with as little as 1 μM of TiO_2 NPs increased surface expression of the maturation markers, CD80 and CD86, and increased HLA-DR, comparably to the level induced by the positive control, LPS. On the other hand, upregulation of CD83, a phenotypic hallmark of DC maturation, was only observed on DCs treated with a higher TiO_2 dose (100 μM). In concert with the observed costimulatory marker upregulation, we demonstrated that exposure to TiO_2 NPs and not CeO_2 NPs induced an increased level expression of the migratory-enhancing C-C chemokine receptor type 7, CCR7 (Figure 19B). CCR7 expression is significant to report because of its role in DC migration towards the lymph nodes where antigen presentation occurs, thus materials which upregulate CCR7 expression may enhance immunity. Interestingly, a 24-hour exposure of the DCs to CeO_2 NPs had no effect on CD83, CD80, CD86, and HLA-DR expression.

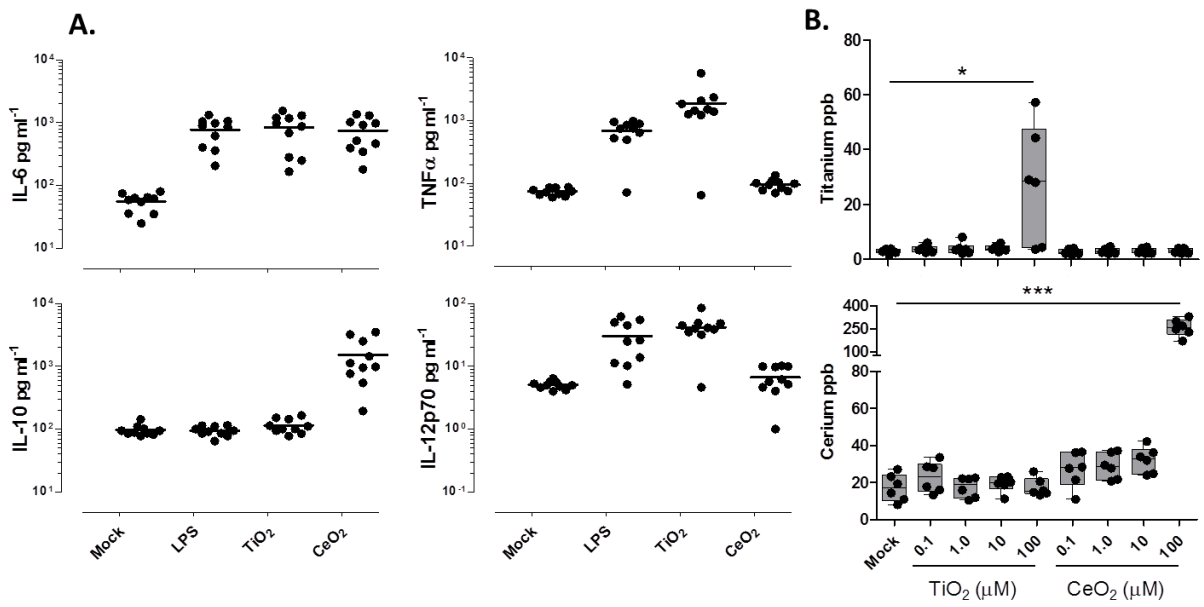

Figure 20. CeO_2 and TiO_2 NPs directly affect the cytokine secretion independent of uptake in DCs following 24 hour incubation.

(A) Supernatants from DCs stimulated with nanomaterials were examined for relevant cytokines. Each dot on the scatter plot represents the signal for an individual donor. Ten (10) donors were examined in total. (B) DCs were subjected to ICP-MS evaluation for metal analysis and ppb detection was determined. 6 donors were analyzed in total. Paired t-test was used for statistical analysis. ICP-MS performed by Chris Reilly.

Besides triggering changes in surface marker expression, maturation programs often stimulate DCs to secrete increased amounts of cytokines that modulate many facets of innate and adaptive immunity. Given that the CeO_2 particles failed to induce measurable phenotypic changes in DCs (Figure 19), we expected they would induce minimal innate cytokine secretion by the DCs. Curiously, though, we found that the CeO_2 particles were capable of stimulating IL-10 production in all the donors examined (Figure 20). On the other hand, TiO_2 particles stimulated strong cytokine responses of a pro-inflammatory slant (IL-12, TNFα) consistent with the DC maturation we observed in Figure 19A. Considering evidence that excessive oxidative stress can result in cytotoxicity and inflammation [155],

we suspect that the differential DC-stimulatory potentials of TiO_2 and CeO_2 NPs observed here might be explained by the opposite surface reactivates of the two particle types.

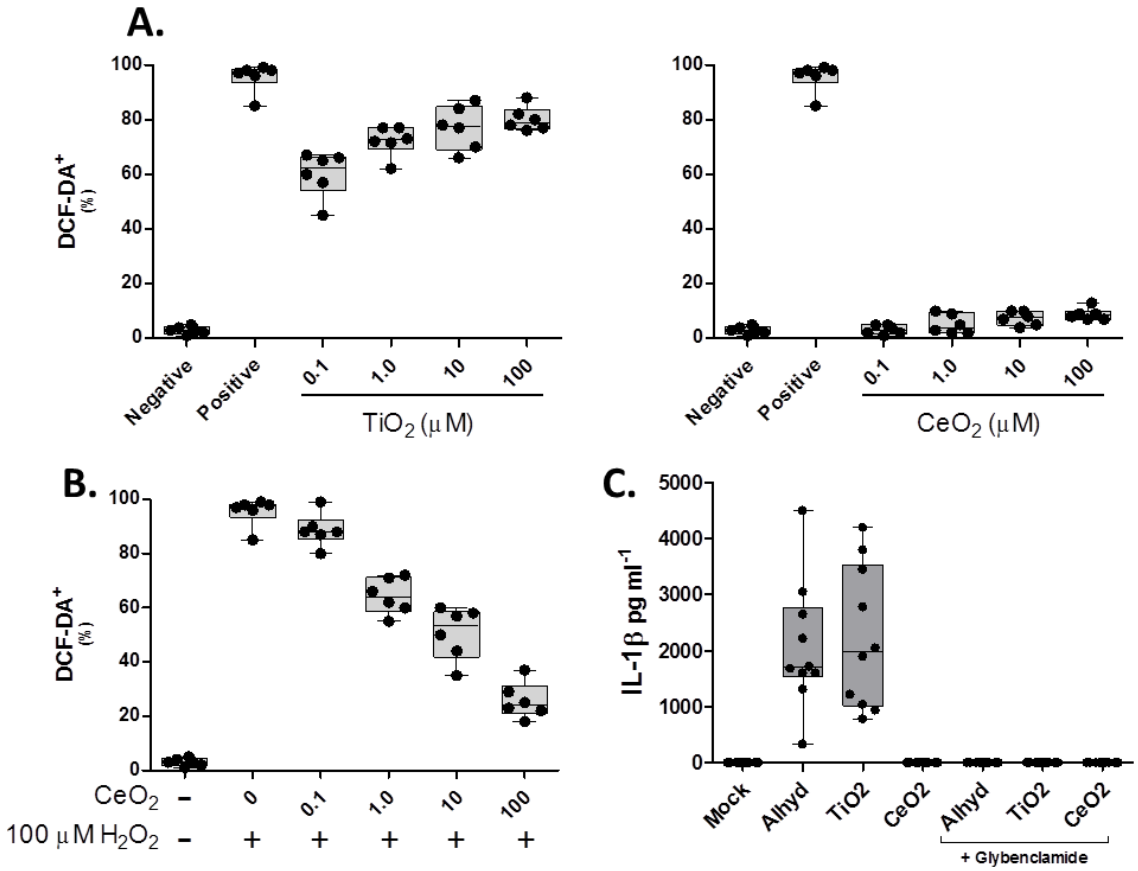

Figure 21. NP-redox dependent ROS production in DCs and activation of NLRP3 inflammasome by TiO_2.

(A) Human DCs were cultured in the absence or presence of the indicated treatment (for 24 hours prior to being examined for ROS. (B) DCs were cultured in the presence of cerium oxide at various concentrations for 8 hours prior to the addition of H_2O_2 for the rest of the 24 hour incubation. Oxidative stress was measured by DCF-DA fluorescence. n=6 patients. (C) DCs were stimulated for 24 hours with Alhydrogel (AlHy, 150 µg/ml) as a positive control for NLRP3 activation. Alternatively, TiO_2 NPs or CeO_2 NPS were delivered at 1 µM to the cultures for 24 hours prior to being measured for the presence of IL-1β in the presence or absence of NLRP3 inhibitor glybenclamide (50µM). Each data point is representative of an individual donor, n=10.

A possible explanation for the observed differences in immunostimulatory potential between TiO_2 and CeO_2 is that CeO_2 do not efficiently interact with DCs. Since ICP-MS has been used to detect NPs within the single digit part-per-billion range within cells [156], we adopted this methodology to examine for the presence of NPs within treated DCs (Figure 20B). We determined that uptake is dose dependent and detectable by ICP-MS at 100 μM for both NPs, leading us to further conclude that the difference between the NP surface chemistries has no influence on their frequency for uptake. It should be noted that in previous studies, uptake of TiO_2 was demonstrated only with much higher dosing (5mg/mL, 62.5mM) reaching only as low as 250μM in another study [157, 158]. Similarly, CeO_2 uptake has only been demonstrated with higher dosing in comparison to our study [159, 160]. Since both materials have the same propensity to be internalized, we speculate that perhaps the unique and opposite behavior of CeO_2 NPs in comparison to TiO_2 is a result of CeO_2 metal properties and reductive surface chemistry. Similar to this excogitation are studies where other antioxidants (reductive molecules) were shown to increase IL-10 production [161, 162].

Intracellular assessment of ROS

Based on our findings of differential activation induced by the CeO_2 and TiO_2 NPs, we pondered whether these differences could be related to the unique capacities of the NPs (TiO_2, oxidative; CeO_2, reductive) to differentially modulate intracellular ROS production. To address this possibility, we analyzed intracellular oxidative stress levels in NP-treated DCs using the intracellular DCF-DA dye, which fluoresces upon contact with ROS. Figure 4 reveals that TiO_2 NPs induced human DCs to generate ROS, in a dose-dependent manner, to levels comparable to the positive control, H_2O_2. Opposite to this were CeO_2 NP-treated DCs, which showed little to no production of ROS (Figure 21). To test the antioxidant

capacity of CeO_2 NPs we pre-treated DCs CeO_2 NPs followed by the addition of H_2O_2 as an oxidant to the cultures and examined the DCs to see if the CeO_2 pre-treatment had an ROS-mitigating effect (Figure 21B).

While ROS acts through a variety of downstream pathways to regulate/potentiate immune reactions, perhaps its most important feature is its ability to activate innate danger sensors, such as the NLRP3 inflammasome [163]. Since the detection of IL-1β has been routinely used as a readout of NLRP3 inflammasome activation [163], we used this cytokine as an indirect measure to examine our hypothesis that TiO_2 NPs, and not CeO2, can activate the NLRP3 inflammasome in human DCs (Figure 21C). Indeed, we found that TiO_2 NP treated DCs do secrete IL-1β, a result that is consistent with prior studies demonstrating TiO_2 NPs activate the NLRP3 inflammasome in mice [163]. In subsequent studies, we added a selective NLRP3 inhibitor, glybenclamide (50μM) [164], to some wells to directly show that TiO_2 NPs act through the NLRP3 inflammasome to induce IL-1b production. When TiO_2 NPs were co-administered with the NLRP3 inhibitor, IL-1β production was abolished (Figure 21C). This provided us with evidence that TiO_2-induced IL-1β production was strictly mediated through the NLRP3 pathway. In contrast to the activation of NLRP3 by TiO_2 NPs, we observed that CeO_2 NPs were unable to instigate IL-1β production. Because ROS is a critical messenger and component of how irritants like TiO_2 activate the NLRP3 inflammasome, it is likely that the lack of ROS-associated danger signaling prevents CeO_2 from activating NLRP3, consistent with its anti-inflammatory behavior.

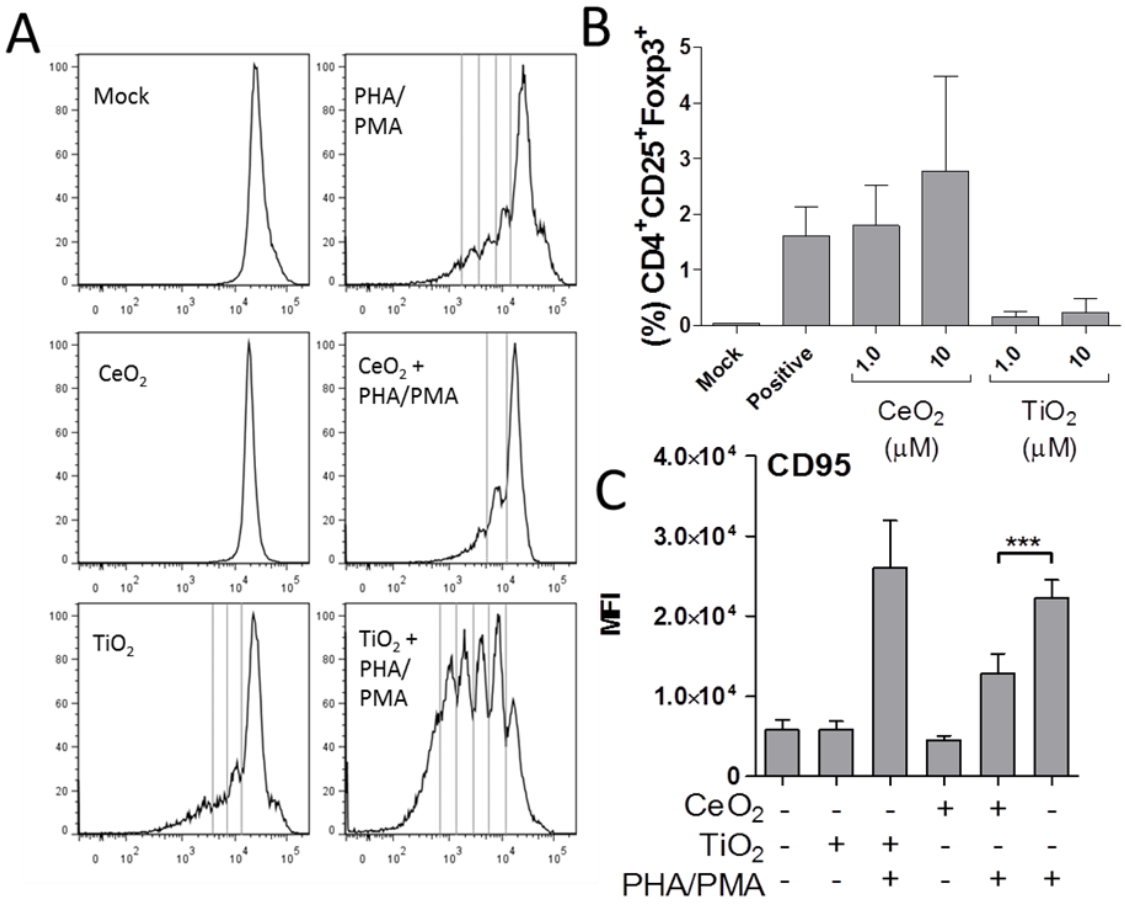

Figure 22. T cell stimulatory property of TiO_2 NPs and response suppression and induction of T_{REGS} by CeO_2 NPs.

(A) CD4+ T cells were isolated and cultured in the absence or presence of 10 µM TiO2 NPs , 10 µM CeO2 NPs, PHA, 10 µM TiO2 NPs with PHA, or 10 µM CeO2 NPs with PHA as indicated for 5 days. (B) Naïve T helpers were cultured in the presence of T cells untouched (mock), co-cultured with matured DCs, pulsed with CeO_2 NPs or TiO_2 NPs. The cultures were harvested on day 7 and stained for Foxp3+ expression. N=8 donors. (C) Reduced Fas expression in CeO_2 NPs/PHA treated cultures as compared to PHA alone. T cell cultures were stained for surface expression of CD95 and acquired using flow cytometry. The data was plotted as histogram overlays for each condition. Plots are representative of 3 donors, each with similar response profiles.

NPs Drive CD4$^+$ T cell Proliferation and T_H1/T_H2 Polarization

Following our finding that CeO_2 and TiO_2 provided DCs with distinct stimulatory/maturation cues, particularly regarding the unique cytokine responses shown in Figure 20, we pondered whether TiO_2 NPs and CeO_2 NPs would impact the capacity of DCs to induce naïve T cell activation. Prior to addressing this question, we felt it was important to demonstrate NPs do not directly activate T cells. Here, isolated CD4$^+$ T cells were simply labeled with CFSE to monitor proliferation and then incubated with the NPs for 24 hrs. To our surprise, TiO_2 had a modest immunostimulatory effect to the T cells, as demonstrated by their capacity to induce a 30% CFSE-low (divided) population. Furthermore, when co-administered with the strong mitogen combo, PHA/PMA, TiO_2 NPs amplified the proliferative response (Figure 22), while CeO_2 NPs moderately reduced the proliferating response (Figure 22A). Considering we observed that CeO_2 NPs had an anti-inflammaotry effect on the DCs, we decided to investigate the influence CeO_2 NPs had on induction of regulatory T cells (T_{Reg}) as determined by staining for Foxp3, a specific marker of T_{Regs} (Figure 5B). Here, we demonstrated the capacity for naked CeO_2 NPs to induce T_{Regs} differentiation. Additionally, since the expression of CD95 in resting T cells has been shown to increase under stress or disease conditions, we examined for modulation of this receptor which has implications in co-stimulatory and effector function [165]. Figure 22C clearly shows that there is a strong correlation for reduced CD95 expression in CeO_2 NP treated T_H cells as compared to the mitogen control or TiO_2 NP treatment. While this evidence doesn't tell us precisely how these NPs are interacting with T cells, the NPs are affecting T cell phenotype and function as measured by these assays.

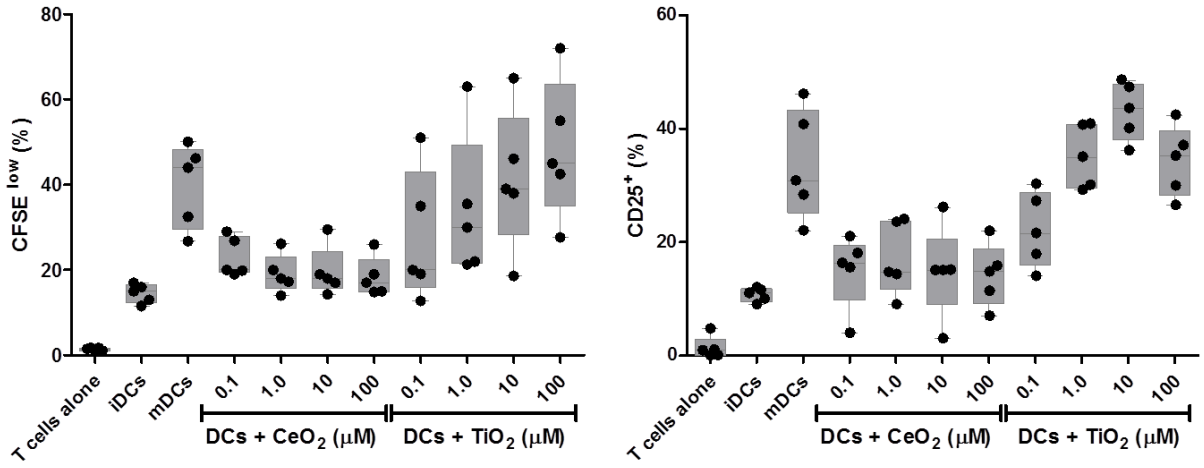

Figure 23. NP primed DCs differentially modulate CD4$^+$ T cells proliferation and CD25 surface expression in response to allogeneic challenge.

DCs were cultured in the absence (iDCs) or presence of the indicated nanomaterials (x-axis) or maturation cocktail of LPS/R848 (mDCs) for 24 hours. They were then harvested and co-cultured with mismatched donor naïve Th cells in the presence of the indicated treatments (legend).

To better define the impact catalytic NPs have towards adaptive immunity we investigated their influence on T cell function by co-culturing NP-treated DCs with mismatched (allogeneic) naïve T cells. With this approach, the engagement of MHC class II with TCR in an antigen-independent fashion is sufficient to induce the activation of the lymphocytes. Here, DCs were left untouched (iDC), matured with cytokine cocktail (mDC) as a control for stimulation of the APCs, or primed with CeO_2 or TiO_2 NPs before being co-cultured with allogeneic CD4$^+$ T cells. Priming the DCs with TiO_2 boosted the magnitude of naïve CD4$^+$ T cells to respond to allogeneic and mitogen challenge as compared to the iDC across the mock condition (Figure 23); whereas the CeO_2 NP-treated DCs had little influence on the proliferation. Indeed, there is a noticeable and disparate effect between the two materials when delivered into the co-culture.

Based on the lack of T cell proliferation in the CeO_2 NP condition, we expected little, if any, cytokine production by these T cells. In contrast, we expected the pro-inflammatory profile of the TiO_2

particles would induce the proliferating lymphocytes to secrete a variety of prototypic T cell cytokines. Instead, we observed both particles triggered cytokine responses, but the profiles were nearly opposite from each other TiO_2 NPs instigated greater production of more pro-inflammatory T_H1 cytokines (IL-2, IFN-γ), while CeO_2 NPs induced an increase in the levels of anti-inflammatory T_H2 cytokines (IL-4, IL-5, and IL-10) that promote humoral immunity. Beyond their capacity to induce a T_H2-biased T cell response, the CeO_2 particles were even capable of hampering the strong T_H1 program induced by mitogens (Figure 24). While we might have anticipated that a well described inflammatory particle like TiO_2 could drive a type 1 immune response, the observed effects induced by CeO_2 NPs such as IL-10 secretion by DCs (Figure 20), upregulation of T_{Regs}, modulation of T cell proliferation, and T_H2 polarization (Figure 22, 23 and 24) suggest a unique functional property of metallic antioxidant NPs that has been unidentified and may provide significant implications across a wide range of therapeutic and prophylactic applications.

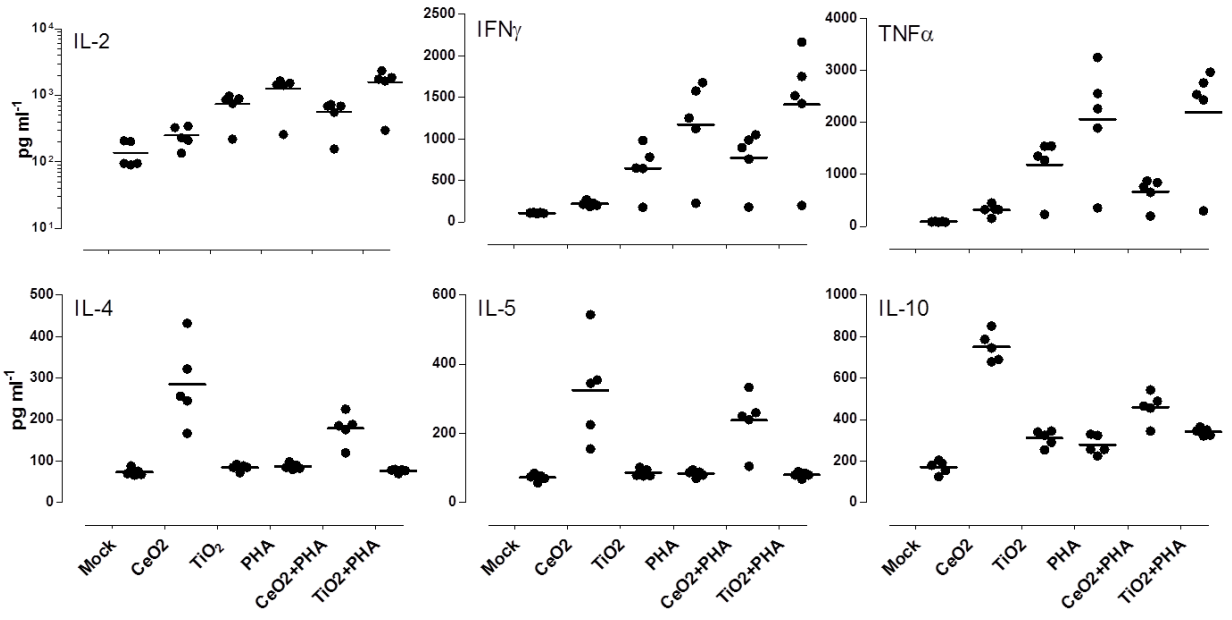

Figure 24. CeO_2 and TiO_2 NPs directly affect the cytokine secretion in human $CD4^+$ T cells following 24 hour incubation.

Supernatants from the T cell stimulatory assays were examined for Th1 and Th2 associated cytokines by BIOPLEX array. Each dot on the scatter plot represents the signal for an individual donor. 10 donors were examined in total.

Discussion

Few studies have targeted the functional impact NPs impose to human immunity. Specifically, we were concerned how catalytic surface physicochemical properties impact immunity, a research focus in much need of further exploration [154, 163, 166, 167]. To address these concerns and establish an understanding of the impact that catalytic NPs have on the immune system we chose to investigate the immunomodulatory capacity of CeO_2 NPs and TiO_2 NPs. We were promted to investigate these materials both for their unique contradictory catalytic behavior and concerns over the high level of exposure risk these materials impose towards consumers [160, 167-169]. Namely, over 4 million tons of pigmentary

TiO_2 being consumed globally each year for use in paints, papers, plastics, sunscreens, and cosmetics [111, 170-174]; CeO_2 NPs having emerged as *next-generation* NPs because of its wide application from solar cells, fuel cells, gas sensors, oxygen pumps, and refining glass/ceramic production to proposed biomedical application making them an appreciable exposure risk [175, 176]. This study has made an attempt to address an unexplored component of how certain physicochemical features of NPs can their impact innate and adaptive immunity which hopefully will be ignite further study into this curious and promising field of study.

While previous studies have largely focused on the inflammatory effect of NPs to cell lines or even phagocytic cells [177], we chose to investigate the effect of NPs to DCs because they are an extremely sensitive cell that is pivotal for induction of prophylactic immunity and long-lived memory. We began by examining the effect these NPs had to the DCs across a range of doses. We found that higher doses (100 μM) of TiO_2 induced increased cell death and apoptosis as compared to CeO_2 NP treated DCs (Figure 19). It is important to note that we chose a physiologically relevant dosing range that was in some cases 100x less concentrated than that used in other studies since our goal was to maintain cell functionality avoiding doses that would otherwise be acutely toxic. Interestingly, we noticed that even at the lower dose range TiO_2 managed to enhance DC pro-inflammatory phenotypic activation, while CeO_2 remained non-proinflammatory. Based on this, it might be assumed that there was a differential level of uptake between either NP as a plausible explanation to the difference in DC response profiles between materials. However, this was not the case as demonstrated in Figure 3B. Although previous work has demonstrated TiO_2 and CeO_2 NP uptake routinely by phagocytic cells at doses 2-100 fold higher than our greatest dose [178, 179], using ICP-MS we observed uptake of both NPs in human DCs only at 100μM (Figure 20B), which we believe is the first report of this finding for CeO_2 NPs. While we believe it to be less reliable, we also visualized increased side-scatter profiling of the

treated cells via flow cytometry (data not shown) as reported by others to be conclusive of NP internalization [180]. Since we noticed phenotypic changes in the DCs at concentrations below 100μM, we suspect either the limits of sensitive for the instrument and assay have been met or that uptake of the material is not necessary to induce such phenotypic changes. While the effect of TiO_2 on the DCs was made clear with the surface marker examination, CeO_2 was more mysterious at this superficial level and required further investigation into the cytokine output of the DCs following treatment to capture its effect on DCs. Indeed, we furthered our commitment to categorizing TiO_2 as pro-inflammatory and were compelled to declare CeO_2 as anti-inflammatory in light of its effect on DCs to produce IL-10.

Building upon our innate discovery, we explored the influence these particles have towards adaptive immunity. Because NPs have been shown to collect in the lymph nodes of treated animals, we chose to look at the effect of NPs on naïve $CD4^+$ T cells since they too are localized in the lymph node where they freely interact with antigen presenting DCs searching to engage their cognate receptor bolstering humoral and cellular immunity. Upon cognate recognition, the CD4 T cells may begin to further differentiate into distinct functional subsets. T_H1 and T_H2 effector T cell populations are among the subsets that have been most well described, although other subsets have been described. T_H1 cells have been defined as secreting interferon IFNγ, IL-2 and TNFα to evoke cell-mediated immunity and phagocyte-dependent inflammatory response, whereas T_H2 cells secret IL-4, IL-5, IL-10, and IL-13 which have been shown *in vivo* to evoke a strong antibody response (including those of the IgE class) and eosinophil accumulation, but inhibit several functions of phagocytic cells (phagocyte-independent inflammation) [181]. Because pathogen clearance is a dynamic process, it is more likely that for some complex diseases multiple subset will be involved, suited to the immune challenge. However, skewing the T_H response in a particular direction could be quite useful in a therapeutic scenario, such as T_H2 responses to intracellular pathogen clearance and wound healing [182]. While we are not the first to

describe that NPs have the propensity to drive a Th polarizing response [183], we believe it is necessary to uncover the relationship various NP physicochemical properties exert onto the T_H1/T_H2 paradigm can provide the basis for safety, development, optimization, and utilization of NPs towards therapeutic strategies against infectious agents. Namely, what we know about the materials in our study are that TiO_2 NPs have been shown to generate ROS as a result of elemental surface chemistry and large porous surface area resultant from the wet chemical synthesis method used to prepare the material [184], while CeO_2 has been described as an antioxidant [176]. We found that in human DC and T cell co-cultures, CeO_2 NPs do not generate detectable levels of ROS, unlike those cultures treated with TiO_2 NPs (Figure 5). Therefore, we can make some general conclusions about NP surface chemistry that ultimately define the resulting ROS levels when delivered to culture systems that align with their immunomodulatory tendency. When under UV-light illumination both materials result in the absorption of a photon with a higher energy than the band gap, creating an electron-hole pair. Unlike CeO_2 NPs where the absorbed UV electron hole pairs recombine together inside the particles, the electron-hole pairs in TiO_2 NPs have a tendency to migrate to the surface of the particles. At the surface, the electron pairs are free to react with oxygen, water or hydroxyls to form free radicals in a process called "photocatalysis." In fact, we observed this process using DCF-DA to analyze TiO_2 NP treated DCs as well as the antioxidant effect of CeO_2 NPs by demonstrating a dose dependent reduction in DCF fluorescence following treatment (Figure 22). While the oxidative reactions observed with TiO_2 NPs is well described, we believe the antioxidant behavior of CeO_2 NPs is a result of its proposed catalase mimetic activity [185]. Considering reports that suggest ROS can function as a second messenger and modulator of the immunity [148, 186-188], we must consider that both NPs may modulate redox-sensitive signal transduction pathways necessary for initiating the innate immune response and a mechanism of downstream adaptive immunomodulation. While it is easy to imagine that ROS-generation by materials

like TiO2 can have downstream proinflammatory effects, catalytic antioxidants have been shown to prevent the initiation of the innate immune response in LPS-stimulated macrophages as evidenced by the suppression of proinflammatory cytokines (TNF-α, IL-1β) and ROS (NO_2^- and O_2^-)[189], thus supporting our claim that ROS-modulating NPs can have immunomodulatory properties. Clearly, delivery of the CeO_2 NPs to T helper cells, perhaps a result of its catalase mimetic property, lent to a reduction in allogeneic-induced proliferation, induction of $Foxp3^+$ regulatory T cells, and increased production of T_H2-type cytokines IL-4, IL-5, and IL-10 as detected in the culture supernatants. It remains unclear how CeO_2 NPs modulate a greater production of these particular cytokines, yet we may speculate that at certain concentrations CeO_2 NPs behave in a manner which abrogates cellular ROS disrupting key pathways leading to an altered immune response profile. In support of this, recent evidence has revealed the capacity for ROS-mediated mechanisms to underlie the development of T_H2 responses in a complex murine model [187]. Other lines of evidence have shown that biological and chemical antioxidants play a role in directed T_H polarization and favor T_H2 shift similar to our observations with CeO_2 NPs [190, 191]. CeO_2 NPs may provide a unique opportunity for use in therapeutic combinations considering the importance of T_H2 responses for driving antibody production, a defining feature of prophylactic vaccination, coupled with the observation that CeO_2 NPs can aggregate (perhaps via intracellular DC transit) in the lymph node [192]. In this context, modulation of these redox reactions by CeO_2 NPs may provide a means of therapeutic benefit for controlling inflammatory-mediated diseases. However, we must remain cautious with such strategies because a T_H2 dominate response has been shown to be present in allergy and autoimmune diseases. TiO_2 NPs were observed to potentiate the proliferative response of T cells along with increased production of T helper type 1 (T_H1) cytokines (IL-2, IFNγ, TNFα). Moreover, naïve $CD4^+$ T cells co-cultured with allogeneic DCs pre-pulsed with TiO_2 NPs had increased proliferative response profile as compared to CeO_2 NP treated

cultures in which the response was observed as largely refractory, even in combination with a mitogen. These data add further implication that the redox activity of the NP can have profound influence over the generation and direction of an immune response.

Based on a summary of the evidence from this work, surface reactivity can have profound influence over immune response and directionality. Specifically, these data suggest that low doses of redox active NPs have the propensity to modulate the activation status of human DCs and alter the direction of CD4 T helper cells in response to challenge. These data illustrate the capacity for NPs to influence Th polarization in a distinct manner which likely coincides with the catalytic behavior of the molecule. While NP-induced T_H polarization has been observed at a limited level by others [183, 193-195], our results differ greatly from previous observations in that we are investigating simple, non-coated metallic NPs that induced a response polarization differential in a human culture. However, as we have previously demonstrated, parameters such as size and therefore exposed surface area can influence immune cell inflammation and activation. Building upon these our understanding of the importance these physicochemical features are towards inflammation are perhaps other material characteristics, such as catalytic status, that may prove useful to serve to drive a T cell biased response in the direction necessary for prophylaxis or conjugating catalytic NPs to an antigen of choice to adaptive responses. This work deepens our knowledge of the kind of physicochemical properties which influence human immunity. With further study, perhaps features like catalytic behavior may be exploited for engineered NPs to meet a particular task such as enhancing responses or mediating tolerance.

APPENDIX: IRB APPROVAL LETTER

Chesapeake Research Review, Inc.

Providing Human Research Protections Services
IRB Services • Consultation • Education
7063 Columbia Gateway Drive, Suite 110
Columbia, MD 21046-3403
410.884.2900

PROTOCOL AND PRINCIPAL INVESTIGATOR APPROVAL

DATE: 16 Jan 2012

TO: William Warren, Ph.D.
VaxDesign Corporation

FROM: Grace Hogan
Project Team Assistant, Chesapeake IRB

CC: Robin Sanders, VaxDesign Corporation

RE: Continuing Review of VaxDesign Corporation Protocol 0906009, Development and Testing of the MIMIC® (Modular Immune In vitro Constructs) and Dr. William Warren (Pro00005129)

Thank you for providing the information required for Chesapeake IRB to conduct continuing review of the protocol and Dr. William Warren.

In addition to the information you provided, the IRB reviewed the current protocol (Number 0906009, Dated September 29, 2011), Informed Consent and Authorization Forms, and other supporting information.

The IRB approved continuation of the above referenced protocol and Dr. William Warren on 14 Jan 2012.

The IRB determined that changes to the IRB Approved Informed Consent and Authorization Forms were not necessary. Continue using the Informed Consent and Authorization Forms electronically available on your CIRBI workspace under the "IRB Issued Documents" tab.

IRB Approval for the protocol and Dr. William Warren expires on 14 Jan 2013 unless re-approved by the IRB. A Continuing Review reminder will be sent prior to your expiration date.

Please review the Chesapeake IRB Investigator Handbook by accessing CIRBI™ (www.cirbi.net). Log on to your CIRBI homepage ("My Home") and select the "Reference Materials" tab for IRB requirements and guidance. A copy of the most recent IRB roster is also available under "Reference Materials".

All documentation related to this study must be submitted electronically through CIRBI™. Please **do not fax or mail** any information to the IRB. If you have any questions or concerns, please use the Contact IRB activity on your CIRBI workspace. We look forward to continuing to work with you on this project.

REFERENCES

1. Banchereau, J., et al., *Immunobiology of dendritic cells.* Annu Rev Immunol, 2000. **18**: p. 767-811.

2. Rossi, M. and J.W. Young, *Human dendritic cells: potent antigen-presenting cells at the crossroads of innate and adaptive immunity.* J Immunol, 2005. **175**(3): p. 1373-81.

3. Ancuta, P., et al., *Fractalkine preferentially mediates arrest and migration of CD16+ monocytes.* J Exp Med, 2003. **197**(12): p. 1701-7.

4. Muller, W.A., *Migration of leukocytes across endothelial junctions: some concepts and controversies.* Microcirculation, 2001. **8**(3): p. 181-93.

5. Randolph, G.J., et al., *Differentiation of phagocytic monocytes into lymph node dendritic cells in vivo.* Immunity, 1999. **11**(6): p. 753-61.

6. Randolph, G.J., et al., *The CD16(+) (FcgammaRIII(+)) subset of human monocytes preferentially becomes migratory dendritic cells in a model tissue setting.* J Exp Med, 2002. **196**(4): p. 517-27.

7. Cabillic, F., et al., *Hepatic environment elicits monocyte differentiation into a dendritic cell subset directing Th2 response.* J Hepatol, 2006. **44**(3): p. 552-9.

8. Despars, G. and H.C. O'Neill, *A role for niches in the development of a multiplicity of dendritic cell subsets.* Exp Hematol, 2004. **32**(3): p. 235-43.

9. Liu, Y.J., *Dendritic cell subsets and lineages, and their functions in innate and adaptive immunity.* Cell, 2001. **106**(3): p. 259-62.

10. Kelsall, B.L. and W. Strober, *Distinct populations of dendritic cells are present in the subepithelial dome and T cell regions of the murine Peyer's patch.* J Exp Med, 1996. **183**(1): p. 237-47.

11. Renn, C.N., et al., *TLR activation of Langerhans cell-like dendritic cells triggers an antiviral immune response.* J Immunol, 2006. **177**(1): p. 298-305.

12. Qu, C., T.M. Moran, and G.J. Randolph, *Autocrine type I IFN and contact with endothelium promote the presentation of influenza A virus by monocyte-derived APC.* J Immunol, 2003. **170**(2): p. 1010-8.

13. Randolph, G.J., et al., *Differentiation of monocytes into dendritic cells in a model of transendothelial trafficking.* Science, 1998. **282**(5388): p. 480-3.

14. Randolph, G.J., et al., *A physiologic function for p-glycoprotein (MDR-1) during the migration of dendritic cells from skin via afferent lymphatic vessels.* Proc Natl Acad Sci U S A, 1998. **95**(12): p. 6924-9.

15. Manna, P.P., et al., *Differentiation and functional maturation of human CD14(+) adherent peripheral blood monocytes by xenogeneic endothelial cells: up-regulation of costimulation, cytokine generation, and toll-like receptors.* Transplantation, 2002. **74**(2): p. 243-52.

16. Romani, N., et al., *Proliferating dendritic cell progenitors in human blood.* J Exp Med, 1994. **180**(1): p. 83-93.

17. Sallusto, F. and A. Lanzavecchia, *Efficient presentation of soluble antigen by cultured human dendritic cells is maintained by granulocyte/macrophage colony-stimulating factor plus interleukin 4 and downregulated by tumor necrosis factor alpha.* J Exp Med, 1994. **179**(4): p. 1109-18.

18. Dye, J.F., et al., *Cyclic AMP and acidic fibroblast growth factor have opposing effects on tight and adherens junctions in microvascular endothelial cells in vitro.* Microvasc Res, 2001. **62**(2): p. 94-113.

19. Ali, M.H., et al., *Endothelial permeability and IL-6 production during hypoxia: role of ROS in signal transduction.* Am J Physiol, 1999. **277**(5 Pt 1): p. L1057-65.

20. Nevo, N., et al., *Increasing endothelial cell permeability improves the efficiency of myocyte adenoviral vector infection.* J Gene Med, 2001. **3**(1): p. 42-50.

21. Geissmann, F., S. Jung, and D.R. Littman, *Blood monocytes consist of two principal subsets with distinct migratory properties.* Immunity, 2003. **19**(1): p. 71-82.

22. Van Furth, R., M.C. Diesselhoff-den Dulk, and H. Mattie, *Quantitative study on the production and kinetics of mononuclear phagocytes during an acute inflammatory reaction.* J Exp Med, 1973. **138**(6): p. 1314-30.

23. Bautista, E.M., D. Gregg, and W.T. Golde, *Characterization and functional analysis of skin-derived dendritic cells from swine without a requirement for in vitro propagation.* Vet Immunol Immunopathol, 2002. **88**(3-4): p. 131-48.

24. Mantegazza, A.R., et al., *CD63 tetraspanin slows down cell migration and translocates to the endosomal-lysosomal-MIICs route after extracellular stimuli in human immature dendritic cells.* Blood, 2004. **104**(4): p. 1183-90.

25. Sato, M., et al., *Direct binding of Toll-like receptor 2 to zymosan, and zymosan-induced NF-kappa B activation and TNF-alpha secretion are down-regulated by lung collectin surfactant protein A.* J Immunol, 2003. **171**(1): p. 417-25.

26. Mahnke, K., et al., *CD14 is expressed by subsets of murine dendritic cells and upregulated by lipopolysaccharide.* Adv Exp Med Biol, 1997. **417**: p. 145-59.

27. Schmitt, N., et al., *Ex vivo characterization of human thymic dendritic cell subsets.* Immunobiology, 2007. **212**(3): p. 167-77.

28. Frentsch, M., et al., *Direct access to CD4+ T cells specific for defined antigens according to CD154 expression.* Nat Med, 2005. **11**(10): p. 1118-24.

29. Kirchhoff, D., et al., *Identification and isolation of murine antigen-reactive T cells according to CD154 expression.* Eur J Immunol, 2007. **37**(9): p. 2370-7.

30. Morse, M.A., et al., *Migration of human dendritic cells after injection in patients with metastatic malignancies.* Cancer Res, 1999. **59**(1): p. 56-8.

31. Thurnher, M., et al., *The disabled dendritic cell.* FASEB J, 2001. **15**(6): p. 1054-61.

32. Edgell, C.J., C.C. McDonald, and J.B. Graham, *Permanent cell line expressing human factor VIII-related antigen established by hybridization.* Proc Natl Acad Sci U S A, 1983. **80**(12): p. 3734-7.

33. Seguin, R., et al., *Human brain endothelial cells supply support for monocyte immunoregulatory functions.* J Neuroimmunol, 2003. **135**(1-2): p. 96-106.

34. Dilioglou, S., J.M. Cruse, and R.E. Lewis, *Costimulatory function of umbilical cord blood CD14+ and CD34+ derived dendritic cells.* Exp Mol Pathol, 2003. **75**(1): p. 18-33.

35. Nelson, E.L., et al., *Cycling of human dendritic cell effector phenotypes in response to TNF-alpha: modification of the current 'maturation' paradigm and implications for in vivo immunoregulation.* FASEB J, 1999. **13**(14): p. 2021-30.

36. Miller, M.J., et al., *T cell repertoire scanning is promoted by dynamic dendritic cell behavior and random T cell motility in the lymph node.* Proc Natl Acad Sci U S A, 2004. **101**(4): p. 998-1003.

37. Banchereau, J. and R.M. Steinman, *Dendritic cells and the control of immunity.* Nature, 1998. **392**(6673): p. 245-52.

38. Zhou, L.J. and T.F. Tedder, *CD14+ blood monocytes can differentiate into functionally mature CD83+ dendritic cells.* Proc Natl Acad Sci U S A, 1996. **93**(6): p. 2588-92.

39. Piemonti, L., et al., *Generation and functional characterisation of dendritic cells from patients with pancreatic carcinoma with special regard to clinical applicability.* Cancer Immunol Immunother, 2000. **49**(10): p. 544-50.

40. Li, G., et al., *P-selectin enhances generation of CD14+CD16+ dendritic-like cells and inhibits macrophage maturation from human peripheral blood monocytes.* J Immunol, 2003. **171**(2): p. 669-77.

41. Macey, M.G., et al., *Rapid flow cytometric identification of putative CD14- and CD64- dendritic cells in whole blood.* Cytometry, 1998. **31**(3): p. 199-207.

42. Butler, M., et al., *Modulation of dendritic cell phenotype and function in an in vitro model of the intestinal epithelium.* Eur J Immunol, 2006. **36**(4): p. 864-74.

43. Memoli, M.J., et al., *An early 'classical' swine H1N1 influenza virus shows similar pathogenicity to the 1918 pandemic virus in ferrets and mice.* Virology, 2009. **393**(2): p. 338-45.

44. Garten, R.J., et al., *Antigenic and genetic characteristics of swine-origin 2009 A(H1N1) influenza viruses circulating in humans.* Science, 2009. **325**(5937): p. 197-201.

45. Hancock, K., et al., *Cross-reactive antibody responses to the 2009 pandemic H1N1 influenza virus.* N Engl J Med, 2009. **361**(20): p. 1945-52.

46. Itoh, Y., et al., *In vitro and in vivo characterization of new swine-origin H1N1 influenza viruses.* Nature, 2009. **460**(7258): p. 1021-5.

47. *Serum cross-reactive antibody response to a novel influenza A (H1N1) virus after vaccination with seasonal influenza vaccine.* MMWR Morb Mortal Wkly Rep, 2009. **58**(19): p. 521-4.

48. Greenbaum, J.A., et al., *Pre-existing immunity against swine-origin H1N1 influenza viruses in the general human population.* Proc Natl Acad Sci U S A, 2009. **106**(48): p. 20365-70.

49. Ampofo, K., et al., *Association of 2009 pandemic influenza A (H1N1) infection and increased hospitalization with parapneumonic empyema in children in Utah.* Pediatr Infect Dis J, 2010. **29**(10): p. 905-9.

50. Ellebedy, A.H., et al., *Impact of prior seasonal influenza vaccination and infection on pandemic A(H1N1) influenza virus replication in ferrets.* Vaccine, 2010.

51. De Groot, A.S., et al., *Immunoinformatic comparison of T-cell epitopes contained in novel swine-origin influenza A (H1N1) virus with epitopes in 2008-2009 conventional influenza vaccine.* Vaccine, 2009. **27**(42): p. 5740-7.

52. Moser, J.M., et al., *Optimization of a dendritic cell-based assay for the in vitro priming of naive human CD4+ T cells.* J Immunol Methods, 2010. **353**(1-2): p. 8-19.

53. Schanen, B.C. and D.R. Drake, 3rd, *A novel approach for the generation of human dendritic cells from blood monocytes in the absence of exogenous factors.* J Immunol Methods, 2008. **335**(1-2): p. 53-64.

54. Sette, A. and J. Sidney, *Nine major HLA class I supertypes account for the vast preponderance of HLA-A and -B polymorphism.* Immunogenetics, 1999. **50**(3-4): p. 201-12.

55. De Groot, A.S., et al., *An interactive Web site providing major histocompatibility ligand predictions: application to HIV research.* AIDS Res Hum Retroviruses, 1997. **13**(7): p. 529-31.

56. Schafer, J.R., et al., *Prediction of well-conserved HIV-1 ligands using a matrix-based algorithm, EpiMatrix.* Vaccine, 1998. **16**(19): p. 1880-4.

57. Sturniolo, T., et al., *Generation of tissue-specific and promiscuous HLA ligand databases using DNA microarrays and virtual HLA class II matrices.* Nat Biotechnol, 1999. **17**(6): p. 555-61.

58. De Groot, A.S., P.M. Knopp, and W. Martin, *De-immunization of therapeutic proteins by T-cell epitope modification.* Dev Biol (Basel), 2005. **122**: p. 171-94.

59. De Groot, A.S., et al., *Identification of immunogenic HLA-B7 "Achilles' heel" epitopes within highly conserved regions of HIV.* Vaccine, 2008. **26**(24): p. 3059-71.

60. Cohen, T., et al., *A method for individualizing the prediction of immunogenicity of protein vaccines and biologic therapeutics: individualized T cell epitope measure (iTEM).* J Biomed Biotechnol, 2010. **2010**.

61. De Groot, A.S. and W. Martin, *Reducing risk, improving outcomes: bioengineering less immunogenic protein therapeutics.* Clin Immunol, 2009. **131**(2): p. 189-201.

62. Richards, K.A., et al., *Cutting Edge: CD4 T Cells Generated from Encounter with Seasonal Influenza Viruses and Vaccines Have Broad Protein Specificity and Can Directly Recognize Naturally Generated Epitopes Derived from the Live Pandemic H1N1 Virus.* J Immunol, 2010.

63. Tu, W., et al., *Cytotoxic T lymphocytes established by seasonal human influenza cross-react against 2009 pandemic H1N1 influenza virus.* J Virol, 2010. **84**(13): p. 6527-35.

64. Ge, X., et al., *Assessment of seasonal influenza A virus-specific CD4 T-cell responses to 2009 pandemic H1N1 swine-origin influenza A virus.* J Virol, 2010. **84**(7): p. 3312-9.

65. Cusick, M.F., S. Wang, and D.D. Eckels, *In vitro responses to avian influenza H5 by human CD4 T cells.* J Immunol, 2009. **183**(10): p. 6432-41.

66. Gioia, C., et al., *Cross-subtype immunity against avian influenza in persons recently vaccinated for influenza.* Emerg Infect Dis, 2008. **14**(1): p. 121-8.

67. Jameson, J., et al., *Human CD8+ and CD4+ T lymphocyte memory to influenza A viruses of swine and avian species.* J Immunol, 1999. **162**(12): p. 7578-83.

68. Richards, K.A., et al., *Direct ex vivo analyses of HLA-DR1 transgenic mice reveal an exceptionally broad pattern of immunodominance in the primary HLA-DR1-restricted CD4 T-cell response to influenza virus hemagglutinin.* J Virol, 2007. **81**(14): p. 7608-19.

69. Richards, K.A., F.A. Chaves, and A.J. Sant, *Infection of HLA-DR1 transgenic mice with a human isolate of influenza a virus (H1N1) primes a diverse CD4 T-cell repertoire that includes CD4 T cells with heterosubtypic cross-reactivity to avian (H5N1) influenza virus.* J Virol, 2009. **83**(13): p. 6566-77.

70. Roti, M., et al., *Healthy human subjects have CD4+ T cells directed against H5N1 influenza virus.* J Immunol, 2008. **180**(3): p. 1758-68.

71. Schneider, C. and M.H. Van Regenmortel, *Immunogenicity of free synthetic peptides corresponding to T helper epitopes of the influenza HA 1 subunit. Induction of virus cross reacting CD4+ T lymphocytes in mice.* Arch Virol, 1992. **125**(1-4): p. 103-19.

72. Alexander, J., et al., *Universal influenza DNA vaccine encoding conserved CD4+ T cell epitopes protects against lethal viral challenge in HLA-DR transgenic mice.* Vaccine, 2010. **28**(3): p. 664-72.

73. Belz, G.T., et al., *Compromised influenza virus-specific CD8(+)-T-cell memory in CD4(+)-T-cell-deficient mice.* J Virol, 2002. **76**(23): p. 12388-93.

74. Brooks, J.W., et al., *Requirement for CD40 ligand, CD4(+) T cells, and B cells in an infectious mononucleosis-like syndrome.* J Virol, 1999. **73**(11): p. 9650-4.

75. Cardin, R.D., et al., *Progressive loss of CD8+ T cell-mediated control of a gamma-herpesvirus in the absence of CD4+ T cells.* J Exp Med, 1996. **184**(3): p. 863-71.

76. Rasmussen, I.B., et al., *The principle of delivery of T cell epitopes to antigen-presenting cells applied to peptides from influenza virus, ovalbumin, and hen egg lysozyme: implications for peptide vaccination.* Proc Natl Acad Sci U S A, 2001. **98**(18): p. 10296-301.

77. Marshall, D., et al., *TH cells primed during influenza virus infection provide help for qualitatively distinct antibody responses to subsequent immunization.* J Immunol, 1999. **163**(9): p. 4673-82.

78. Boon, A.C., et al., *Recognition of homo- and heterosubtypic variants of influenza A viruses by human CD8+ T lymphocytes.* J Immunol, 2004. **172**(4): p. 2453-60.

79. Kreijtz, J.H., et al., *Primary influenza A virus infection induces cross-protective immunity against a lethal infection with a heterosubtypic virus strain in mice.* Vaccine, 2007. **25**(4): p. 612-20.

80. Ulmer, J.B., et al., *Protective CD4+ and CD8+ T cells against influenza virus induced by vaccination with nucleoprotein DNA.* J Virol, 1998. **72**(7): p. 5648-53.

81. Goy, K., et al., *Heterosubtypic T-cell responses against avian influenza H5 haemagglutinin are frequently detected in individuals vaccinated against or previously infected with human subtypes of influenza.* Influenza Other Respi Viruses, 2008. **2**(4): p. 115-25.

82. Zinckgraf, J.W., et al., *Identification of HLA class II H5N1 hemagglutinin epitopes following subvirion influenza A (H5N1) vaccination.* Vaccine, 2009. **27**(39): p. 5393-401.

83. McMurry, J.A., et al., *Epitope-driven TB vaccine development: a streamlined approach using immuno-informatics, ELISpot assays, and HLA transgenic mice.* Curr Mol Med, 2007. **7**(4): p. 351-68.

84. Otero, M., et al., *Efficacy of novel plasmid DNA encoding vaccinia antigens in improving current smallpox vaccination strategy.* Vaccine, 2006. **24**(21): p. 4461-70.

85. Meister, G.E., et al., *Two novel T cell epitope prediction algorithms based on MHC-binding motifs; comparison of predicted and published epitopes from Mycobacterium tuberculosis and HIV protein sequences.* Vaccine, 1995. **13**(6): p. 581-91.

86. Bond, K.B., et al., *An HLA-directed molecular and bioinformatics approach identifies new HLA-A11 HIV-1 subtype E cytotoxic T lymphocyte epitopes in HIV-1-infected Thais.* AIDS Res Hum Retroviruses, 2001. **17**(8): p. 703-17.

87. Dong, Y., et al., *HLA-A2-restricted CD8+-cytotoxic-T-cell responses to novel epitopes in Mycobacterium tuberculosis superoxide dismutase, alanine dehydrogenase, and glutamine synthetase.* Infect Immun, 2004. **72**(4): p. 2412-5.

88. McMurry, J.A., B.E. Johansson, and A.S. De Groot, *A call to cellular & humoral arms: enlisting cognate T cell help to develop broad-spectrum vaccines against influenza A.* Hum Vaccin, 2008. **4**(2): p. 148-57.

89. Carbone, R., et al., *Biocompatibility of cluster-assembled nanostructured TiO2 with primary and cancer cells.* Biomaterials, 2006. **27**(17): p. 3221-9.

90. Rasmusson, L., J. Roos, and H. Bystedt, *A 10-year follow-up study of titanium dioxide-blasted implants.* Clin Implant Dent Relat Res, 2005. **7**(1): p. 36-42.

91. Chen, F., et al., *Biocompatibility of electrophoretical deposition of nanostructured hydroxyapatite coating on roughen titanium surface: in vitro evaluation using mesenchymal stem cells.* J Biomed Mater Res B Appl Biomater, 2007. **82**(1): p. 183-91.

92. Liu, X., et al., *Plasma-treated nanostructured TiO(2) surface supporting biomimetic growth of apatite.* Biomaterials, 2005. **26**(31): p. 6143-50.

93. Annesi-Maesano, I. and W. Dab, *[Air pollution and the lung: epidemiological approach].* Med Sci (Paris), 2006. **22**(6-7): p. 589-94.

94. Auger, F., et al., *Responses of well-differentiated nasal epithelial cells exposed to particles: role of the epithelium in airway inflammation.* Toxicol Appl Pharmacol, 2006. **215**(3): p. 285-94.

95. Brunekreef, B. and S.T. Holgate, *Air pollution and health.* Lancet, 2002. **360**(9341): p. 1233-42.

96. Lin, W., et al., *Toxicity of cerium oxide nanoparticles in human lung cancer cells.* Int J Toxicol, 2006. **25**(6): p. 451-7.

97. Oberdorster, G., et al., *Association of particulate air pollution and acute mortality: involvement of ultrafine particles?* Inhal Toxicol, 1995. **7**(1): p. 111-24.

98. Wildhaber, J.H., *Aerosols: the environmental harmful effect.* Paediatr Respir Rev, 2006. **7 Suppl 1**: p. S86-7.

99. Baan, R., et al., *Carcinogenicity of carbon black, titanium dioxide, and talc.* Lancet Oncol, 2006. **7**(4): p. 295-6.

100. Baan, R.A., *Carcinogenic hazards from inhaled carbon black, titanium dioxide, and talc not containing asbestos or asbestiform fibers: recent evaluations by an IARC Monographs Working Group.* Inhal Toxicol, 2007. **19 Suppl 1**: p. 213-28.

101. Nel, A.E., et al., *Enhancement of allergic inflammation by the interaction between diesel exhaust particles and the immune system.* J Allergy Clin Immunol, 1998. **102**(4 Pt 1): p. 539-54.

102. Wang, J., et al., *Potential neurological lesion after nasal instillation of TiO(2) nanoparticles in the anatase and rutile crystal phases.* Toxicol Lett, 2008. **183**(1-3): p. 72-80.

103. Xia, T., N. Li, and A.E. Nel, *Potential Health Impact of Nanoparticles.* Annu Rev Public Health, 2009.

104. Chung, C.J., et al., *An antimicrobial TiO2 coating for reducing hospital-acquired infection.* J Biomed Mater Res B Appl Biomater, 2008. **85**(1): p. 220-4.

105. Erli, H.J., et al., *The effect of surface modification of a porous TiO2/perlite composite on the ingrowth of bone tissue in vivo.* Biomaterials, 2006. **27**(8): p. 1270-6.

106. Goto, K., et al., *Bioactive bone cements containing nano-sized titania particles for use as bone substitutes.* Biomaterials, 2005. **26**(33): p. 6496-505.

107. Karpagavalli, R., et al., *Corrosion behavior and biocompatibility of nanostructured TiO2 film on Ti6Al4V.* J Biomed Mater Res A, 2007. **83**(4): p. 1087-95.

108. Popat, K.C., et al., *Influence of engineered titania nanotubular surfaces on bone cells.* Biomaterials, 2007. **28**(21): p. 3188-97.

109. Warheit, D.B., et al., *Pulmonary toxicity study in rats with three forms of ultrafine-TiO2 particles: differential responses related to surface properties.* Toxicology, 2007. **230**(1): p. 90-104.

110. Warheit, D.B., et al., *Pulmonary instillation studies with nanoscale TiO2 rods and dots in rats: toxicity is not dependent upon particle size and surface area.* Toxicol Sci, 2006. **91**(1): p. 227-36.

111. Vamanu, C.I., et al., *Formation of potential titanium antigens based on protein binding to titanium dioxide nanoparticles.* Int J Nanomedicine, 2008. **3**(1): p. 69-74.

112. Yao, Z., et al., *Polymerization from the surface of single-walled carbon nanotubes - preparation and characterization of nanocomposites.* J Am Chem Soc, 2003. **125**(51): p. 16015-24.

113. Zhang, S., et al., *Formation mechanism of H2Ti3O7 nanotubes.* Phys Rev Lett, 2003. **91**(25): p. 256103.

114. Muller, W.A. and G.J. Randolph, *Migration of leukocytes across endothelium and beyond: molecules involved in the transmigration and fate of monocytes.* J Leukoc Biol, 1999. **66**(5): p. 698-704.

115. Penolazzi, L., et al., *Evaluation of chemokine and cytokine profiles in osteoblast progenitors from umbilical cord blood stem cells by BIO-PLEX technology.* Cell Biol Int, 2008. **32**(2): p. 320-5.

116. Chew, J.L., et al., *Chitosan nanoparticles containing plasmid DNA encoding house dust mite allergen, Der p 1 for oral vaccination in mice.* Vaccine, 2003. **21**(21-22): p. 2720-9.

117. Kapetanovic, R. and J.M. Cavaillon, *Early events in innate immunity in the recognition of microbial pathogens.* Expert Opin Biol Ther, 2007. **7**(6): p. 907-18.

118. van Vliet, S.J., et al., *Innate signaling and regulation of Dendritic cell immunity.* Curr Opin Immunol, 2007. **19**(4): p. 435-40.

119. D'Elia, R. and K.J. Else, *In vitro antigen presenting cell-derived IL-10 and IL-6 correlate with Trichuris muris isolate-specific survival.* Parasite Immunol, 2009. **31**(3): p. 123-31.

120. Harizi, H. and N. Gualde, *Pivotal role of PGE2 and IL-10 in the cross-regulation of dendritic cell-derived inflammatory mediators.* Cell Mol Immunol, 2006. **3**(4): p. 271-7.

121. Afaq, F., et al., *Activation of alveolar macrophages and peripheral red blood cells in rats exposed to fibers/particles.* Toxicol Lett, 1998. **99**(3): p. 175-82.

122. Matsuzawa, A., et al., *ROS-dependent activation of the TRAF6-ASK1-p38 pathway is selectively required for TLR4-mediated innate immunity.* Nat Immunol, 2005. **6**(6): p. 587-92.

123. Aukrust, P., F. Muller, and S.S. Froland, *Enhanced generation of reactive oxygen species in monocytes from patients with common variable immunodeficiency.* Clin Exp Immunol, 1994. **97**(2): p. 232-8.

124. Park, E.J. and K. Park, *Oxidative stress and pro-inflammatory responses induced by silica nanoparticles in vivo and in vitro.* Toxicol Lett, 2009. **184**(1): p. 18-25.

125. Takahashi, M., et al., *Roles of reactive oxygen species in monocyte activation induced by photochemical reactions during photodynamic therapy.* Front Med Biol Eng, 2002. **11**(4): p. 279-94.

126. Reeves, J.F., Davies, S.J., Dodd, N.J.F., Jha, A.N., *Hydroxyl radicals are associated with Titanium dioxide nanoparticle induced cytotoxicity and oxidative DNA damage in fish cells.* Mutation Research, 2008.

127. Soto, K.F., L.E. Murr, and K.M. Garza, *Cytotoxic responses and potential respiratory health effects of carbon and carbonaceous nanoparticulates in the Paso del Norte airshed environment.* Int J Environ Res Public Health, 2008. **5**(1): p. 12-25.

128. Demento, S.L., et al., *Inflammasome-activating nanoparticles as modular systems for optimizing vaccine efficacy.* Vaccine, 2009. **27**(23): p. 3013-21.

129. Sharp, F.A., et al., *Uptake of particulate vaccine adjuvants by dendritic cells activates the NALP3 inflammasome.* Proc Natl Acad Sci U S A, 2009. **106**(3): p. 870-5.

130. Moss, O.R. and V.A. Wong, *When nanoparticles get in the way: impact of projected area on in vivo and in vitro macrophage function.* Inhal Toxicol, 2006. **18**(10): p. 711-6.

131. Pickl, W.F., et al., *Molecular and functional characteristics of dendritic cells generated from highly purified CD14+ peripheral blood monocytes.* J Immunol, 1996. **157**(9): p. 3850-9.

132. Kohl, K., et al., *Subpopulations of human dendritic cells display a distinct phenotype and bind differentially to proteins of the extracellular matrix.* Eur J Cell Biol, 2007. **86**(11-12): p. 719-30.

133. Wang, J.J., B.J. Sanderson, and H. Wang, *Cyto- and genotoxicity of ultrafine TiO2 particles in cultured human lymphoblastoid cells.* Mutat Res, 2007. **628**(2): p. 99-106.

134. Wang, J.J., B.J. Sanderson, and H. Wang, *Cytotoxicity and genotoxicity of ultrafine crystalline SiO2 particulate in cultured human lymphoblastoid cells.* Environ Mol Mutagen, 2007. **48**(2): p. 151-7.

135. Godfrey, D.I., J. Rossjohn, and J. McCluskey, *The fidelity, occasional promiscuity, and versatility of T cell receptor recognition.* Immunity, 2008. **28**(3): p. 304-14.

136. Patil, S., et al., *Protein adsorption and cellular uptake of cerium oxide nanoparticles as a function of zeta potential.* Biomaterials, 2007. **28**(31): p. 4600-7.

137. Colon, J., et al., *Cerium oxide nanoparticles protect gastrointestinal epithelium from radiation-induced damage by reduction of reactive oxygen species and upregulation of superoxide dismutase 2.* Nanomedicine, 2010. **6**(5): p. 698-705.

138. Hirst, S.M., et al., *Anti-inflammatory properties of cerium oxide nanoparticles.* Small, 2009. **5**(24): p. 2848-56.

139. Fan, A.M. and G. Alexeeff, *Nanotechnology and nanomaterials: toxicology, risk assessment, and regulations.* J Nanosci Nanotechnol, 2010. **10**(12): p. 8646-57.

140. Dobrovolskaia, M.A., et al., *Preclinical studies to understand nanoparticle interaction with the immune system and its potential effects on nanoparticle biodistribution.* Mol Pharm, 2008. **5**(4): p. 487-95.

141. McNeil, S.E., *Nanotechnology for the biologist.* J Leukoc Biol, 2005. **78**(3): p. 585-94.

142. Hanley, C., et al., *The Influences of Cell Type and ZnO Nanoparticle Size on Immune Cell Cytotoxicity and Cytokine Induction.* Nanoscale Res Lett, 2009. **4**(12): p. 1409-20.

143. Mayer, A., et al., *The role of nanoparticle size in hemocompatibility.* Toxicology, 2009. **258**(2-3): p. 139-47.

144. Schanen, B.C., et al., *Exposure to titanium dioxide nanomaterials provokes inflammation of an in vitro human immune construct.* ACS Nano, 2009. **3**(9): p. 2523-32.

145. Deng, Z.J., et al., *Nanoparticle-induced unfolding of fibrinogen promotes Mac-1 receptor activation and inflammation.* Nat Nanotechnol, 2011. **6**(1): p. 39-44.

146. Duffin, R., et al., *Proinflammogenic effects of low-toxicity and metal nanoparticles in vivo and in vitro: highlighting the role of particle surface area and surface reactivity.* Inhal Toxicol, 2007. **19**(10): p. 849-56.

147. Shin, S.H., et al., *The effects of nano-silver on the proliferation and cytokine expression by peripheral blood mononuclear cells.* Int Immunopharmacol, 2007. **7**(13): p. 1813-8.

148. Finkel, T., *Redox-dependent signal transduction.* FEBS Lett, 2000. **476**(1-2): p. 52-4.

149. Karakoti, A.S., et al., *PEGylated nanoceria as radical scavenger with tunable redox chemistry.* J Am Chem Soc, 2009. **131**(40): p. 14144-5.

150. Banerjee, D.K., et al., *Expansion of FOXP3high regulatory T cells by human dendritic cells (DCs) in vitro and after injection of cytokine-matured DCs in myeloma patients.* Blood, 2006. **108**(8): p. 2655-61.

151. Xu, M., et al., *Photoexcited TiO2 nanoparticles through •OH-radicals induced malignant cells to necrosis.* Supramolecular Science, 1998. **5**(5-6): p. 449-451.

152. Zhang, A.P. and Y.P. Sun, *Photocatalytic killing effect of TiO2 nanoparticles on Ls-174-t human colon carcinoma cells.* World J Gastroenterol, 2004. **10**(21): p. 3191-3.

153. Bar-Ilan, O., et al., *Titanium dioxide nanoparticles produce phototoxicity in the developing zebrafish.* Nanotoxicology. **0**(0): p. 1-10.

154. Yang, D., et al., *[Gd@C(82)(OH)(22)](n) nanoparticles induce dendritic cell maturation and activate Th1 immune responses.* ACS Nano, 2010. **4**(2): p. 1178-86.

155. Warheit, D.B., K.L. Reed, and C.M. Sayes, *A role for nanoparticle surface reactivity in facilitating pulmonary toxicity and development of a base set of hazard assays as a component of nanoparticle risk management.* Inhal Toxicol, 2009. **21 Suppl 1**: p. 61-7.

156. Zhu, Z.J., et al., *Multiplexed screening of cellular uptake of gold nanoparticles using laser desorption/ionization mass spectrometry.* J Am Chem Soc, 2008. **130**(43): p. 14139-43.

157. Churg, A., B. Stevens, and J.L. Wright, *Comparison of the uptake of fine and ultrafine TiO2 in a tracheal explant system.* Am J Physiol, 1998. **274**(1 Pt 1): p. L81-6.

158. Teste, B., et al., *Microchip integrating magnetic nanoparticles for allergy diagnosis.* Lab Chip, 2011. **11**(24): p. 4207-13.

159. Zhu, Y., et al., *G-quadruplex DNAzyme-based microcystin-LR (toxin) determination by a novel immunosensor.* Biosens Bioelectron, 2011. **26**(11): p. 4393-8.

160. Di Gioacchino, M., et al., *Immunotoxicity of nanoparticles.* Int J Immunopathol Pharmacol, 2011. **24**(1 Suppl): p. 65S-71S.

161. Chauveau, C., et al., *Heme oxygenase-1 expression inhibits dendritic cell maturation and proinflammatory function but conserves IL-10 expression.* Blood, 2005. **106**(5): p. 1694-702.

162. Wang, P., et al., *Interleukin (IL)-10 inhibits nuclear factor kappa B (NF kappa B) activation in human monocytes. IL-10 and IL-4 suppress cytokine synthesis by different mechanisms.* J Biol Chem, 1995. **270**(16): p. 9558-63.

163. Yazdi, A.S., et al., *Nanoparticles activate the NLR pyrin domain containing 3 (Nlrp3) inflammasome and cause pulmonary inflammation through release of IL-1alpha and IL-1beta.* Proc Natl Acad Sci U S A, 2010. **107**(45): p. 19449-54.

164. Lamkanfi, M., R.K. Malireddi, and T.D. Kanneganti, *Fungal zymosan and mannan activate the cryopyrin inflammasome.* J Biol Chem, 2009. **284**(31): p. 20574-81.

165. Paulsen, M., et al., *Modulation of CD4+ T-cell activation by CD95 co-stimulation.* Cell Death Differ, 2011. **18**(4): p. 619-31.

166. Zolnik, B.S., et al., *Nanoparticles and the immune system.* Endocrinology, 2010. **151**(2): p. 458-65.

167. Dobrovolskaia, M.A. and S.E. McNeil, *Immunological properties of engineered nanomaterials.* Nat Nanotechnol, 2007. **2**(8): p. 469-78.

168. Hussain, S., J.A.J. Vanoirbeek, and P.H.M. Hoet, *Interactions of nanomaterials with the immune system.* Wiley Interdisciplinary Reviews: Nanomedicine and Nanobiotechnology, 2011: p. n/a-n/a.

169. Kitchin, K.T., R.Y. Prasad, and K. Wallace, *Oxidative stress studies of six TiO(2) and two CeO(2) nanomaterials: Immuno-spin trapping results with DNA.* Nanotoxicology, 2010.

170. Donaldson, K., P.H. Beswick, and P.S. Gilmour, *Free radical activity associated with the surface of particles: a unifying factor in determining biological activity?* Toxicol Lett, 1996. **88**(1-3): p. 293-8.

171. Gilmour, P.S., et al., *Free radical activity of industrial fibers: role of iron in oxidative stress and activation of transcription factors.* Environ Health Perspect, 1997. **105 Suppl 5**: p. 1313-7.

172. Goncalves, D.M., S. Chiasson, and D. Girard, *Activation of human neutrophils by titanium dioxide (TiO2) nanoparticles.* Toxicol In Vitro, 2010. **24**(3): p. 1002-8.

173. Jin, C.Y., et al., *Cytotoxicity of titanium dioxide nanoparticles in mouse fibroblast cells.* Chem Res Toxicol, 2008. **21**(9): p. 1871-7.

174. Sayes, C.M., et al., *Correlating nanoscale titania structure with toxicity: a cytotoxicity and inflammatory response study with human dermal fibroblasts and human lung epithelial cells.* Toxicol Sci, 2006. **92**(1): p. 174-85.

175. Celardo, I., et al., *Pharmacological potential of cerium oxide nanoparticles.* Nanoscale, 2011. **3**(4): p. 1411-20.

176. Celardo, I., E. Traversa, and L. Ghibelli, *Cerium oxide nanoparticles: a promise for applications in therapy.* J Exp Ther Oncol, 2011. **9**(1): p. 47-51.

177. Valles, G., et al., *Differential inflammatory macrophage response to rutile and titanium particles.* Biomaterials, 2006. **27**(30): p. 5199-211.

178. Singh, S., et al., *Endocytosis, oxidative stress and IL-8 expression in human lung epithelial cells upon treatment with fine and ultrafine TiO2: role of the specific surface area and of surface methylation of the particles.* Toxicol Appl Pharmacol, 2007. **222**(2): p. 141-51.

179. Asati, A., et al., *Surface-charge-dependent cell localization and cytotoxicity of cerium oxide nanoparticles.* ACS Nano, 2010. **4**(9): p. 5321-31.

180. Zucker, R.M., et al., *Detection of TiO2 nanoparticles in cells by flow cytometry.* Cytometry A, 2010. **77**(7): p. 677-85.

181. Romagnani, S., *T-cell subsets (Th1 versus Th2).* Ann Allergy Asthma Immunol, 2000. **85**(1): p. 9-18; quiz 18, 21.

182. Allen, J.E. and T.A. Wynn, *Evolution of Th2 immunity: a rapid repair response to tissue destructive pathogens.* PLoS Pathog, 2011. **7**(5): p. e1002003.

183. Liu, Y., et al., *The effect of Gd@C82(OH)22 nanoparticles on the release of Th1/Th2 cytokines and induction of TNF-alpha mediated cellular immunity.* Biomaterials, 2009. **30**(23-24): p. 3934-45.

184. Jiang, J., et al., *Does Nanoparticle Activity Depend upon Size and Crystal Phase?* Nanotoxicology, 2008. **2**(1): p. 33-42.

185. Pirmohamed, T., et al., *Nanoceria exhibit redox state-dependent catalase mimetic activity.* Chem Commun (Camb), 2010. **46**(16): p. 2736-8.

186. Lander, H.M., et al., *Redox regulation of cell signalling.* Nature, 1996. **381**(6581): p. 380-1.

187. Tang, H., et al., *The T helper type 2 response to cysteine proteases requires dendritic cell-basophil cooperation via ROS-mediated signaling.* Nat Immunol, 2010. **11**(7): p. 608-17.

188. Fialkow, L., Y. Wang, and G.P. Downey, *Reactive oxygen and nitrogen species as signaling molecules regulating neutrophil function.* Free Radic Biol Med, 2007. **42**(2): p. 153-64.

189. Tse, H.M., M.J. Milton, and J.D. Piganelli, *Mechanistic analysis of the immunomodulatory effects of a catalytic antioxidant on antigen-presenting cells: implication for their use in targeting oxidation-reduction reactions in innate immunity.* Free Radic Biol Med, 2004. **36**(2): p. 233-47.

190. Fraternale, A., et al., *Antiviral and immunomodulatory properties of new pro-glutathione (GSH) molecules.* Curr Med Chem, 2006. **13**(15): p. 1749-55.

191. Schroecksnadel, K., et al., *Antioxidants suppress Th1-type immune response in vitro.* Drug Metab Lett, 2007. **1**(3): p. 166-71.

192. Cassee, F.R., et al., *Exposure, health and ecological effects review of engineered nanoscale cerium and cerium oxide associated with its use as a fuel additive.* Crit Rev Toxicol, 2011. **41**(3): p. 213-29.

193. Conway, M.A., et al., *Protection against Bordetella pertussis infection following parenteral or oral immunization with antigens entrapped in biodegradable particles: effect of formulation and route of immunization on induction of Th1 and Th2 cells.* Vaccine, 2001. **19**(15-16): p. 1940-50.

194. He, Q., et al., *Calcium phosphate nanoparticle adjuvant.* Clin Diagn Lab Immunol, 2000. **7**(6): p. 899-903.

195. Lutsiak, M.E., G.S. Kwon, and J. Samuel, *Biodegradable nanoparticle delivery of a Th2-biased peptide for induction of Th1 immune responses.* J Pharm Pharmacol, 2006. **58**(6): p. 739-47.